Civilian Radioactive Waste Management System

Management & Operating Contractor

THERMAL TEST PROGRESS REPORT #1

December 23, 1998

Prepared for:

U.S. Department of Energy
Yucca Mountain Site Characterization Office
P.O. Box 30307
North Las Vegas, NV 89036-0307

Prepared by:
Natural Environment Program Operations
Civilian Radioactive Waste Management System
Management and Operating Contractor
1261 Town Center Drive
Las Vegas, NV 89134-6352

Under Contract Number
DE-AC08-91RW0034

9903020042 990223
PDR WASTE
WM-11 PDR

EXECUTIVE SUMMARY

As explained in Section 1, this Thermal Test Progress Report # 1 is the first of a series of informal reports intended to communicate the progress of the in-situ thermal tests. The progress reports will be prepared and distributed every three months or so.

The Single Heater Test (SHT), the Large Block Test (LBT) and the Drift Scale Test (DST) are the three components of the current in-situ thermal testing program at Yucca Mountain.

The SHT, covered in Section 2, is nearly complete and the final report is being prepared. The findings of the SHT are discussed in detail in Section 2.2.1 through 2.2.3. The principal findings of the SHT are:

- Conduction is the dominant heat transfer mechanism, although pore water in the rock plays a role via the convection mode in both liquid and gas phases. This needs to be taken into account in modeling, to correctly predict the effects of heating the rock such as rise in temperature and movement of water.

- The dual permeability (DKM) model is more effective than the equivalent continuum (ECM) model in simulating the thermo-hydrologic processes in the SHT block.

- The SHT provides a basis, in site-specific field measurements, to rock mass thermal properties such as thermal conductivity and thermal expansion. The SHT shows that, below 200°C, rock mass thermal expansion is as much as 50% less than the values measured in the laboratory using small hand samples. The SHT also indicated that the thermal conductivity of the in-situ rock is substantially higher than that of the dried rock because of its moisture content. This difference needs to be taken into account in modeling the thermo-hydrologic processes.

- Chemical analysis of the water mobilized by heating in the SHT and subsequent modeling to recreate the characteristics of this water demonstrated that gas-phase reactions will play an important role in the thermal-chemical response of repository rock. The depressed measured pH of the SHT water samples indicates that CO_2 partial pressures in the SHT have been as much as two orders of magnitude higher than that at ambient condition.

- Pneumatic measurements in the SHT suggest that air-permeability, in certain regions of the test block some distance away from the heater, decreased by a factor of 3 to 5 during the heating phase due to the filling of fractures by the condensation of mobilized moisture. Permeability recovered with the progress of cooling as liquid water drained from the fractures by gravity.

- Electric resistivity tomography (ERT) and ground penetrating radar (GPR) measurements in the SHT tend to suggest, as does DKM modeling, that rock moisture mobilized by heating may drain by gravity via fractures to below the heated region rather than stay perched above it.

The Large Block Test is discussed in Section 3. The heating and cooling phases of the LBT are complete and measurements of temperature and moisture content of the block have been terminated. Overcoring for post-test characterization of the block is currently underway. Laboratory testing, modeling and analysis will continue over the next several months and the final report is expected to be completed in August, 1999.

The Drift Scale Test is covered in Section 4. The heating phase of the test is in its 13th month now. It is expected to extend over another three years or so. Results measurements of various kinds being made in

the DST are presented and discussed in Section 4. The recently completed Drift Scale Test Progress Report #1 discusses and performs extensive analysis of test results for first six months of the heating phase.

1 INTRODUCTION

Two types of formal reports have generally been employed to date to present and discuss results of the in-situ thermal tests. These are the level 4 deliverable reports and the level 3 deliverable reports. The level 4 or the more numerous kind of reports cover one or a few aspects/subjects associated with a particular test such as the Single Heater Test or the Drift Scale Test. Usually, they cover all the work performed by a teammate organization with respect to a specific test. The level 3 reports, which are fewer, are intended to document in a comprehensive and integrated fashion all aspects of a particular test over a specific period of time. The contents of a level 4 report are incorporated in a subsequent level 3 report associated with the test. Both level 4 and level 3 reports are subject to rigorous guidelines of product quality in terms of reference citations, data presentations and interpretations, to ensure traceability, transparency and QA pedigree of information presented and discussed.

Because of the unavoidable overlap/duplication of efforts in preparing both the level 3 and level 4 reports and in order to streamline the process so that resource utilization is optimized, it has been decided to prepare only integrated level 3 reports for the thermal tests starting in FY99. There will still be some level 4 deliverables from each teammate organization comprising of semi-annual data submittals to the technical database. However, there will be no formal level 4 reports. Elimination of the level 4 reports is not expected to adversely impact the communication within the thermal test team. Such communication is continuously ongoing and is greatly enhanced by the workshops every three months. Since the level 3 reports will be approximately 12 months apart, the absence of the more frequent level 4 reports may cause a gap in others' awareness about the progress of the thermal tests. To avoid such a situation, this informal report, covering all aspects of the thermal tests, is prepared and distributed. This report, designated Thermal Test Progress Report #1, is the first of a series of informal reports which will be prepared shortly after each quarterly workshop to ensure wider dissemination of information on the progress of the thermal tests. Although, much of the information in the progress reports will be derived from the preceding workshop, these reports will not be limited to be a summary of the workshop presentations and discussions. Any information, relevant to the in-situ thermal tests, available at the time of publication of an progress report will be included and discussed in it.

This Thermal Test Progress Report #1 is prepared following the sixth workshop held in Lawrence Livermore National Laboratory in October, 1998.

2 SINGLE HEATER TEST

The Single Heater Test (SHT), the first of the in-situ thermal tests, was fielded in Alcove # 5 in the Exploratory Studies Facility (ESF). The SHT is described in the report, "Test Design, Plans and Layout for the ESF Thermal Test", document # BAB000000-01717-4600-00025 REV 01 of September 20, 1996. The as-built SHT and some of the test results from the heating phase of the SHT are presented in the report, "Single Heater Test Status Report", document # BAB000000-01717-5700-00002 REV 01 of December 11, 1997.

2.1 Status

The heater of the SHT, energized on August 26, 1996, was turned off on May 27, 1997. Measurements and data collection continued till the end of January, 1998. Post-test characterization of the test block and analysis of results are complete. Several level 4 reports on various aspects of the SHT have been published. The final report is being prepared and is expected to be completed in March, 1999.

2.2 Outcome of Single Heater Test

2.2.1 LBNL's perspective/thermo-hydrological focus (from Yvonne Tsang on Input to progress report on ESF thermal test, November, 1998)

The Single Heater Test (SHT) is successful in meeting the stated objective of the YMP Thermal Test Program, namely, to acquire a more in depth understanding of the coupled processes: thermal, mechanical, hydrological and chemical processes in fractured, partially saturated tuff under the influence of heat. The good agreement between the modeling results and the extensive data set from the SHT indicates that the fundamental basis of our understanding of the thermo-hydrological coupled processes is sound, although detailed behavior are impacted by site specific features and local heterogeneities that have a higher degree of uncertainty. Table 2-1 gives a statistical measure of goodness of fit for simulated and all measured temperature in the SHT, at three instance of time during the test: 3 and 9 months after heating, and 3 months after cooling. Both the statistical measures Mean-Error and Root-Mean-Square-Error use the same weighting scheme Ë inversely proportional to the number of temperature measurements in a given temperature subrange Ë in order to give equal importance to all temperatures observed.

The success of the SHT is a direct result of the multidisplinary and multi-laboratory teamwork of the Thermal Test Team (TTT) in closely integrating modeling studies and field and laboratory measurements. The SHT has afforded the TTT an opportunity to refine an iterative approach between modeling and measurements. The approach is such that ambient pre-test characterization data serve as input to predictive modeling efforts, and measured data serve to discriminate and confirm alternative hypothesis in the conceptual models, and modeled results are allowed to guide further active testing and post-test characterization. This kind of iteration between model and test data is effective for reducing conceptual model and parameter uncertainty. As the first of the *in situ* thermal tests in the ESF, the SHT has functioned also as a testbed for the longer-duration, larger-scale Drift Scale Test (DST). Insights gained with regards to overall approach, testing methods, instrumentation, analysis strategies are presently applied to conducting of the DST. Two examples are: (1) while only water sampling and analysis was planned for the SHT, outcome of the SHT underlines the importance of gas chemistry in deciphering the thermo-hydrological-chemical processes, thus a rigorous gas sampling and isotopic analysis program is put in place for the DST; (2) while water sampling was originally planned only from the chemistry holes, the occurence of water in the hydrology hole 16 in SHT promoted a revised design of the packer system for the DST. The present packer string design in the DST is such that each borehole section isolated by packers in the 12 hydrology holes also double as water and gas sampling ports.

Despite the difference in scale and configuration between the two thermal tests (SHT and DST), the conceptual model of various coupled processes developed based on the SHT experience has been equally

successful in matching the extensive temperature data set from 9 months of heating of the DST. This is a strong confirmation that the fundamental understanding and formulation of the thermo-hydrological coupled processes obtained in SHT is valid, thus significantly increase the confidence level of our ability to predict the performance of a high-level nuclear waste repository in heterogeneous, partially saturated, fractured tuff.

The main technical findings from the SHT (thermo-hydrological focus) are:

(1) Heat conduction accounts for most of the temperature rise, and is therefore the dominant heat transfer mechanism in the SHT.
(2) Complementary field and laboratory techniques are important in tracking the drying/condensation front. The simulated moisture redistribution in the SHT using a dual-permeability 3D model is well supported by field data, which include those from ERT, neutron logging, cross-hole radar tomography, air injection tests, and laboratory measurements of matrix liquid saturation from post-test cores. The model predicts a drying zone of about 1.2 m around the heater at the end of the heating phase, as well as a condensation zone further away with a large increase in fracture liquid saturation, which gives rise to significant water drainage through the fractures by gravity, and the drained water is subsequently imbibed into the rock matrix below the heater horizon. Both electrical resistivity and cross-hole radar tomograms for the heating phase of the SHT hint at a larger liquid saturation in the matrix below the heater horizon rather than above it, suggesting water drainage in the fractures. The air permeability values in the condensation zone (zone 3 of boreholes 16 and 18), while remaining depressed throughout the heating phase because of increased liquid saturation in the fractures, returned to pre-heat values after the termination of heating, suggesting that water was not held in the fractures once the vaporization and condensation processes ceased at heater turn-off, again supporting the presence of water drainage in the fractures. This observation led the TTT to design placement of the three post-test boreholes 199, 200, and 201 (Figure 2.2-1), based on the drying, condensation, and drainage zones as predicted by the model results. The determination of the liquid saturation of these cores from the laboratory measurements (Figure 2.2-1) show that (a) drying due to heat has occurred near the heater, as evidenced by the lower liquid saturation of cores within the 1-m radius from the heater; (b) the liquid saturation in the anticipated "condensing" zone between the two dashed circles are generally lower than those values in borehole 201 (drainage zone). These observations are consistent with the predictions from a dual-permeability conceptual model, while an effective continuum approximation would predict no drainage in the fractures and a symmetric condensation zone about the heater horizon.

(3) The water collected in the SHT is confirmed by THC modeling to be result of steam condensation in fractures.

(4) Small thermo-mechanical changes due to heating were detected by post-test air permeability tests in the SHT block. There is an overall increase in air permeability from about 20% to a factor of 3.5, which may be attributed to overall microfracturing. Heating may cause some fractures to close and some to open. However, since air-permeability tests are conducted over length scale of meters, and since fluid always seek the least resistive path, air-permeability tests preferentially register the effect of fracture opening.

2.2.2 SNL Perspective

The Single Heater Test was a great success for the YMP for the following reasons:

- It was the first large-scale in situ coupled-process test at Yucca Mountain, and the experience gained from its successful implementation was used toward the Drift Scale Test.
- The range and quality of data produced was outstanding.
- The test successfully combined the results of field and laboratory data to describe hydrological, mechanical, and chemical changes occurring to the heated rock.
- The data allowed a realistic evaluation of the predictive codes and conceptual models used to describe complex coupled processes expected at Yucca Mountain.

Thermal-Hydrologic Results

Equivalent continuum conceptual models do not adequately capture or describe details of the thermal-hydrological behavior at the scale of the Single Heater Test. Dual permeability models match the data much better. For T-H modeling, the equivalent continuum model washes out the convective effects of the presence of fractures. The presentation by SNL pointed out the difference between the predicted and measured temperatures for the High k_b ECM, Low k_b ECM, and Low k_b DKM models.

At r>1 m, where T(measured)<100°C, the three models yield essentially the same results, indicating that conduction is the primary heat transfer mechanism. Also in this region the models overpredict temperature (measured) by as much as 7°C. This overprediction could be corrected by increasing the wet thermal conductivity of the rock in the simulations, which would cool the predicted rock temperatures.

The most important differences between the three models occur at radial distances from the heater between about 0.8 to 1.2 meters:

- For the Low k_b ECM model in this annular region, the temperature is at the boiling point of water and liquid water and water vapor coexist in the pores of the rock. The vapor cannot readily escape from the pores of the rock
- In the High k_b model water vapor can readily escape from the pores of the rock.
- In the DKM model the separate but connected matrix and fracture continua results in a much smoother temperature profile through the boiling region, similar to the measured data.

Thermal-Mechanical Data

Field and laboratory thermal-mechanical data from the Single Heater Test provided necessary insights into the behavior of the Topopah Springs middle non-lithophysal rock in which the test was implemented

- Rock mass modulus, rock mass thermal expansion, and thermal stress are significantly reduced by the presence of fractures. Rock mass modulus values were obtained through Goodman Jack testing, and those values (3-10 GPa) were much less than the intact rock value (32.4 GPa). Rock mass thermal expansion values were determined from the displacement measurements of the MPBXs; those values (2.5-6 μstrain/°C) were less than the intact rock values (7-14 μstrain/°C) over the same temperature range. Thermally induced stresses were estimated for the range of modulus and expansion values with numerical modeling.
- Intact rock thermomechanical properties (thermal conductivity, thermal expansion, modulus, Poisson's ratio, and peak stress) are largely unaffected by the thermal pulse of the Single Heater Test. Thermomechanical properties of intact rock should not change over time, based on current laboratory test results.

A slight difference was noted for the thermal conductivity measurements of post-test samples. Those obtained from a region within the boiling isotherm had a slightly higher thermal conductivity than those from outside the boiling isotherm. It is thought that, if anything, the "inside" samples should have a lower conductivity because of the greater likelihood of microcrack formation due to the higher temperatures. Others at the workshop expressed the opinion that the data reflect their belief that the radiation across the microcrack would be more efficient than conduction of the intact rock, thus increasing the overall conduction. This is a likely topic for future discussion.

Thermal-Mechanical Modeling

The T-M data provided a realistic basis for comparison of elastic and compliant joint modeling. Previous calculations employing the elastic model and encompassing the range of rock mass and in situ values for modulus and thermal expansion matched the behavior of the MPBXs to some extent; however, seemingly inelastic behavior was observed, particularly in the three MPBXs parallel to the heater. The compliant joint model incorporates temporally and spatially averaged inelastic behavior of fractures. Results with the CJM

with fracture apertures and spacings correlating to the low bulk permeability predict elastic behavior, with maximum displacements closer to the measured values than were the elastic model predictions. Results with the CJM for fracture characteristics correlating to the high bulk permeability predict very different behavior that somewhat mimics the inelastic regions seen in the data. There is some correlation between locations of inelastic behavior and high permeability regions as indicating by air-perm tests and tunnel fracture mapping. Also, predictions of fracture aperture closure by the CJM indicate near-complete closure for the low-perm case, and only partial closure for the much larger fractures of the high-perm case. Although the CJM is very valuable for predicting fracture aperture behavior on a large scale, it does not identify discrete joint slippage events and poses mesh scaling problems for the observed joint spacing at the SHT site.

2.2.3 LLNL Perspective - Outcome of the Single Heater Test by Stephen C. Blair

The Single Heater Test is considered to be successful due, in part, to the tremendous amount of cooperation between the participants, and due to the success in measurements and interpretations of coupled processes that took place in the SHT.

Electrical Resistance Tomography (ERT) was used during the SHT to monitor the rock water saturation, with a special interest in the movement of steam condensate out of the system. Images of resistivity change were calculated using data collected before, during, and after the heating episode. These images were used to calculate changes in water saturation (after accounting for temperature effects) during or after heating.

Thermal neutron-logging was also used to monitor moisture content in four boreholes during the SHT. The ERT imaging and the neutron logs indicated that heating of the rock generally caused drying (decreased liquid saturation) near and above the heater and wetting (increased liquid saturation) in rock below and to the north of the heater. Figure 2.2-2 presents a compilation of the ERT and neutron measurements made near the end of the heating phase (day 270). This figure shows very good agreement between the two data sets. The transition from drying to wetting regions observed from neutron logs in Boreholes 22 and 23 especially well matches the drying/wetting transition derived from ERT measurements.

The most extensive drying is observed in regions at the heater elevation and above. However, the dry zone detected by ERT is not centered on the heater and is not symmetric about the heater; rather, it has lobes that extend upward from and to either side of the heater (Figure 2.2-2). The ERT measurements do indicate that the driest region was right around the heater and that it had a saturation of approximately 10%. In addition, temperature measurements in the neutron holes indicated that drying occurred at temperatures in the range of 60 to 90°C. Figure 2.2-3 presents the ERT tomograph for 270 days overlaid with temperatures calculated for 275 days. This figure shows that, for the region below the level of the heater, measurable drying is indicated for rock at temperatures greater than 60°C.

In late November 1996, early February 1997, late February 1997, and mid-May 1997, water samples were collected from one of the boreholes in the SHT. Geochemical analysis of water composition and associated modeling show that the waters collected were slowly evolving while still maintaining consistent compositional characteristics. These characteristics are that Na and Si were the dominant cations in solution, followed by Ca, K, and Mg. Values of pH at about 6.5 all reflect slightly acidic waters. The low pH is indicative of higher CO_2 partial pressures (approximately two orders of magnitude, relative to ambient).

The evolution is consistent with a simple model in which condensate interacts with fracture-lining minerals only. Preliminary modeling suggests that the flow distance was 3 to 6Ým from the heater and also that the concentration of Ca followed precisely that expected if calcium concentration reflects the interaction of calcite and a water in which pH is externally controlled, that the solution concentration remains saturated with respect to quartz, and that the concentrations of K are consistent with K-feldspar dissolution.

These conclusions are also consistent with the primary characteristics of the solution chemistry developing within a few meters of the heater, at temperatures and flow conditions expected in the actively convecting portion of the heated region.

X-ray analysis of samples taken from the ESF has shown the uniformity of the total SiO2 polymorph and feldspar abundances in the repository horizon (Topopah Spring tuff). Within this horizon and adjacent zones, the relative abundance of quartz plus tridymite is positively correlated with gray, altered zones adjacent to lithophysal and fractures. Work presented here indicates that the relative abundance of cristobalite relative to quartz plus tridymite could potentially be used to assess the density of paleo fluid pathways. A strong negative correlation between cristobalite and quartz plus tridymite abundances was observed and may reflect post-devitrification alteration by aqueous fluids.

An optical extensometer, developed at LLNL, was installed in two boreholes in the SHT. This prototype instrument was developed for use in the high-temperature environment that is expected in a geologic repository for nuclear waste. The system has many advantages over conventional rod extensometers because there are no moving parts in the borehole, and a system correction for temperature is incorporated in the design. Precision of data gathered during the SHT with this system was not adequate to monitor small deformations. However, valuable field experience with this system was gained, and, because the system is still under development, it is hoped that the system performance and data quality will be improved in future realizations of this instrument.

The thermo-hydrologic (TH) behavior during the heating and cooling stages of the SHT was modeled with the NUFT code, using the December 1997 TSPA-VA base-case hydrologic parameter set, which was modified to include the field measurements of bulk permeability in the SHT area. Two different conceptual models for fracture-matrix interaction were considered: the ECM, which assumes equilibrium between the fracture and matrix continua, and the DKM that accounts for disequilibrium processes between the fracture and matrix continua. Unlike earlier TH models of the SHT, all of the models in this study included the influence of vapor and heat flow along the heater borehole.

The DKM model predicted temperatures that were in outstanding agreement with the observed temperatures throughout the heating stage of the SHT; the ECM model predicted lower temperatures, but a more extensive dry-out region, than did the DKM model. Both the ECM and DKM models predict a pronounced cold-trap effect in the heater borehole. Vapor and latent-heat flow from the heated interval of the heater borehole to the cool end of the heater borehole adjacent to its collar, where the vapor condenses, resulting in focused condensate drainage and a local increase in Sliq in the matrix. The cold-trap effect efficiently transfers heat along the heater borehole toward the TM alcove. The cold-trap effect is a potentially important mechanism influencing TH behavior in emplacement drifts.

This work also showed that The SHT was ineffective for distinguishing between alternative conceptual models of the fracture/matrix interaction (FMX) factor. Both approaches result in the same outstanding agreement with observed temperatures, and both approaches predict the same distribution of Sliq in the matrix continua. This analysis also showed that the SHT was not a useful test for diagnosing the magnitude of percolation flux qpere. The lack of sensitivity of the SHT to qpere arises from the heat-driven condensate fluxes being much greater than any of the values of qpere that were considered.

Scientists at LLNL also performed a simple TM analysis of the SHT . This analysis was designed to assess the potential for TM stresses developed in the SHT to cause shear slip on fracture sets occurring in the rock mass heated during the SHT. Shear slip has been shown to increase rock-mass permeability. This analysis shows that thermal gradients and associated thermal stresses induced by heating and cooling of the SHT are relatively low, and regions where shear slip could be expected are also small and unlikely to influence permeability.

The Single-Heater Test (SHT) was one phase of the field-scale thermal testing program of the Yucca Mountain Site Characterization Project. It was conducted to obtain data on thermal, mechanical, hydrologic, and chemical processes in situ. The resulting d -Earth & Environmental Sciences-Earth & Environmental Sciences.

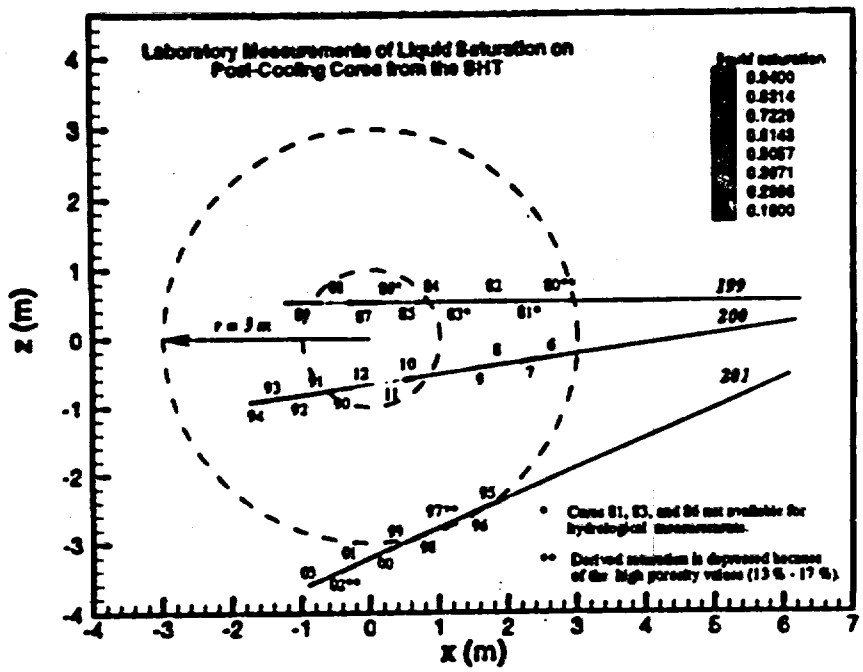

Figure 2.2-1. Liquid saturation of cores from boreholes 199, 200, 201, dry-drilled after the cooling. (DTN LB980901123142.006)

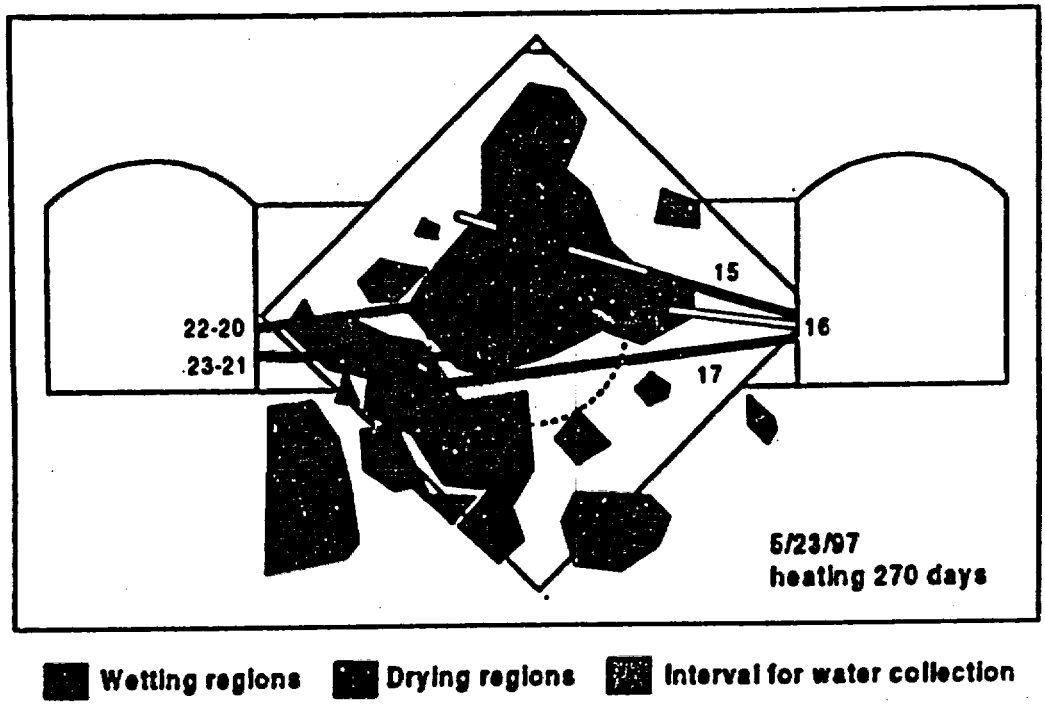

Figure 2.2-2 Zones of relative drying nd wetting after 270 days of heating in the SHT, as observed from ERT and Neutron measurements.

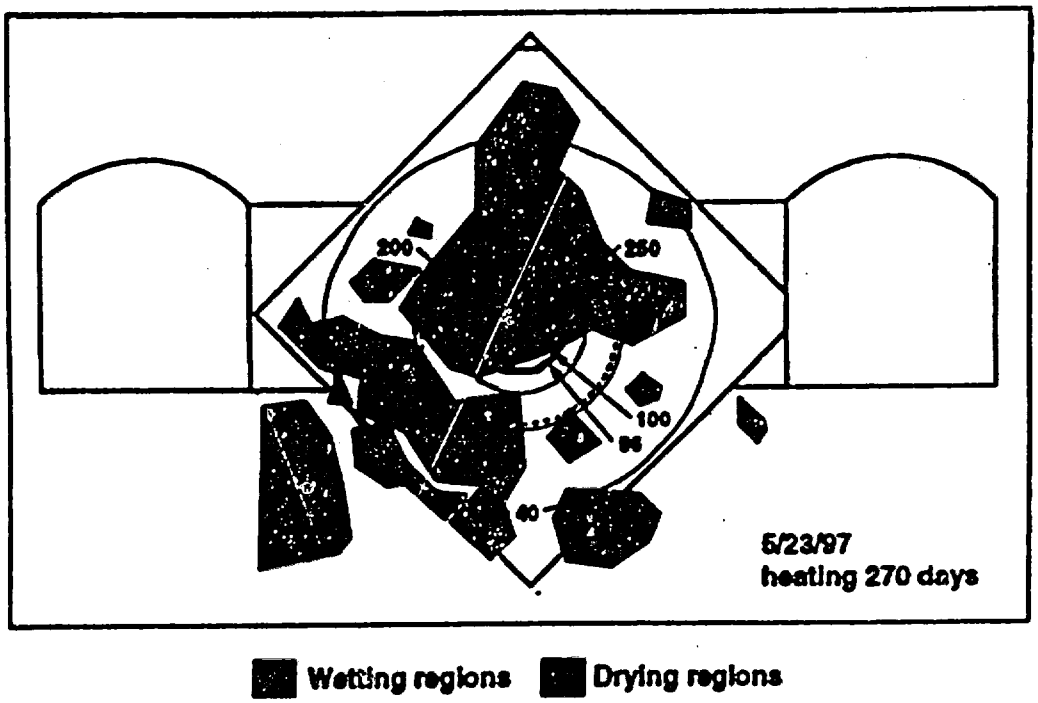

Figure 2.2-3 Comparison of relative drying and wetting regions with predicted temperature distribution at end of heating phase of SHT

DRAFT DISCLAIMER

This contractor document was prepared for the U.S. Department of Energy (DOE), but has not undergone programmatic, policy, or publication review, and is provided for information only. The document provides preliminary information that may change based on new information or analysis, and is not intended for publication or wide distribution; it is a lower level contractor document that may or may not directly contribute to a published DOE report. Although this document has undergone technical reviews at the contractor organization, it has not undergone a DOE policy review. Therefore, the views and opinions of authors expressed do not necessarily state or reflect those of the DOE. However, in the interest of the rapid transfer of information, we are providing this document for your information.

Patterson
Deb

TRW

TRW Environmental
Safety Systems Inc.

1261 Town Center Drive
Las Vegas, NV 89134
702.295.5400

QA: N

Contract #: DE-AC01-91RW00134
LV.NEPO.LRH.01/99-034
January 4, 1999

Dennis R. Williams
Deputy Assistant Manager for Licensing
U.S. Department of Energy
Yucca Mountain Site Characterization Office
P.O. Box 30307
North Las Vegas, NV 89036-0307

Dear Mr. Williams:

Subject: Thermal Test Progress Report No. 1

I am pleased to transmit herewith the Thermal Test Progress Report No. 1 which is the first of a series of informal reports to be prepared every three months. This report has been prepared following the Sixth Thermal Test Workshop held at Livermore in October 1998. These progress reports are intended to help communicate the progress of the in-situ thermal tests, are not a Level 4 or 3 baseline commitment and should be considered draft in nature. Therefore, they are not subject to the provisions of the CRWMS M&O YAP 30.63 (Submittal, Review, and Acceptance of Deliverables) and should not be used in support of/or cited in QA activities.

Should you have any questions, please feel free to contact Robin Datta of my staff at (702) 295-5741 or me at (702) 295-5604.

Sincerely,

Larry R. Hayes

Larry R. Hayes, Manager
Natural Environment Program Operations
Management and Operating Contractor

cc:
R. E. Spence, DOE/YMSCO, Las Vegas, NV
R. L. Patterson, DOE/YMSCO, Las Vegas, NV
Deborah Barr, USGS, Las Vegas, NV
M. T. Peters, M&O, Las Vegas, NV

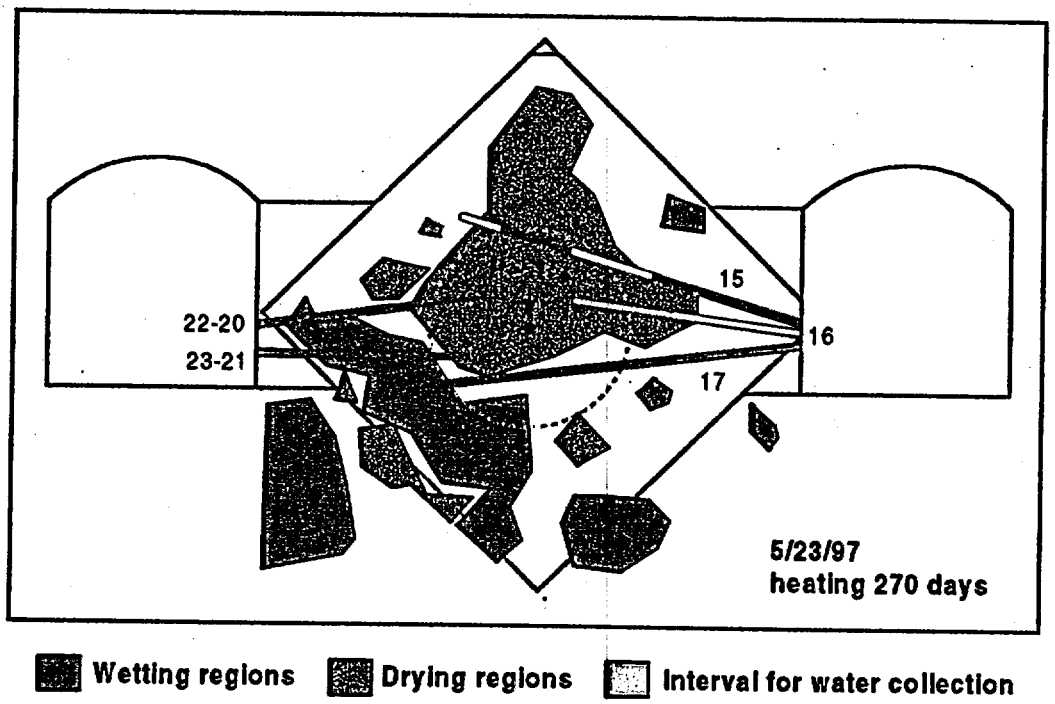

Figure 2.2-2 Zones of relative drying nd wetting after 270 days of heating in the SHT, as observed from ERT and Neutron measurements.

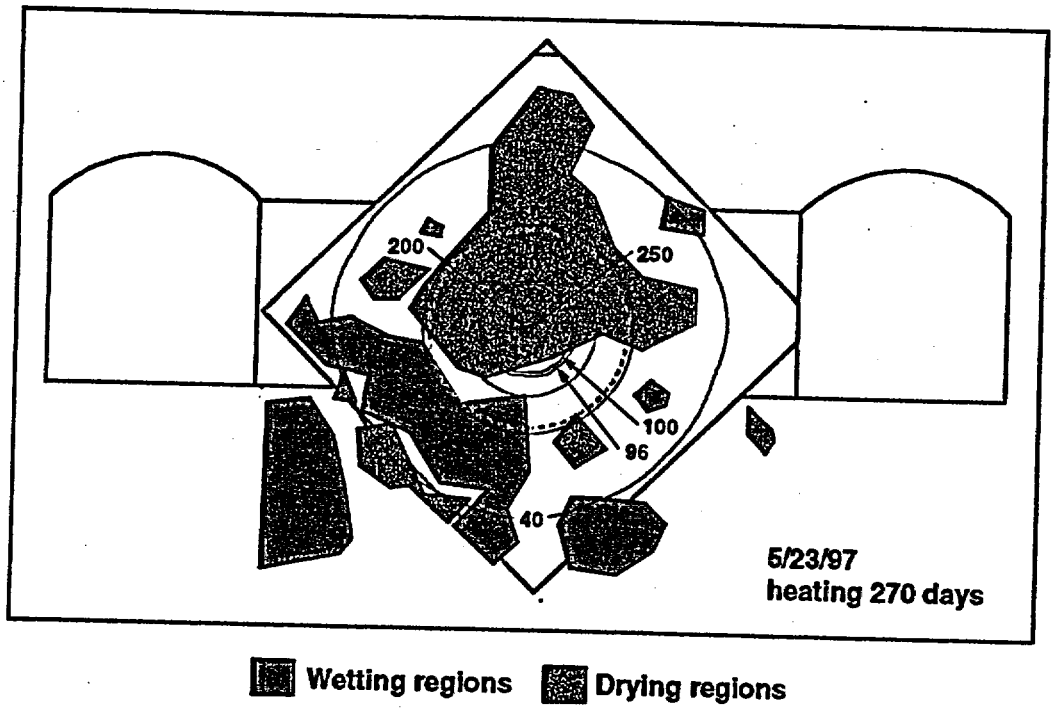

Figure 2.2-3 Comparison of relative drying and wetting regions with predicted temperature distribution at end of heating phase of SHT

3 LARGE BLOCK TEST

The Large Block Test (LBT), located at Fran Ridge south of Yucca Mountain, is the second in-situ thermal test conducted for the Yucca Mountain project. It is a test with controlled boundary conditions to evaluate the coupled thermal-mechanical-hydrological-chemical (TMHC) processes in the nearfield rock of the proposed repository. Specifically, the LBT is expected to help us understand the dominant heat transfer mechanism, condensate refluxing, relationship between boiling point isotherm and the drying of the rock mass, rewetting of the dry-out zone following the cool-down of the block, displacement in fractures, and rock–water interaction. The LBT will evaluate the corrosion/oxidation potential of coupons of candidate waste package materials. The LBT will also investigate the survivability and migration of the local microbes in a heated environment. The current status of the test, and the temperature, neutron logging results, and the microbial observations obtained so far are discussed in the rest of this section.

Description of the LBT

An outcrop area at Fran Ridge was selected because of its suitable rock type and accessibility. A 3 x 3 x 4.5 m block of nonlithophysal Topopah Spring tuff was isolated at Fran Ridge. Instruments and heaters were installed within and on the surface of the block. The instruments installed in the block included resistance temperature devices (RTD) to measure temperatures, electrodes to conduct electrical resistivity tomography (ERT), Teflon liners for the neutron logging in boreholes, Humicaps to measure relative humidity, pressure transducers to measure gas phase pressure, conventional and optical multiple point borehole extensometers (MPBX) for measuring displacements along boreholes, fracture gauges mounted across fractures on the block surface to monitor fracture deformation, Rapid Estimation of K and Alpha (REKA) probes to measure in-situ thermal conductivity and diffusivity, and visual observation of the drainage of water near the bottom of the block. Coupons of waste package material and introduced material were placed within the block to study the effect of the heated environment on the materials. Labeled local microbes were introduced back into the block to study their survivability and migration. The temperature measurements included the spatial and temporal variation of the temperature in the block and the thermal gradient on the block surfaces. One heater of 450 Watts was installed in each of the five horizontal heater holes at about 2.75 m below the block top. A heat exchanger was installed to control the temperature on the block top. A layer of RTV and Viton were installed on the block sides to minimize moisture flux. Three layers of insulation materials (Ultratemp, fiberglass building insulation, and Reflectix) were installed on the outside of the moisture barrier. All of the instrument holes were sealed either by cement grout, packers, or an RTV/Teflon membrane. Straps were used to stabilize the block and insulation during the test. Figure 3-1 shows a schematic diagram of the block displaying borehole location, orientation and purpose.

To conduct the test, the block is heated from within to reach a temperature of 140°C at the heater horizon, and the heat exchanger is used to keep the top temperature at about 60°C. Temperatures will be maintained constant for at least one month, after which the heaters will be turned off to start a cooling phase. Vapor is allowed to leave the top of the block. Background data were prior to heating. Data acquisition will continue throughout the test. The following parameters are measured continuously by an automated data acquisition system: heater power, temperatures, displacement by MPBX, relative humidity, pore gas pressure. Neutron logging, ERT, REKA, and optical MPBX are performed periodically. Air permeability and gas tracer tests were conducted before the heaters were energized, and will be performed again after the block is cooled. After the test, the block will be dismantled to examine for evidence of rock–water interactions, characteristics of the waste package material coupons and the introduced material coupons, and the survivability and migration of the microbes. Currently the data acquisition phase of the test has been completed. The data acquisition system was turned off on 9/30/98. Some of the instruments are being recovered for calibration and evaluation. Air permeability will be measured in the block. Coring and over-coring for samples for analyzing the rock-water interaction will be started soon.

Test Results and Discussion

The heaters were energized to a planned power of 450 Watts each at 10 AM on February 28, 1997. Except for a few short periods of power outages, the heater power has been quite stable. The highest recorded temperatures in the block were measured by RTD TT1-14, which is located about 5 cm above the heater horizon in the vertical RTD hole TT1. TT1 is one of the two vertical RTD holes, and is located about 1.22 m from the north side, and 1.83 m from the east side (Figure 3-1). Figure 3-2 shows the measured temperature at TT1-14 as a function of elapsed time. A heater power rampdown was started at about 12 noon on October 6, 1997. The heater power rampdown is designed to keep the temperatures in the block at about 135°C. The heaters were turned off on 3/10/98 to start a natural cool-down phase. The temperatures at TT1-14 show a brief period of boiling at about 1000 hours. The temperature drops at 2520 and 4475 hours were thermal-hydrological events on June 13, 1997 and September 2, 1997, respectively. Temperatures measured from many RTDs in the two vertical RTD holes (TT1 and TT2 in Figure 3-1) converged to about the boiling point of water (~97°C) during those two events at 2520 and 4475 hours, and remained at that temperature for extended periods of time. The temperatures then began to rise and fluctuate at about 2900 and 4520 hours.

Our interpretation of these temperature fluctuations is that they may be related to condensate refluxing. The convergence of the measured temperature at many RTDs to approximately 97°C is a strong indication that the thermal events were caused by episodic infiltration of water, and boiling had taken place over a substantial vertical distance above the heater horizon. The block cooled off quicker than that predicted. Figure 3-3 shows the temperatures measured at TT2-14. TT2 is the second vertical temperature hole which is located at about 1.82 m from the north side and 0.6 m from the east side, and #14 RTD is at the heater horizon in that hole. As shown in Figure 3-3, the rock at TT2-14 was involved in boiling for much longer period of time than that at TT1-14. Then the temperature fluctuations at the end of the 6/13/97 event, and the 9/2/97 event are similar to that at TT1-14. The cooling off of the block at TT2-14 is the same as at TT1-14.

Figure 3-4 shows the difference in the fraction volume water of the last three neutron measurements before the termination of the data acquisition system, with respect to the pre-heat baseline, in Hole TN3, which is one of the vertical neutron holes located at 1.83 m from the north face and 1.83 m from the east face of the block (Figure 3-1). A maximum drying at the heater horizon is shown. And there was very little sign of re-wetting in the last three months of the cool-down phase. Figure 3-5 shows the difference fraction volume water at four locations in TN3 as a function of time. Again, not much re-wetting is observed since the de-energization of the heaters at 375 days. The difference fraction volume water measured by the neutron logging in other vertical holes are similar to those shown in Figures 3-4 and 3-5.

The moisture distribution measured by neutron logging in the horizontal holes shows fairly uniform drying in the horizontal cross sections in the block. Two exceptions were observed. Those are shown in Figures 3-6 and 3-7 below. Figure 3-6 shows the smoothed difference fraction volume water content at four depths from collar (the west side of the block), as a function of time in WN4. WN4 is one of the four horizontal neutron holes drilled from the west side at about 1.67 m from the top, and about 2.12 m from the north side. An increase of moisture near the middle of the block occurred in May of 1997 (about 100 days of heating). This is in agreement with the ERT results at that time. And a significant drying occurred at about 0.8 m from the west side during much of the heating phase and the entire cool-down phase. Both of these two locations are closely associated with major fractures in the block. Thermal mechanical data of those fractures are available so that an integrated interpretation of the thermal hydrological and thermal mechanical processes can be performed. Figure 3-7 shows the smoothed difference fraction volume water content at four depths from collar (the north side) in NN6 as a function of time. NN6 is one of the six horizontal holes drilled from the north side of the block, at about 3.79 m from the top, and 2.12 m from the east side. This hole is about 1 m below the heater horizon. A significant increase in moisture content was observed during much of the heating phase in this region. And the increase in moisture content disappeared after the heating phase was ended. This region is also associated with major fractures. This is an indication that water drained away in the fractured zone.

The neutron results in NN6 agree with the observation of the migration of the microbes in the observation holes EO3, NO1, and NO2 below the heater horizon (Figure 3-1). The native microbes which were cultured to be double drug resistant, and placed in the heater holes, were detected in the observation holes during the heating phase. No microbes were observed after the end of the heating phase. It is likely that the microbes migrated from the heater holes along with the water that drained away in the fractures.

Summary

The data acquisition phase of the LBT has been completed. The LBT has provided experimental data of thermal-hydrological-mechanical processes. We observe a zone of dry-out at the heater horizon, and a condensate zone above it. Condensate refluxing is indicated by the temperature fluctuation, at least along boreholes TT1 and TT2. Water drainage away from the heater horizon was observed by the neutron logging and the microbial migration test. Core samples will be obtained from the block for studying rock-water interaction in the matrix and on the fracture surfaces. The thermal-hydrological results presented in this presentation will be incorporated with other observations, such as the displacement measurements, ERT, and the post-test analyses of the rock water interaction to enhance our understanding of the coupled TMHC processes.

Thermal-hydrological, thermal-mechanical, thermal-chemical, and the coupled processes models will be constructed to compare with the observed results. Through the comparison of the observations and the model calculations, the coupled TMHC processes will be better understood. The processes may be included in models used to predict characteristics of the near-field environment of a repository.

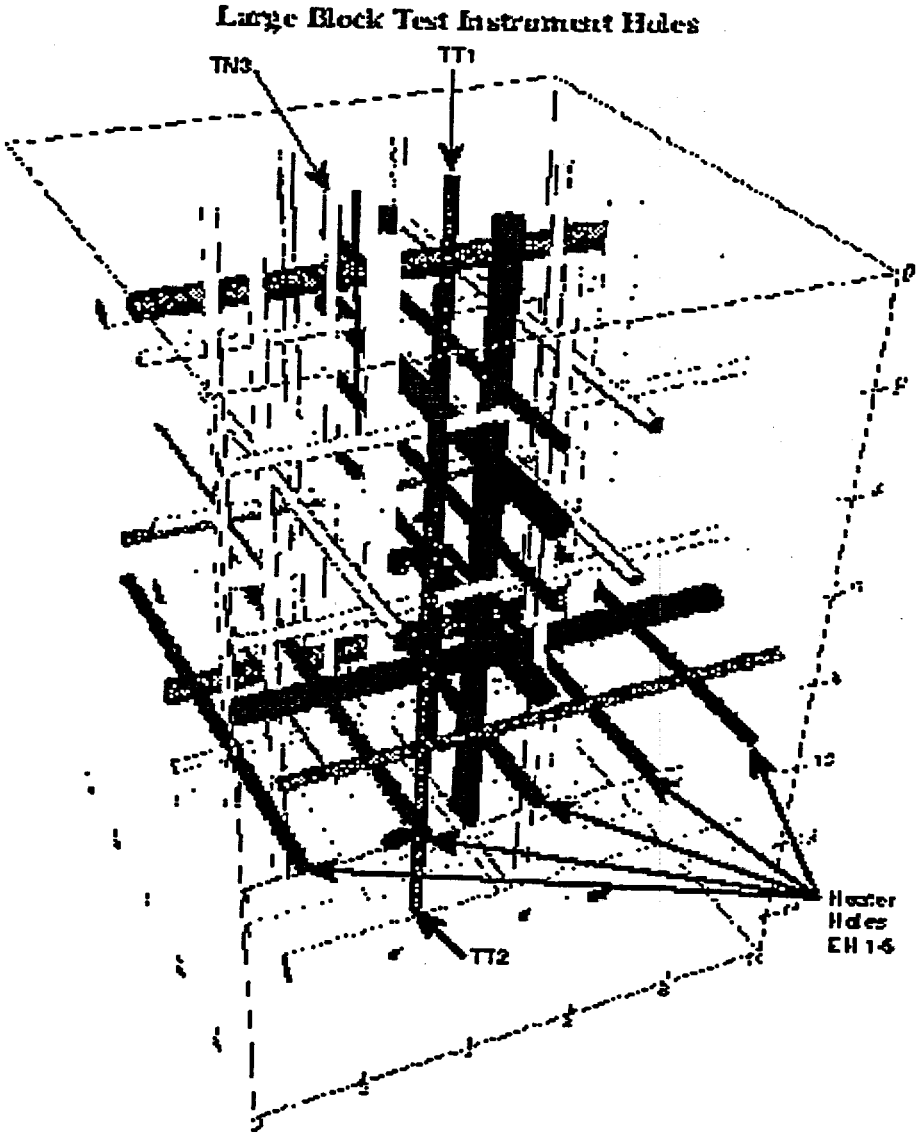

Figure 3-1. Schematic diagram of the large block with all of the boreholes. The color codes for the boreholes are: brown for RTD, yellow for MPBX, purple for packers, red for heaters, white for observation, green for neutron, black for REKA, orange for microbes, and blue for ERT.

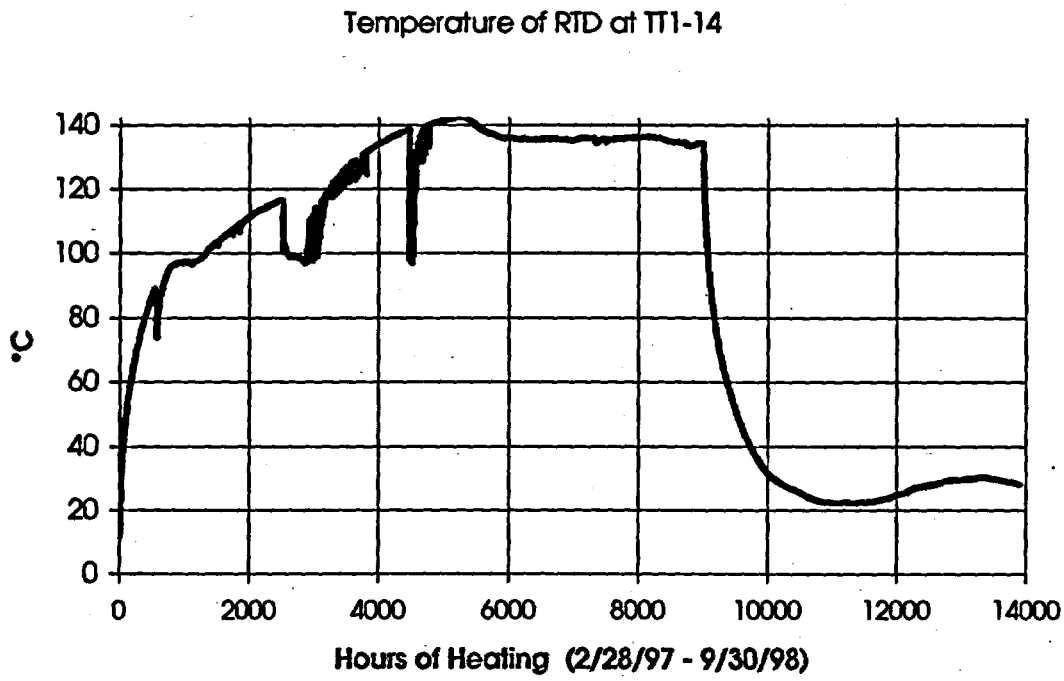

Figure 3-2. Temperatures at TT1-14 as a function of elapsed time.

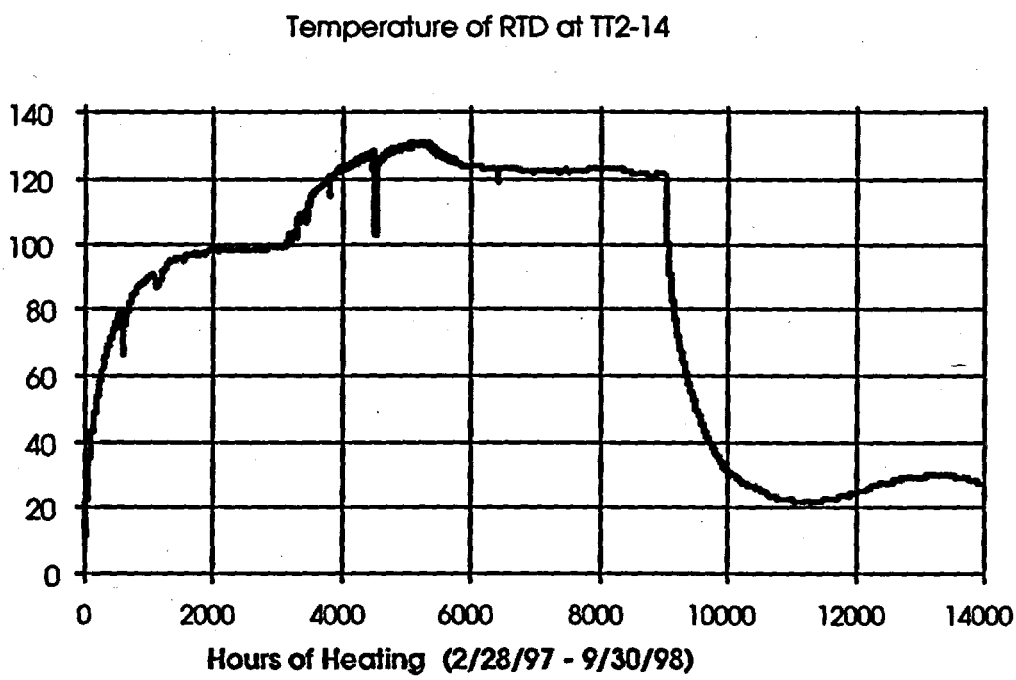

Figure 3-3. Temperatures measured at TT2-14 as a function of time.

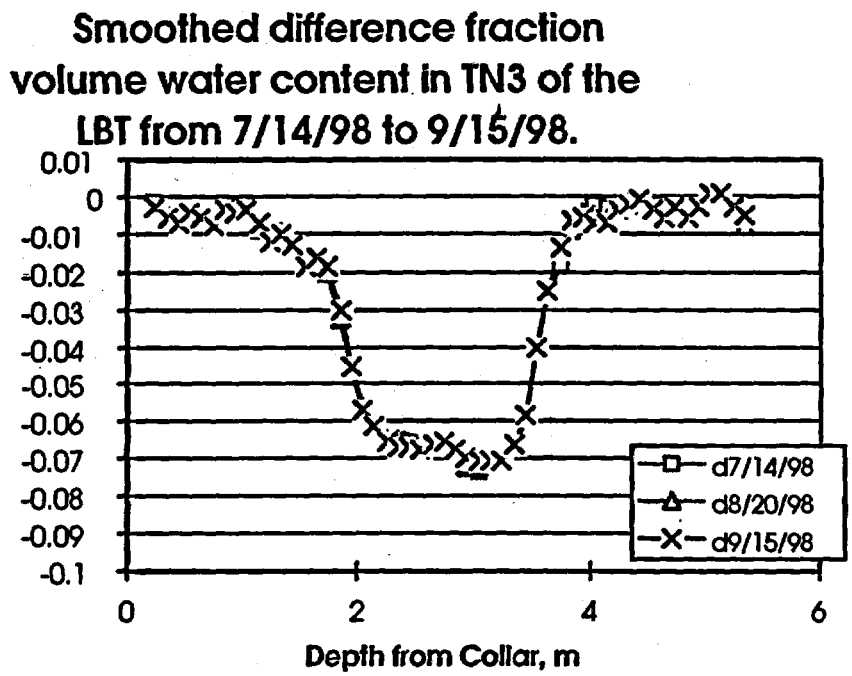

Figure 3-4. Smoothed difference fraction volume water content in TN3 as a function of depth from collar.

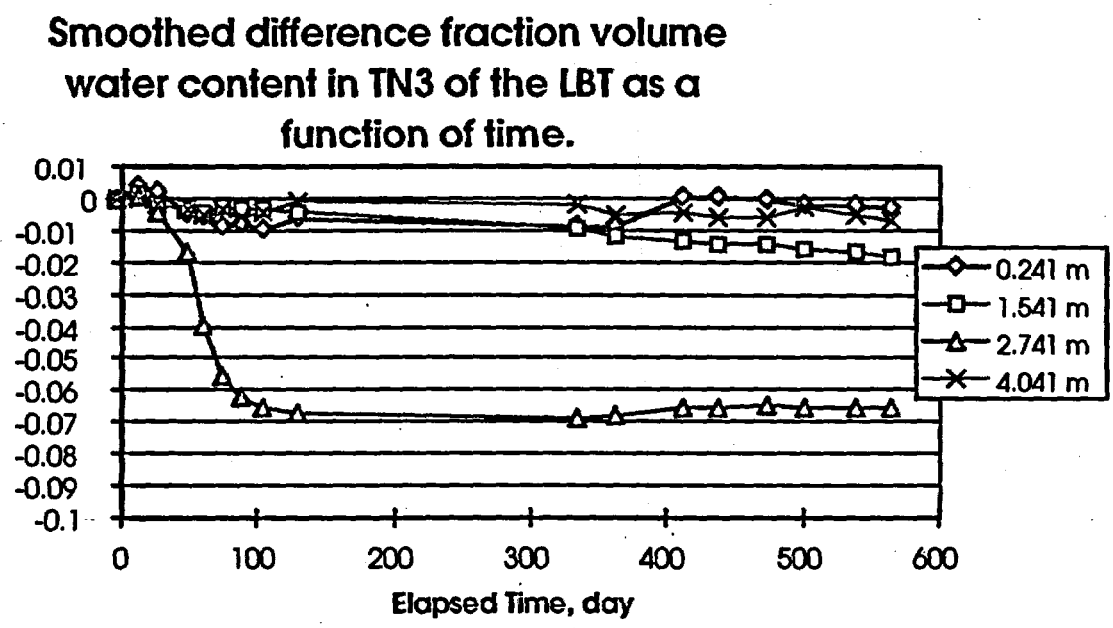

Figure 3-5. Smoothed difference fraction volume water content at four depths from collar in TN3 as a function of time.

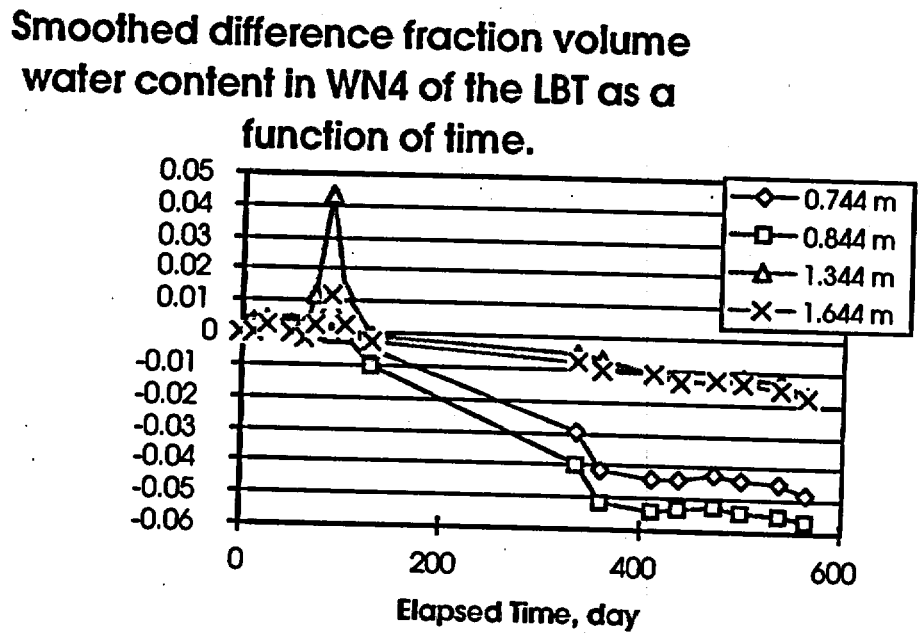

Figure 3-6. Smoothed difference fraction volume water content at four depths from collar in WN4 as a function of time.

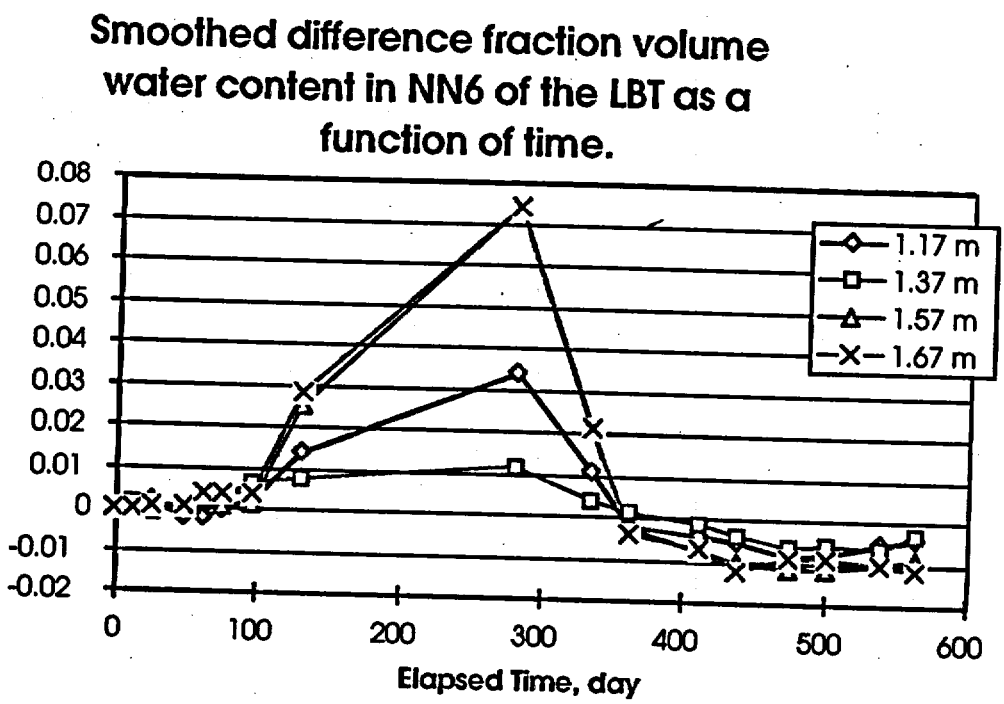

Figure 3-7. Smoothed difference fraction volume water content I at four depths from collar in NN6 as a function of time.

4 DRIFT SCALE TEST

The Drift Scale Test (DST), located in Alcove #5 in the ESF, is described in the report, "Drift Scale Test Design and Forecast Results", document # BAB000000-01717-4600-00007 REV 00 of July 16, 1997. The heating phase of the DST, initiated on December 3, 1997, is scheduled to continue for approximately four years to be followed by a cooling phase of similar duration. The "as-built" DST and the pre-heating baseline measurements are in the report, "Drift Scale Test As-Built Report", document # BAB000000-01717-5700-00003 REV 01 of July 1998. Test results until May 31, 1998 are presented and discussed in the report, "Drift Scale Test Progress Report #1", document # BAB000000-01717-5700-00004 REV 01 of November 1998.

4.1 POWER AND TEMPERATURE DATA

Heater power and temperature data from the start of measurements to September 30, 1998 are presented and discussed in this Section.

Power Data

Figure 4.1-1 illustrates the total power being supplied to all of the wing heaters and all of the canister heaters.. These total power data are Q measurements. The power being supplied to individual canister heaters and to individual wing heater elements are illustrated in Figures 4.1-2 and 4.1-3, respectively. These individual heater element power data are not Q measurements.

The wing heater power was fairly constant up until about day 185 (6/6/1998), when it dropped a few percent. This was a result of the loss of power to the inner and outer elements of wing heater 29. On day 211 (7/3/1998) the outer element of wing heater 26 failed. The power distribution to individual wing heater elements on day 301 (9/30/1998) is illustrated in Figure 4.1-4.

The canister heater power decreased from about 53 kW at the beginning of the test to about 51 kw on day 244 (8/4/1998), a drop of about 2%. From day 244 to 270 (8/30/1998) the power increased to about 53.5 kW. This increase is likely due to changes in the ventilation system just outside the Heated Drift, which were implemented on 8/4/1998. These changes resulted in increased airflow near the cables supplying power to the canister heaters. This increased airflow likely cooled the cables, thereby decreasing the cable resistance. Decreased resistance increased the current flow in the heater circuit, thereby increasing the power to the heaters.

Thermal Data from the Heated Drift

Figures 4.1-5, 4.1-6 and 4.1-7 illustrate the temperatures on the canister heaters, in the air in the Heated Drift and on the walls of the Heated Drift, respectively. By day 301 (9/30/1998) the canisters had reached temperatures of about 150 °C while the air and wall surface temperatures were about 135 °C. For each of these three data sets, the temperatures started out at about 30 °C just prior to the start of the test. When the heaters were activated, the temperatures rose very rapidly at first, but then the rate of increase of temperature decreased with time up until about day 130 (4/12/1998). From day 130 to day 239 (7/30/1998) the temperatures increased nearly linearly. The reason the rate of temperature increase stabilized is likely due to the presence of the wing heaters; without them, the rate of temperature increase would likely have continued to decrease. On day 239, there was a drop in the canister, air and surface temperatures of about 5 °C. This was a result of cool, ambient air being forced into the Heated Drift through a hole in the bulkhead. This condition persisted for about 5 days. When the hole was closed, the temperatures started to increase again. It is interesting to note that after the hole was sealed the rate of temperature increase, while still nearly constant, appears to be slightly less than the rate of temperature increase prior to the incident with the hole. The reason for this is not known. The air and surface temperatures in the Heated Drift indicate that by day 301 (9/30/1998), the middle part of the drift was about 5 or 6 °C warmer than the ends (Figures 4.1-8 and 4.1-9).

Figure 4.1-10 illustrates the air pressure and humidity measured inside the Heated Drift. These measurements are correlated. When the air pressure increases, relatively dry air from outside the Heated Drift if forced into the drift decreasing the humidity. During the time that outside air was being forced into the drift through the hole in the bulkhead there was a pronounced decrease in humidity in the Heated Drift, but no appreciable change in air pressure,.

Figure 4.1-11 illustrates the temperatures recorded by the temperature sensors mounted on the hot side of the thermal bulkhead. The pronounced changes in the temperature distribution on the bulkhead which occurred on day 239 were caused by changes in the thermal insulation on the outside of the bulkhead and in the ventilation system just outside the drift.

Rock Temperature

Figure 4.1-12 illustrates temperature contours on a vertical plane that is perpendicular to the axis of the drift and which intersects the drift at approximately its midpoint (Y = 23 m). The dots indicate the locations of the temperature sensors grouted into eight boreholes radiating out from the drift at this location. The contours in Figure 4.1-12 honor the data measured at these locations after 301 days of heating (9/30/1998). The warmest temperatures are measured near the wing heaters and surrounding the top of the Heated Drift. The region immediately below the drift is slightly cooler than the top of the drift because of the insulating effect of the concrete invert in the drift. Analysis of the contours in Figure 4.1-12 indicates that an area of approximately 160 m^2 is warmer than the boiling point of water (97°C). If it is assumed that the temperature distribution is identical all along the length of the 47.5 meter long drift, then approximately 7600 m^3 of rock has been heated to temperatures exceeding the boiling point. This estimate is likely slightly high since the cross sectional area above boiling likely decreases as the ends of the drift are approached. This tendency to overestimate the volume of rock above boiling is balanced somewhat however by ignoring regions of rock beyond the ends of the drift which are above boiling.

Figure 4.1-13 shows the temperatures observed after 301 days of heating (9/30/1998) in the four horizontal boreholes emanating from the Heated Drift. The data indicate that the rock adjacent to the wing heaters is warmer than the rock near the Heated Drift. This is because of the higher power output of the wing heaters as compared to the canister heaters in the drift. The temperatures near the wing heaters show two pronounced "humps", which correspond to the locations of the two wing heater elements deployed in each borehole. The data from the left side of the drift at Y=23 meters do not exhibit a noticeable "hump" associated with the outer wing heater since this hole is located midway between wing heaters 6 and 7 and the outer heating element of wing heater 7 is operating at only about 75% power. Three of the four temperature profiles exhibit a slight shoulder about 14 meters from the drift at a temperature corresponding to the boiling point of water. These are manifestations of a region of rock where water in the pores of the rock is boiling.

Figure 4.1-14 illustrates the temperature recorded by the temperature gage located at approximately X= -11 meters in borehole 160 (Y = 23 meters). The rock near this gage reached a temperature of about 96 °C 70 days after the start of the test. It remained near that temperature for more than 20 days, during which time the heat entering the rock near this location was devoted almost entirely to vaporizing water instead of to raising the temperature of the rock. After 20 days, all the water in the rock near this location had vaporized and the temperature started to increase again. By day 301 (9/30/1998) the rock near this gage had reached a temperature of 167 °C.

Figure 4.1-15 illustrates the temperatures measured by the gages in borehole 79 every 10 days since heater activation. This hole is oriented parallel to the axis of the Heated Drift at X = +9.5 meters. Near the bulkhead, it is located about 4 meters above the plane of the wing heaters but dips downward such that it is closer to the wing heaters at the bottom of the hole. The general warming with depth in the hole is due to the increasing proximity to the wing heaters with depth. What is noteworthy in this hole is that portions of the hole seem to develop positive temperature anomalies with respect to the rest of the hole. The most notable is located at around Y = 13 meters, where the temperatures begin to warm, as compared to rocks shallower and deeper in the hole, after about 130 days of heating. Less pronounced anomalies exist at Y = 24, 31 and 36 meters. These anomolously warm regions may be located near fractures where warm fluids are flowing upwards, away from the plane of the wing heaters located below the borehole. Also note how the rate of temperature increase slows dramatically as the boiling temperature is approached.

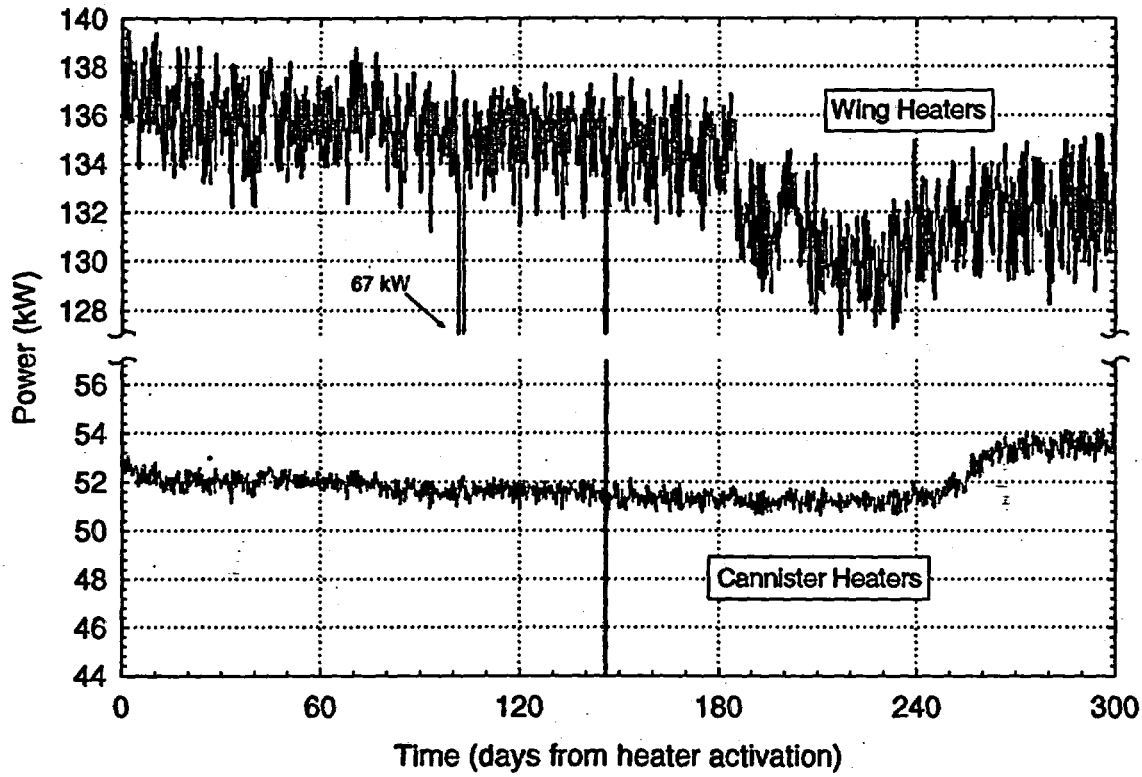

Figure 4.1-1 Heater Power – Qualified Measurements

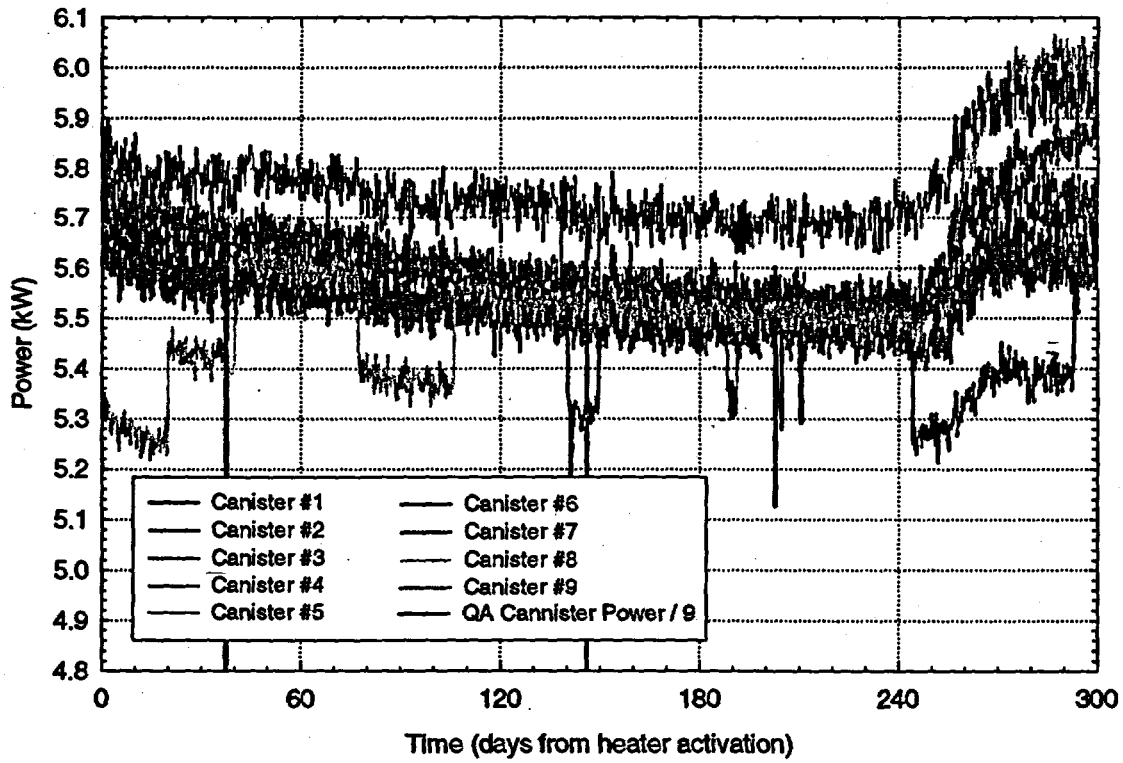

Figure 4.1-2 Canister Heater Power – Unqualified Measurements

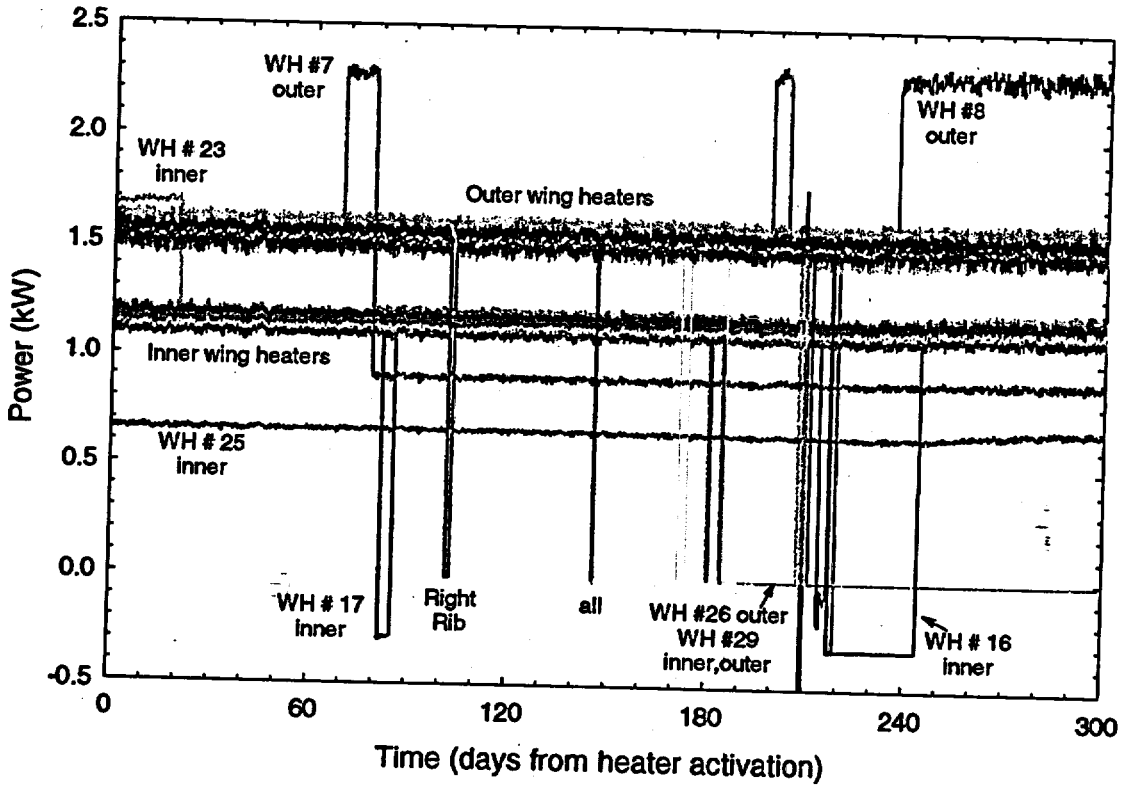

Figure 4.1-3 Wing Heater Power – Unqualified Measurements

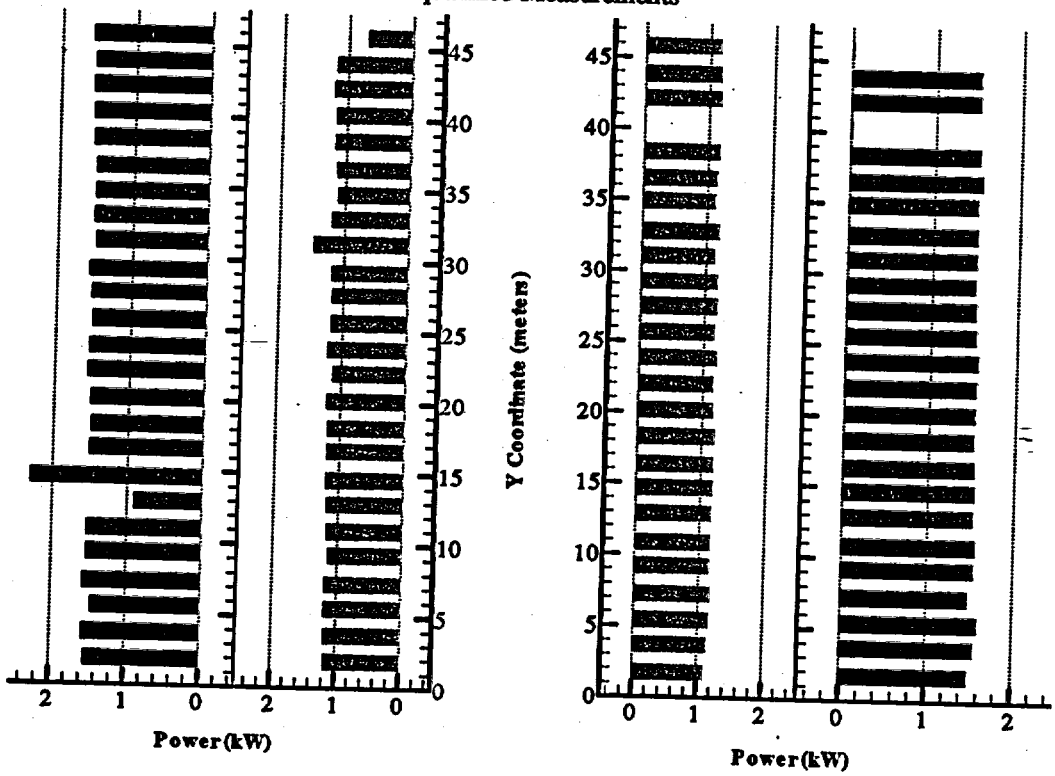

Figure 4.1-4 Wing Heater Power After 300 Days of Heating (9/30/1998).

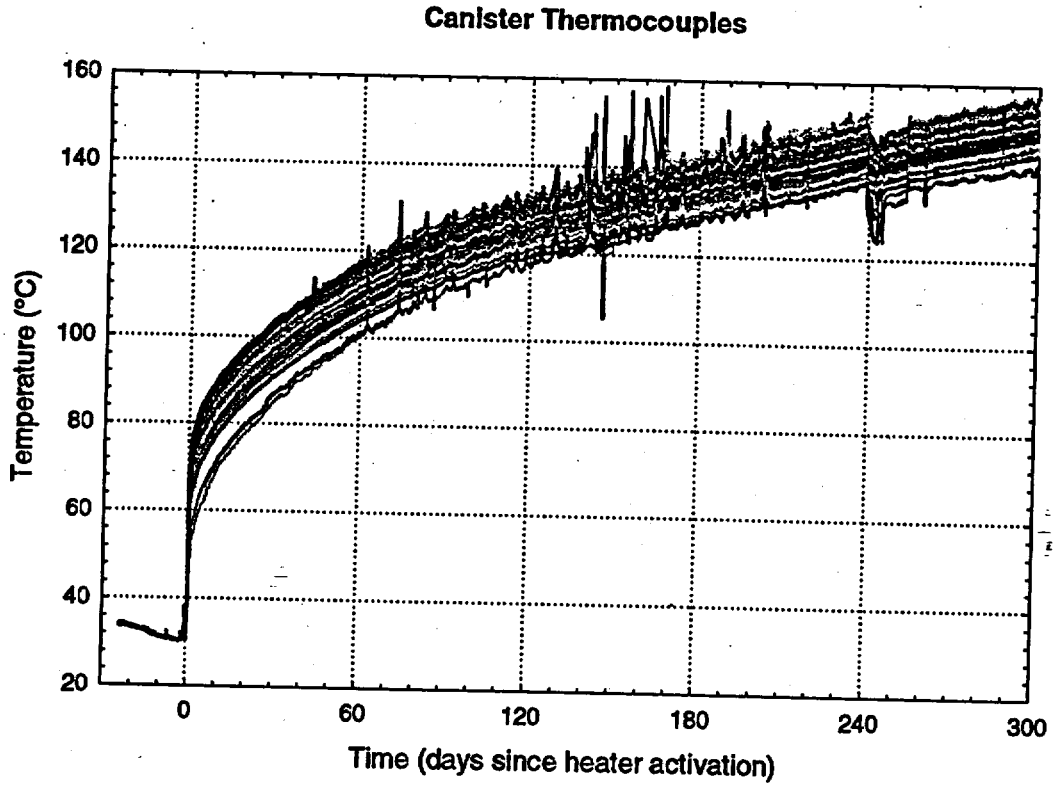

Figure 4.1-5 Canister Thermocouples

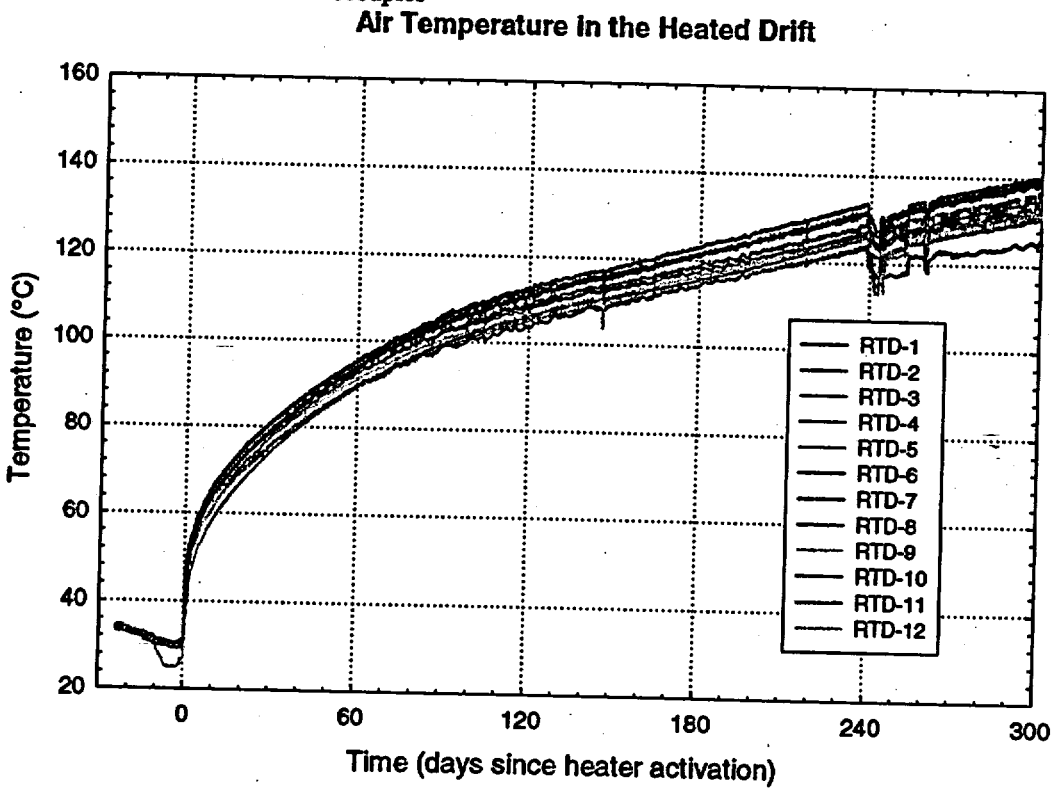

Figure 4.1-6 Air Temperature in the Heated Drift

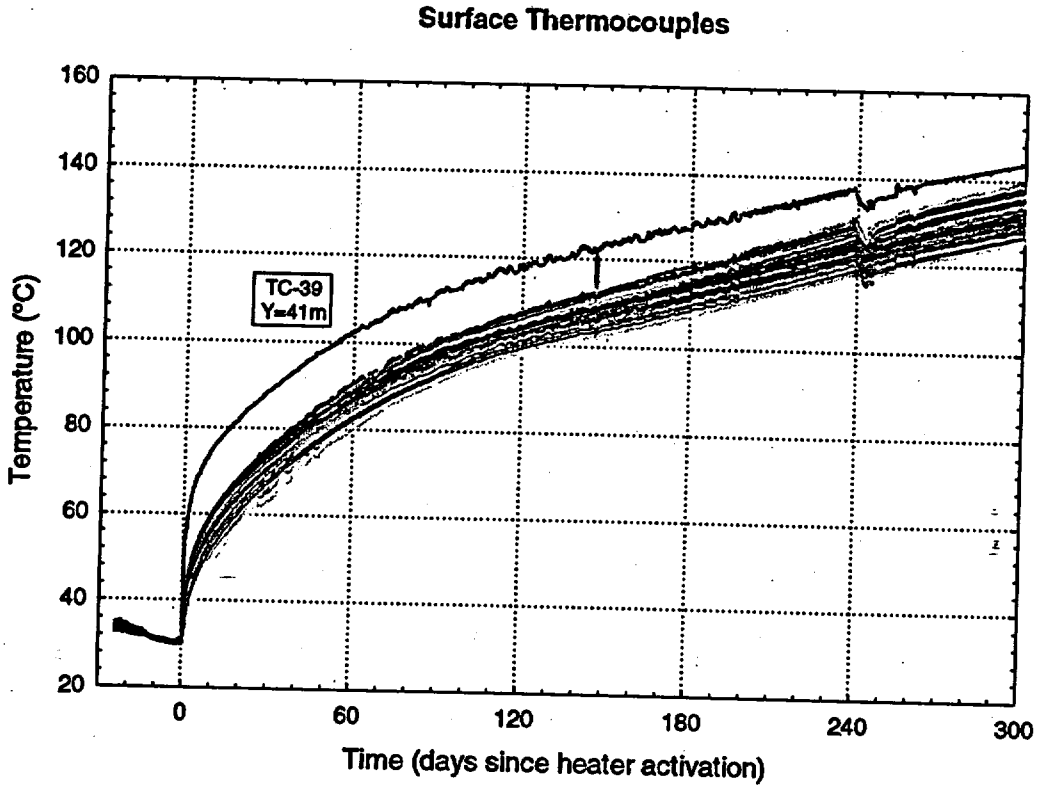

Figure 4.1-7 Surface Thermocouples

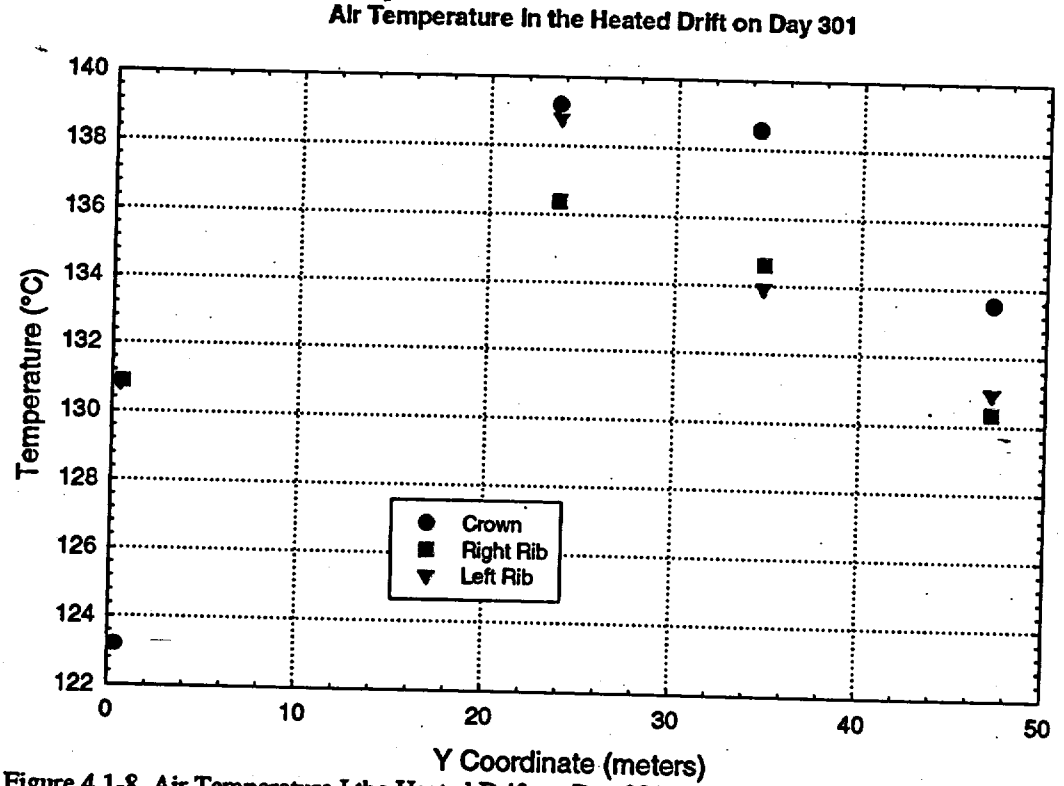

Figure 4.1-8 Air Temperature I the Heated Drift on Day 301

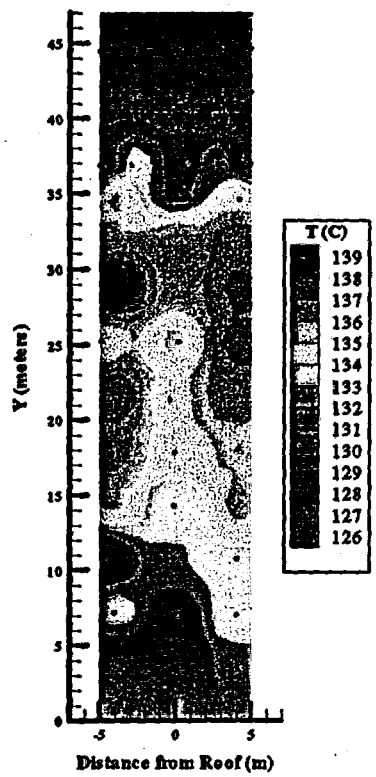

Figure 4.1-9 Temperature distribution on Wall of Heated Drift

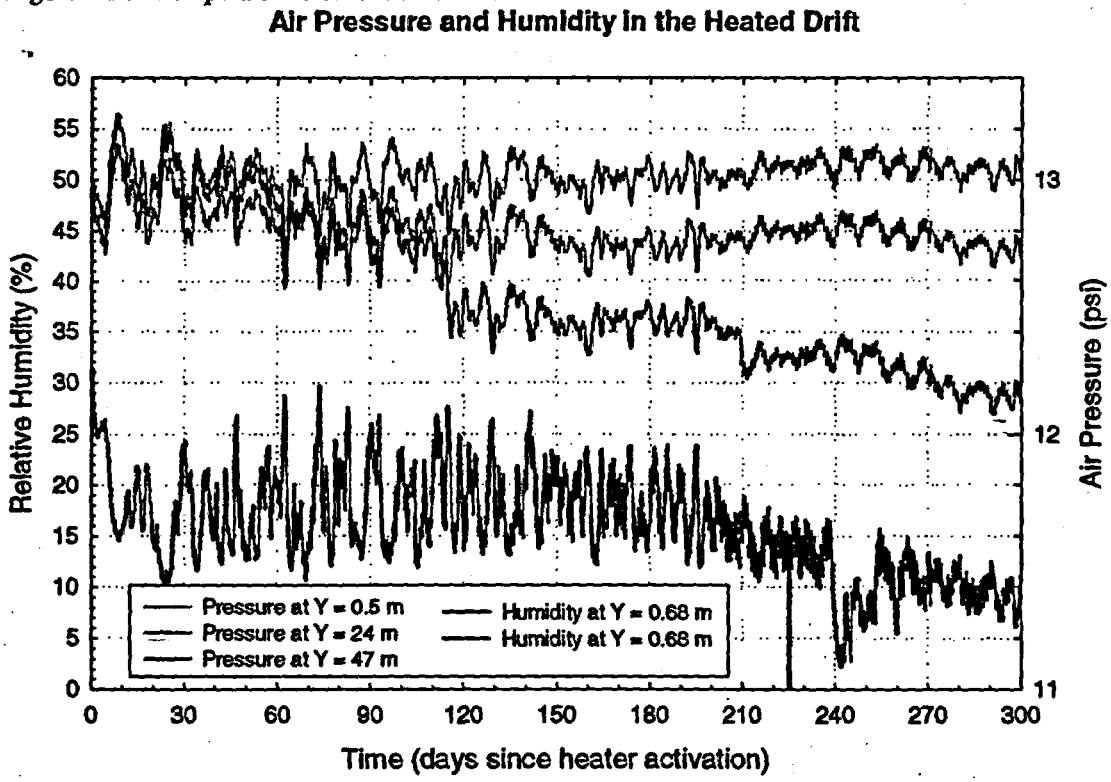

Figure 4.1-10 Air Pressure and Humidity in the Heated Drift

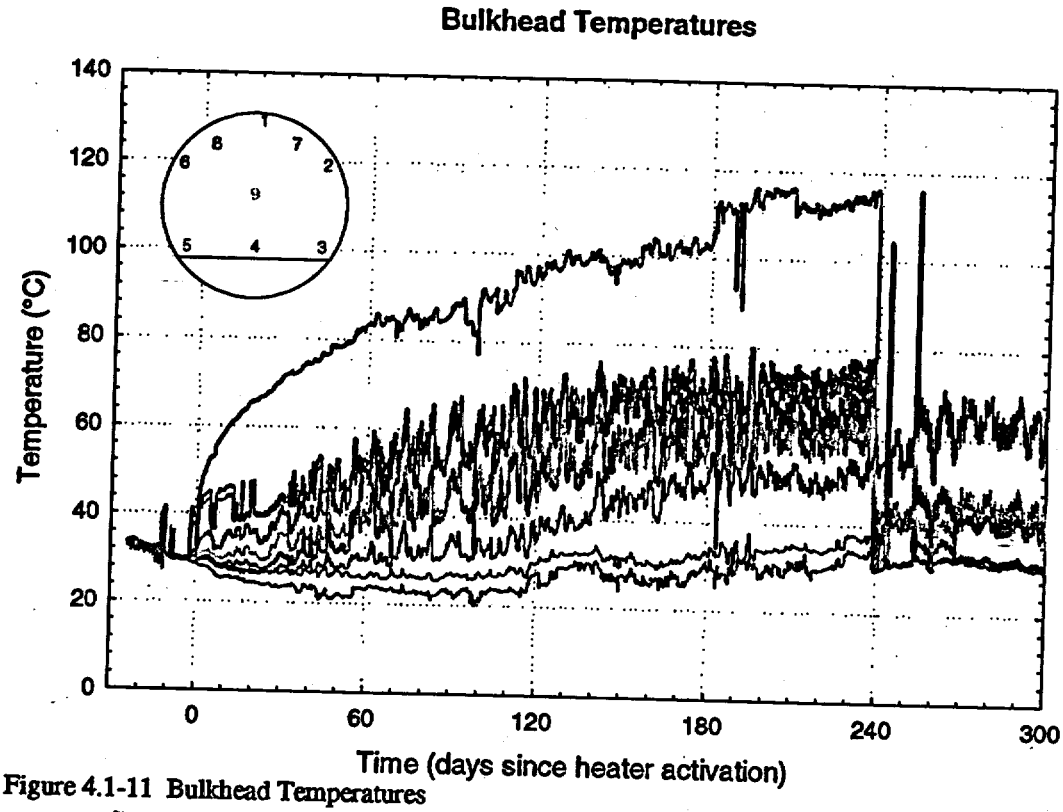

Figure 4.1-11 Bulkhead Temperatures

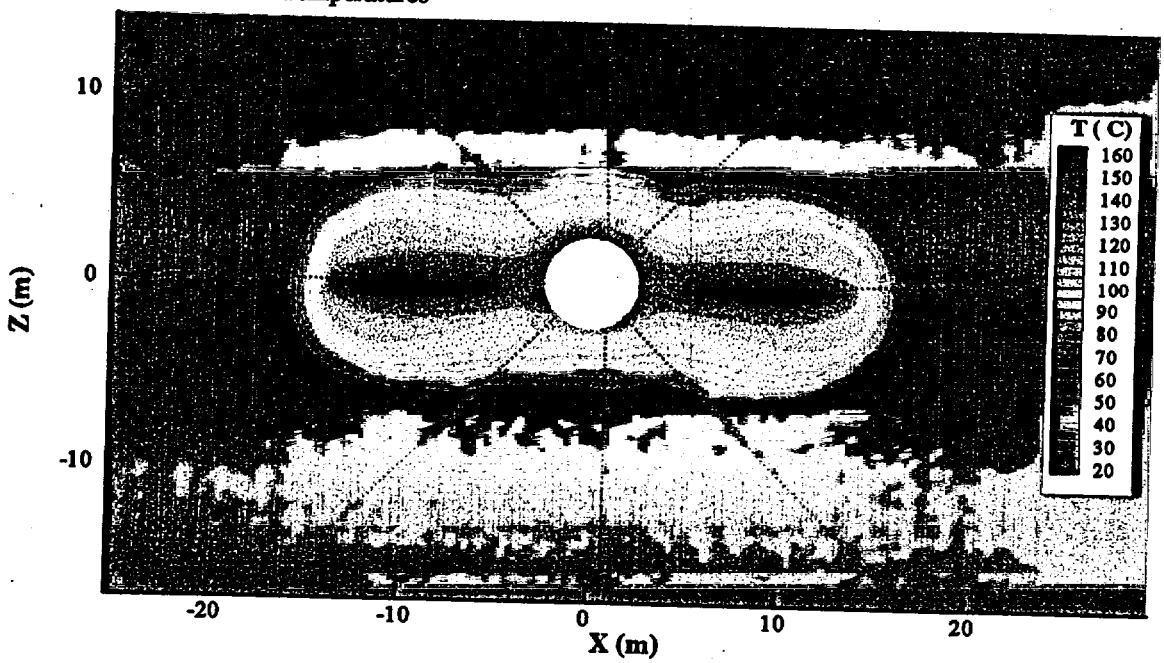

Figure 4.1-12 Temperature contours on the Vertical Plane at Y= 23 m After 301 Days of Heating

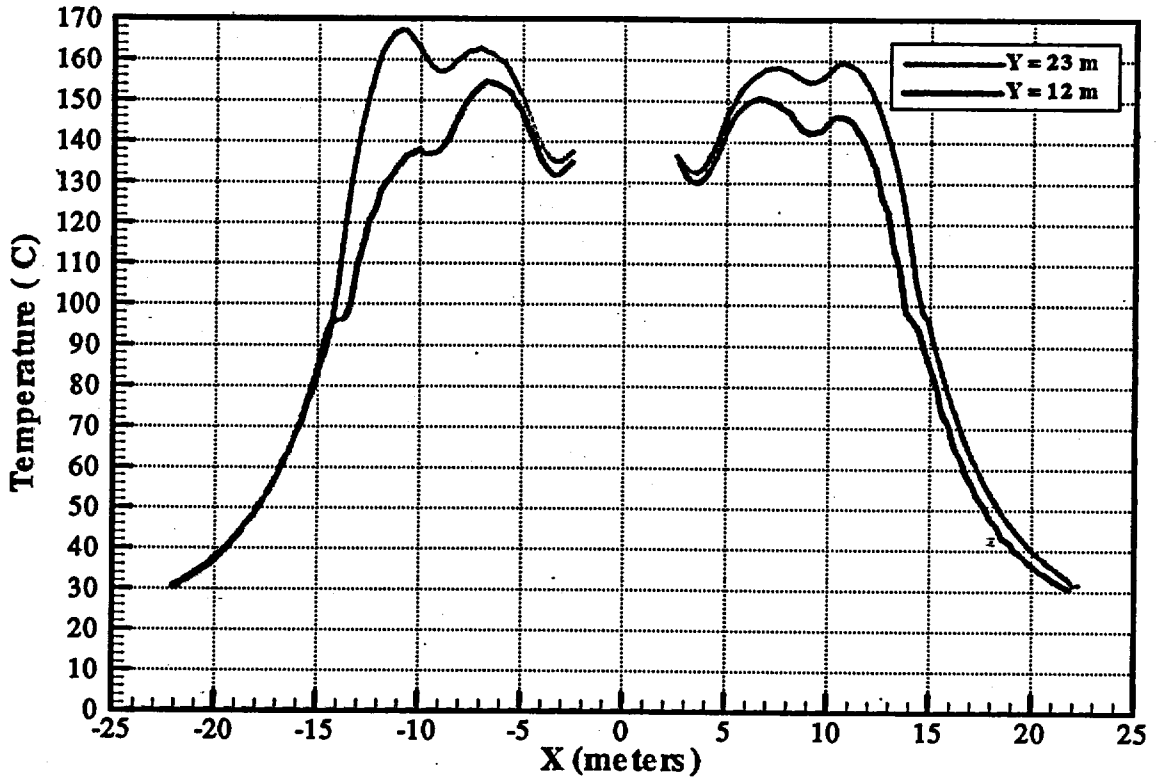

Figure 4.1-13 Temperatures in horizontal RTD Holes After 300 Days of Heating

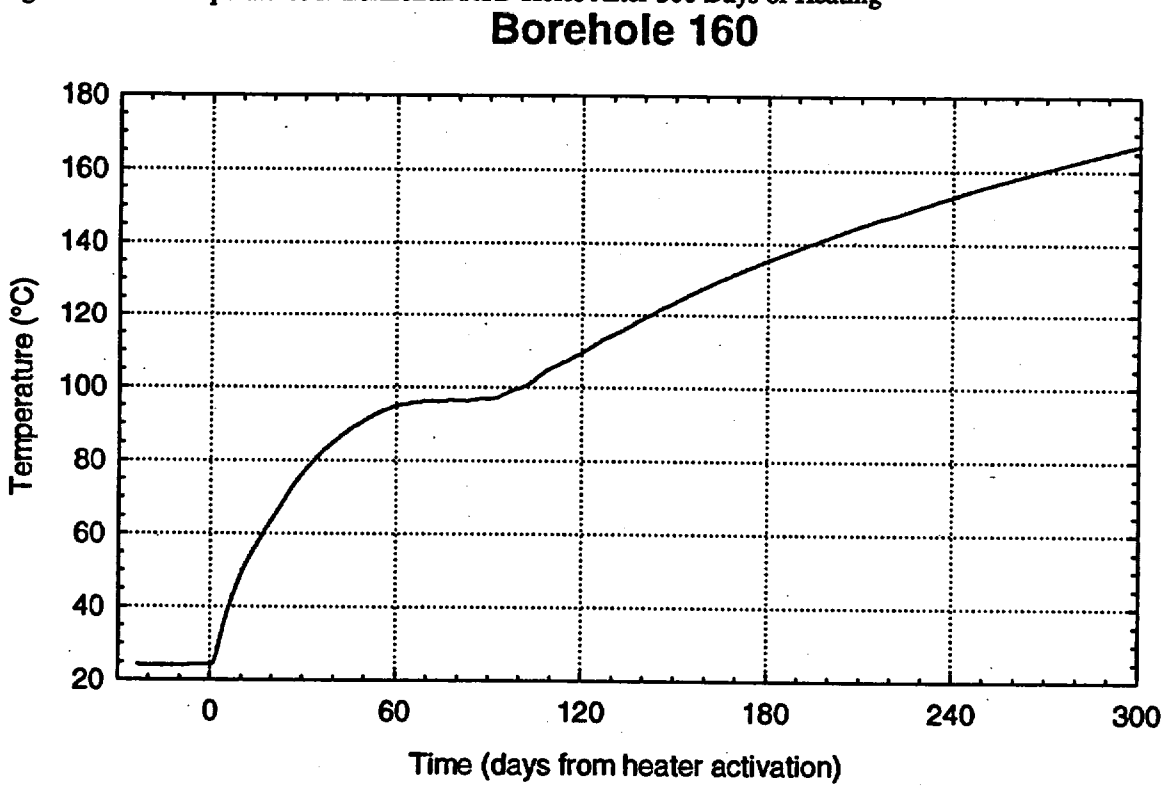

Figure 4.1-14 Borehole 160

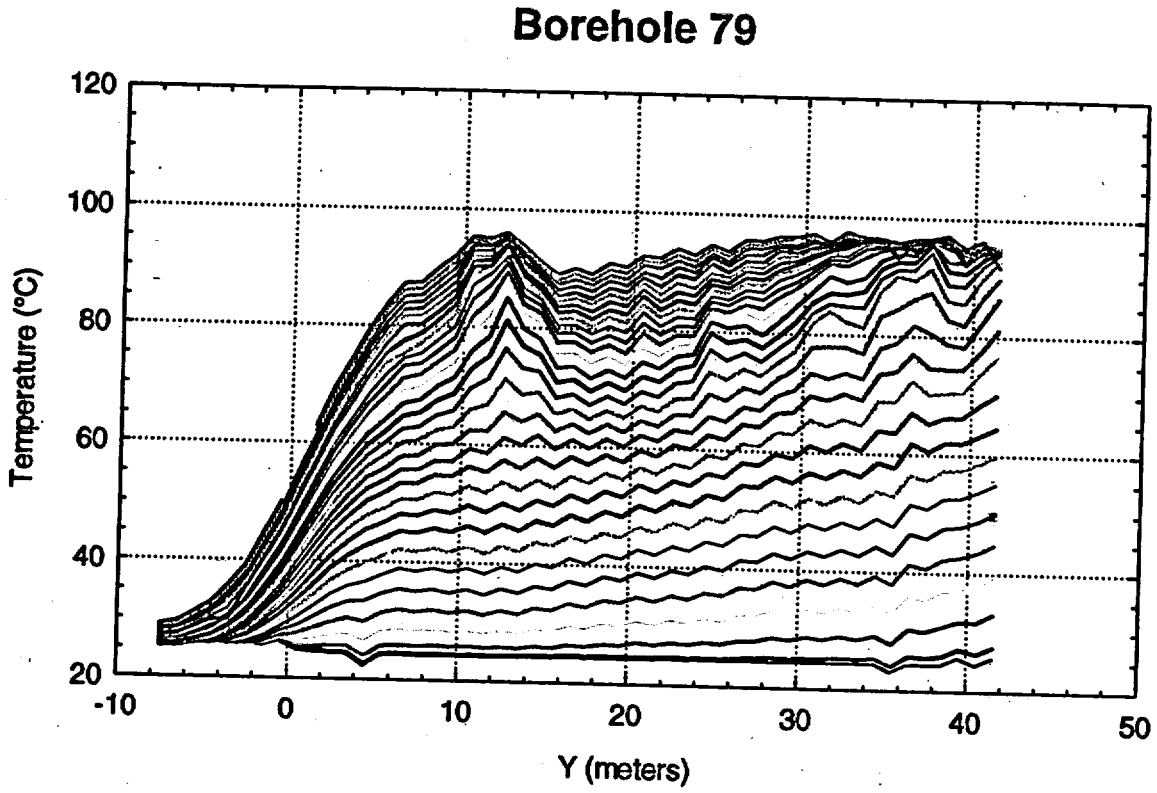

Figure 4.1-15 Borehole 79

4.2 Mechanical Measurements

One of the most significant events during the 3rd quarter time period was a change in the ventilation in the Thermal Test Alcove which caused a cooldown in the Heated Drift. According to the Test Coordination Office, on Thursday 7/30/1998 at approximately 1130 hours, the new Alcove #5 high power ventilation system was started. As per A/E Design Drawing BABFAA000-01717-2100-44110-00, the new system delivers approximately 20,000 cubic feet per minute (CFM) to a location about 10 feet from the Thermal Bulkhead. If conditions near the bulkhead exceed 98°F (37°C), a second duct delivers another 20,000 CFM until the temperature drops below this threshold. Sometime after the system was started on 7/30/1998, the insulation that plugs the hole in the bulkhead allowing the camera rail to pass through the bulkhead became dislodged. This provided an open conduit for a large quantity of ambient air to be forced into the Heated Drift. The Heated Drift experienced a cooldown as shown by the various temperature sensors in the drift. This hole was discovered the evening of Wednesday 8/5/1998 and re-sealed. Until the hole was sealed, the air temperature in the drift had dropped from around 272°F (133°C) on Thursday to around 259°F (126°C) on Wednesday.

Temperature changes resulting from the increased ventilation through the bulkhead were observed all the way to the deep end of the drift, where decreases of 2-5°C were observed on the surface thermocouples on the concrete liner.

Another problem with temperatures was found with the TCs along MPBX-1 (Borehole 81, the long borehole parallel to the drift axis on the north side of the drift). On June 19, all the temperatures in this borehole undergo a precipitous drop, with the TCs in the deep end of the borehole dropping as much as 10 °C. For about a month afterward, the temperatures apparently rise at a higher rate. Then on July 28, the temperatures drop again, to curves which seem to be what they would have been if they had risen according to the original rates.

The second drop in temperature near July 28th is most probably related to the high power ventilation system being turned on. The first drop around June 19th is more difficult to explain. The dates do not correspond to Plate Loading Test activities, so that may be eliminated as a cause. The TCO reports that no hardware or scan changes were made to the DST DCS during this month interval. The only potentially related event uncovered thus far is that the main ESF ventilation system was shut down at about 15:00 UTC (08:00 PDT) on June 20th for 48 hours for LBNL to conduct seismic testing/monitoring in the ESF. The Alcove 5 old ventilation system continued to operate as normal.

Mechanical Data

The behavior exhibited thus far by the MPBXs continues to be similar to the elastic model predictions, with the exception of MPBX-14, which demonstrates separation between the invert and liner. The deepest anchor (Anchor #4) for the MPBXs is progressing toward having the largest displacement from the collar. Most of the MPBX sensors are working well; however, MPBX-5, -7, and –11 have gone totally bad, and MPBX-3, -6, and -14 have gotten progressively noisier during the 3rd quarter.

Due to a problem with the revision of the scan software done on August 4th, the CDEX-1 and CDEX-2 data were not read properly by the DCS for the interval from 8/4/1998 until 9/25/1998. The raw data and Q Engineering readings do not exist for these sensors during this interval. After 9/25/1998 the readings are done the normal manner.

The strain gages placed on the concrete liner and on unconstrained concrete samples in the Heated Drift continue to show the combined effects of thermal expansion, dehydration-induced shrinkage, and mechanical stress imposed by the interaction of the concrete with the heated rock surrounding the drift. The results from the strain gages on the unconstrained samples exhibit behavior indicative of drying shrinkage due to dehydration, a phenomenon seen elsewhere in engineering literature. The cirumferential

strain gages on the liner consistently show that the crown of the liner is in compression while the rest of the liner experiences smaller magnitudes of compression and tension.

The strain gage and liner surface temperature gage data experienced precipitous drops starting on July 30 and lasting 3-4 days due to the new high power ventilation system in Alcove 5. The temperatures dropped 2-5°C, and the strains dropped by 20-100 microstrains, as high as 15% of their values before the drop. These values recovered after the bulkhead was re-sealed on August 5.

4.2.1 Rock Thermal Expansion

The coefficient of thermal expansion (CTE) of repository horizon rocks, especially the middle non-lithophysal sub-unit (Tptpmn) of TSw2, have been measured extensively in the laboratory using small hand samples which can be taken to be intact rock. In earlier years, these tests were done on samples obtained by surface-based drilling. Recently, laboratory testing for thermal expansion has been carried out on samples from the SHT and DST test blocks as well as the thermal test alcove in general. Measurements have been made on both pre-heating and post-heating samples for the SHT and only pre-heating samples for the DST. The results of lab measurements of CTE associated with the SHT and DST are shown in Figure 4.2-1. In this figure, CTE in $10^{-6}/^{0}C$ is plotted against temperature. As the plots show, below $200^{0}C$ lab measured CTE of Tptpmn is approximately 10×10^{-6}. Above $200^{0}C$ however, CTE dramatically increases, by as much as a factor of 5 or 6 at $300^{0}C$. This sharp increase in lab measured CTE above 2000C is thought to be due to volume changes associated with phase changes of silica polymorphs above approximately $230^{0}C$.

It is recognized that in a fractured rock formation, the CTE of the rock mass would be less than that of the intact rock as measured in the laboratory. The extent of the decrease is thought to depend on the scale at which measurements are made as well as the temperature level. Measurements of the displacements in the rock during the heating in the SHT and the DST provide an opportunity to derive values for rock mass CTE at various gage lengths (scales) and levels of temperatures. Values of the CTE of Tptpmn thus derived are presented in Table 4.2-1 along with relevant lab measured value. The data in Table 4.2-1 show that rock mass thermal expansion as measured by the SHT and DST are substantially lower than the lab measured CTE of intact rock.

Rock mass CTE values from Table 4.2-1 are plotted in Figure 4.2-2 to show the relationship between CTE and temperature in Figure 4.2-2a and that between CTE and gage length in Figure 4.2-2b. Figure 4.2-2 clearly shows that CTE increases, as expected, with the increase in temperature. The database for gage length is not adequate. Nonetheless, the expected trend of decreasing CTE with increasing gage length is there.

Table 4.2-1. Comparison of Rock Mass Matrix Thermal Expansion

Test Name	Gage Length (m)	Average Temp./ Temp. Range (°C)	Coefficient of Thermal Expansion (10^{-6}/°C)
Single Heater Test	2.84	160	5.88
Single Heater Test	4.14	70	4.14
Single Heater Test	2.36	116	3.4
Drift Scale Test	7	25-50	1.65
Drift Scale Test	7	50-75	2.51
Drift Scale Test	7	75-100	3.25
Laboratory	0.1	25-200	~10

Figure 4.2-1. Increase in Thermal Expansion Above 200°C. Due to silica Phase Change

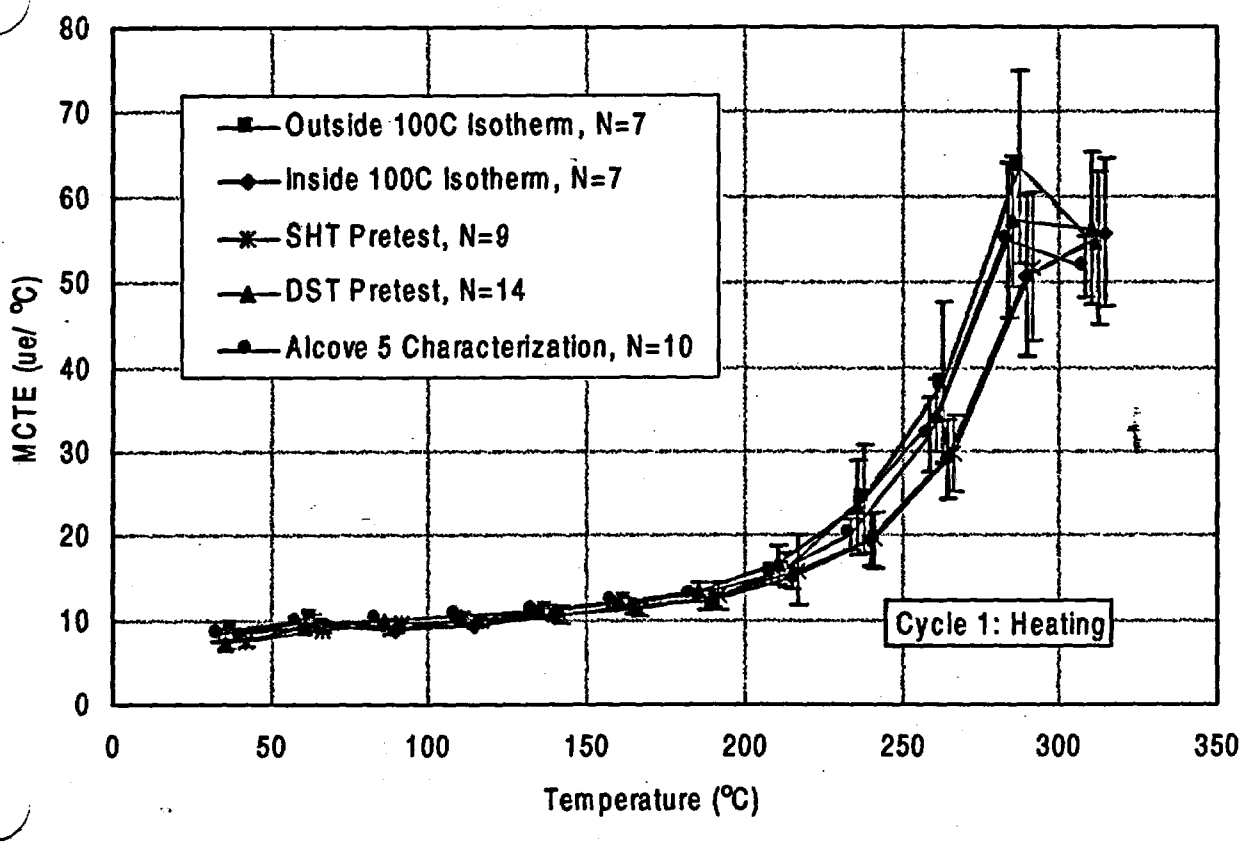

Figure 4.2-2. Relationship of Thermal Expansion vs. Temperature (a) and Gage Length (b)

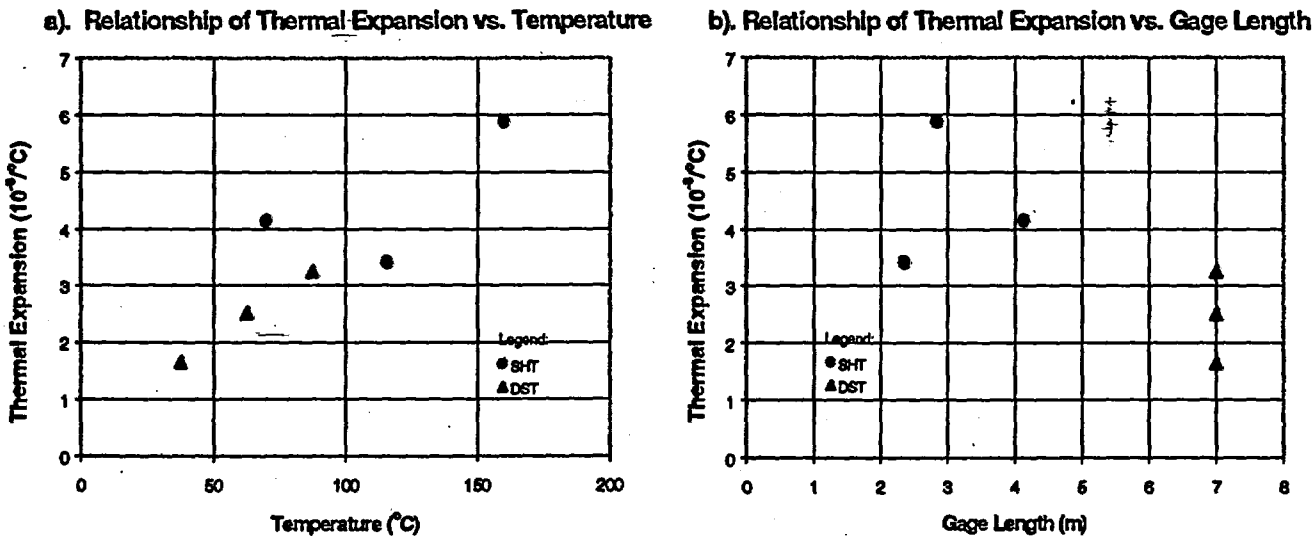

4.3 Air-K and Gas Tracer Tests

Input to progress report on ESF thermal test, November, 1998
from Yvonne Tsang on
Hydrological measurements in the Drift Scale Test

The most prominent thermal-hydrological processes anticipated in the Drift Scale Test (DST) is the redistribution of moisture by vapor transport and subsequent condensation. Air injection tests in 4 consecutive zones in each of the twelve hydrology holes, carried out at approximately three month intervals, are intended to monitor the changes in liquid saturation in the fractures due to vaporization and condensation. In particular, results of the air injection tests are used to locate those zones where liquid saturation in the fracture has increased, thus giving rise to a reduction in the local permeability value. In Figures 4.3-1 and 4.3-2 are shown the air permeability of respective zones in the hydrology boreholes, measured at different stages of the test up to 9 months of heating. The permeability is plotted as a ratio with respect to their respective pre-heat November 1997 values. Only those measurements which indicate more than a reduction of 10% (precision of air injection measurements) are shown in Figures 4.3-1 for zones in boreholes 57 through 61, and in Figure 4.3-2 for zones in boreholes 74 through 78. Borehole sections where decrease in permeability were measured at different stages of heating as displayed in Figures 4.3-1 and 4.3-2 are consistent with those condensation zones predicted from the numerical model (Birkholzer and Tsang, 1998). The simulated fracture liquid saturation at 3, 6, and 9 months of heating are shown in Figures 4.3-3 and 4.3-4, in the xz cross sections containing the fan of boreholes 57 through 61, and the fan of boreholes 74 through 78 respectively. Denotation for borehole sections by borehole number follow by the zone number in Figures 4.3-1 and 4.3-2 are such that zone 1 refers to the borehole section closest to the borehole collar, and zone 4 refers to the borehole section between the fourth packer and the bottom of the borehole. In Figures 4.3-3 and 4.3-4 the locations of the packers in the boreholes are denoted by the white circles. In most boreholes the first packer closest to the collar is off-scale, the exception is borehole 58, where only 3 packers were installed and therefore 58-3 refers to the borehole section between the third packer and the bottom of the borehole. Furthermore, in borehole 77, of the three packers installed, the third packer has been damaged and deflated since March 1998, leaving essentially only one zone, 77-1 for which air permeability measurements are meaningful. Simulated results in Figure 4.3-4 show that saturation build-up in the fractures occur in zones 60-2 and 61-2 as early as 3 months after initiation of heating. As heating progress to 6 and 9 months, condensation also extends to 60-3, 60-4, 61-3, and eventually to those boreholes above the heated drift, 59-2, 59-3, 59-4, as well as in 58-1 and 58-2. Air permeability data in Figure 4.3-1 indicate that the only borehole sections which show decrease in permeability are 60-2, 3, 4; 61-2, 59-2, 3 and 58-2. The measured permeability in 58-2 and 60-4 show an initial large decrease, then subsequent rise (though not reaching their pre-heat values) as the heater test progresses. This behavior is not anticipated in the simulated results based on a homogeneous description of the fracture continuum. It can be caused by gravity drainage through fractures after an initial build up of condensation; drainage can be expected to be spatially heterogeneous, since fracture can have different orientations, and are of different length scales. Data in Figure 4.3-2 show that zones of decreased air permeability occurred in boreholes 78 and 76 for the first 9 months of heating, which is again consistent with the predicted fracture liquid saturation at 3, 6, and 9 months of heating shown in Figure 4.3-4.

Though air-injection tests in the hydrology holes were intended mainly to locate zones of increased fracture liquid saturation from condensation, post-test characterization of the Single Heater Test have indicated an overall increase in air permeability in the test block which may be attributed to microfracturing. For this reason, the air permeability data in the Drift Scale Test were also studied to unveil any thermal-mechanical coupled effects. We screened our data to investigate only those upward inclining boreholes that are farthest from the heaters, i.e. boreholes 57 and 74, where condensation was not yet anticipated at 9 months of heating. The measurements do show an increase in permeability during tests for zones 57-3, 57-4 and 74-4. These and air-injection data yet to be collected as the heating phase progress will be studied closely in order to sort out the thermal-hydrological and thermal-mechanical coupled processes.

Gas tracer tests in boreholes 74, 75 and 76 have indicated an effective fracture porosity on the order of 0.01. This values is orders of magnitude higher than what is deduced from a parallel plate conceptualization of fractures together with the ESF fracture mapping data. It was suggested that the large value of fracture

porosity perhaps arises from the connected pore space of the lithophysal cavities that seem pervasive in the DST according to the borehole videos. During this quarter gas tracer tests have been carried out in Niche 3107 in the ESF. Niche 3107, though in the same middle non-lithophysal welded tuff unit as the DST, is rather intact. While in the DST area the tracer tests were carried out in borehole sections of 8 to 9 meters, in Niche 3 the corresponding length of the borehole section was less than 1 m. The estimated fracture porosity from gas tracer tests in Niche 3 is 0.012-0.02, again on the order of 0.01 as was measured for the DST. The rather consistent fracture porosity of 0.01 at different locations, on different length scales, and for welded tuff of apparently different fracture characteristics, indicate that fractures in the Topopah Spring welded tuff in fact occupy a pore space on the order of 1%, which is considerably larger than previously estimated from fracture mapping data, thus implying that transport in the fractures of the proposed repository middle nonlithophysal unit would be one or two orders of magnitude slower than transport estimated using previously calculated fracture porosity.

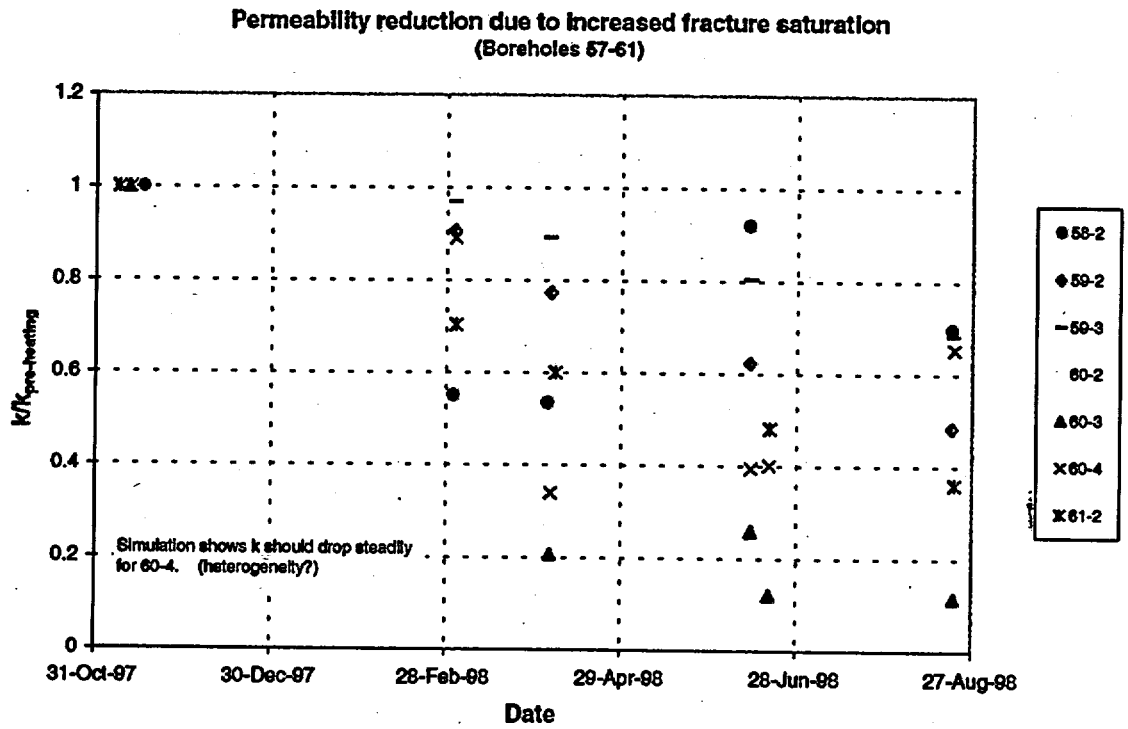

Figure 4.3-1 Decrease in measured air permeability (normalized to respective pre-heat values) due to increase liquid saturation for zones in boreholes 57 through 61.

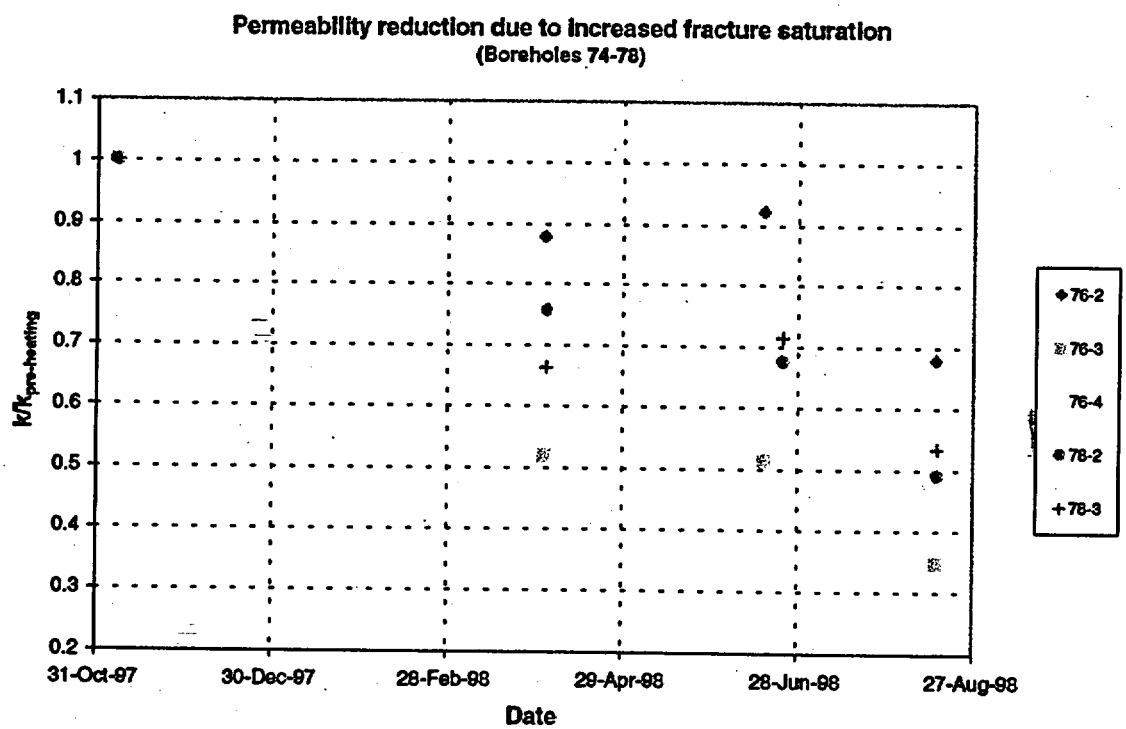

Figure 4.3-2 Decrease in measured air permeability (normalized to respective pre-heat values) due to increase liquid saturation for zones in boreholes 74 through 78. (DTN:LB981016123142.002)

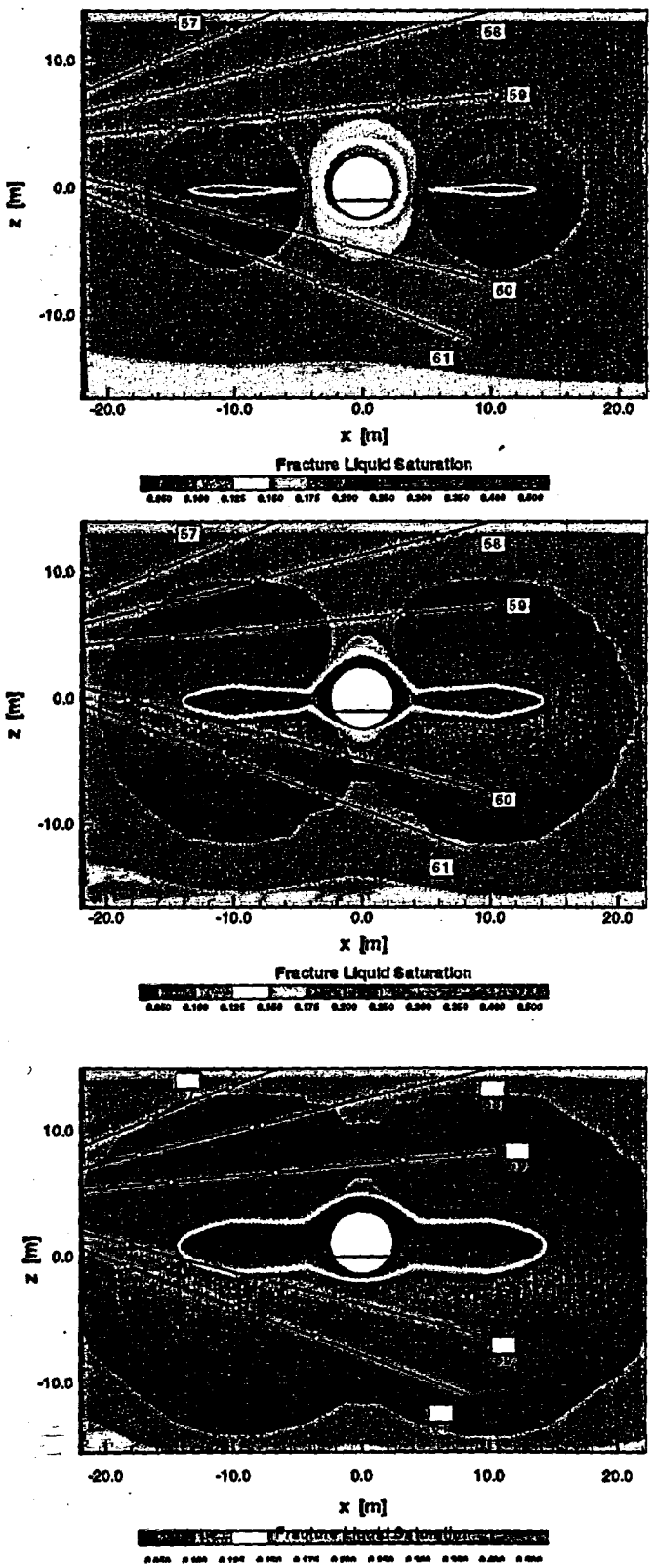

Figure 4.3-3 . Simulated fracture liquid saturation at 3 (top), 6, and 9 (bottom) months after heating in boreholes 57 through 61.

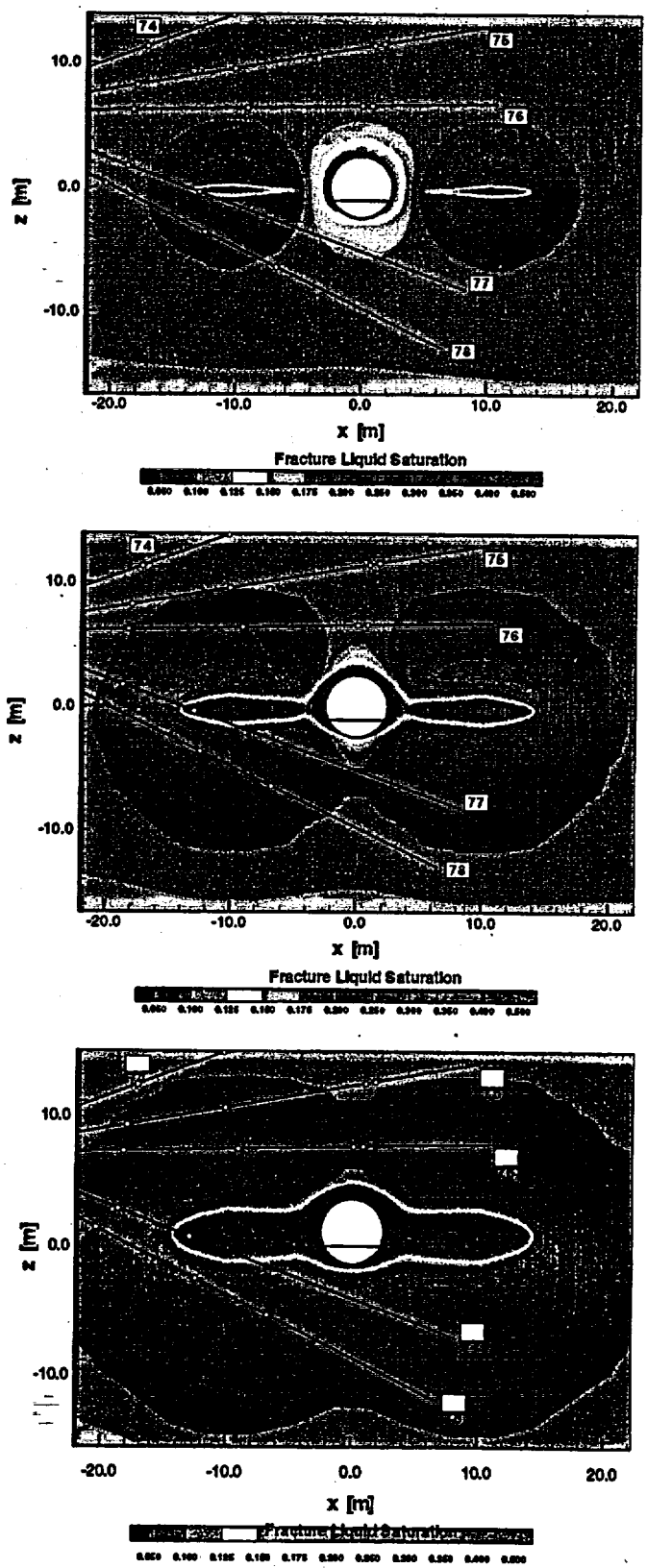

Figure 4.3-4 Simulated fracture liquid saturation at 3 (top), 6, and 9 (bottom) months of heating for boreholes 74 through 78

4.4 ERT MEASUREMENTS

Electrical Resistivity Monitoring of the Drift Scale Test: June-August, 1998
A. Ramirez, W. Daily

Introduction:

This letter report describes electrical resistance tomography (ERT) surveys made at the Drift Scale Test (DST), during the June to August, 1998 time period. ERT is one of the several thermal, mechanical, and hydrologic measurements being used to monitor the rock-mass response during the DST. The purpose of this work is to map the changes in moisture content caused by the heating of the rock mass water, with a special interest in the movement of condensate out of the system..

The purpose of this letter report is to provide a brief synopsis of the progress made during the time period of interest. A comprehensive discussion of the process followed to produce the results shown here, equipment used, and assumptions made can be found in Wagner, 1998, pages 7-13 to 7-21.

Changes in Electrical Resistivity:

Tomographs of resistivity change corresponding to the time period between June 3, 1998, and August 18, 1998, are shown in Figures 4.4-1, 4.4-2, and 4.4-3. The top part of each of these figures shows the tomographs collected along a cross-section parallel to the Heated Drift (HD). The lower left portion of the figures shows tomographs corresponding to a vertical plane intersecting the HD at right angles, and about 5 meters in from the bulkhead; we will refer to this plane as AOD 1. The lower right portion of the figures corresponds to a second vertical plane intersecting the HD at right angles, about 24 meters in from the bulkhead; we will refer to this plane as AOD 5.

The upper part of Figure 4.4-1 shows the changes in resistivity along the HD, calculated after 182 days of heating. Note that most of the tomographs are yellow-green in color, thereby indicating resistivity ratios near 1.0 (no change relative to the pre-heat case). Near the walls of the HD, the tomographs show resistivity ratios less than 1.0, thereby indicating that the resistivity has decreased relative to the pre-heating condition. After 224 days of heating(upper portion of Figure 4.4-2), most of the rock still shows a ratio of 1.0, but the rock near the crown and invert of the HD shows stronger resistivity decreases (ratios farther removed from 1.0). These decreases become stronger as heating time increases (upper portion of Figure 4.4-3). The tomographs also indicate that the resistivity changes above the HD are stronger than those below the HD. We believe that these resistivity changes are due primarily to increases in temperature that have developed close to the walls of the HD.

The lower left portions of Figures 4.4-1, 4.4-2 and 4.4-3, shows the tomographs corresponding to AOD 1. Although the mesh consists of a large region around the electrode arrays, only the region inside the ERT electrode array is shown in the figure because the region outside the array is poorly constrained by the data. The region inside the HD is also masked because the technique does not measure rock properties in the excavated region. The tomograph sequence shows a region of resistivity decrease near the walls of the HD. The resistivity decreases become stronger with time and they extend farther into the rock above the HD. Surprisingly, the region corresponding to the wing heaters location (nine o'clock position relative to the HD) shows relatively weak resistivity decreases.

The lower right portions of Figures 4.4-1, 4.4-2 and 4.4-3, depicts resistivity-change tomographs sampling the rock mass along AOD 5, which is a second vertical plane that intersects the HD at right angles near its middle. The images show both increases (ratios greater than 1.0) and decreases near the location of the wing heaters. Resistivity decreases are also observed near the walls of the HD. We suggest that the resistivity changes observed through August, 1998, are caused by temperature increases as well as saturation decreases. The AOD 5 results in Figures 4.4-1, 4.4-2 and 4.4-3 make it clear that resistivity increases are observed in the rock closest to the wing heaters while resistivity decreases are observed

farther away. This behavior is caused by the competing effects that saturation decreases and temperature increases have on electrical resistivity . In rock where rock temperature has increased but relatively little drying has occurred, the resistivity will decrease because the temperature increase has enhanced the mobility of the ions in the pore water. As significant drying occurs and the saturation is higher than about 30%, the pore water paths through which electrical charge moves become smaller, thereby tending to increase the water resistivity. However, the net change in bulk resistivity is a decrease relative to baseline because the increases in ion mobility more than compensate for the volumetric reduction of the pore water pathways. As the temperature continues to increase and the saturation drops below 30%, the pore water paths through which electrical charge moves starts to become discontinuous. This makes the bulk resistivity increase exponentially even though the increases in ion mobility caused by temperature are still present. Thus, the net effect on the bulk resistivity is an increase above baseline (i.e., the ratio becomes greater than 1.0) in hot dry rock with saturations less that 30%.

There are both similarities and differences between the AOD 1 and AOD 5 planes. Both show resistivity decreases, near the walls of the HD, that extend deeper into the rock above the crown of the HD than below its invert. A significant difference between the AOD 1 and AOD 5 results is observed in the vicinity of the wing heaters were the AOD 1 tomographs show weaker decreases in resistivity near the bulkhead. Possible reasons for this difference can be found in Wagner, 1998.

Estimates of Saturation Change:

The resistivity changes shown in Figures 4.4-1, 4.4-2 and 4.4-3 are influenced by changes in moisture content, temperature, and ionic strength of the water. To estimate saturation, it is assumed that the dominant factors affecting resistivity changes are temperature and saturation. That is, an increase in temperature or water saturation causes a resistivity decrease. Near the heaters, there may be regions where the increasing temperature reduces the resistivity, while rock drying changes the resistivity in the opposite sense (increases the resistivity). Our goal in this section is to use the images of resistivity change near the HD, along with the measured temperature field and what is known of initial conditions in the rock mass, to estimate moisture change during heating. A detailed description of this approach can be found on a previous milestone report pertaining to the Single Heater Test (Ramirez and Daily, 1997).

To estimate moisture content changes, the effects of both rock temperatures and resistivity changes measured by ERT must be taken into account. Interpolation of temperature measurements made at discrete points was necessary to develop the temperature fields showing temperature values at each tomograph pixel. The interpolations can sometimes be in error when the interpolation algorithm is not sufficiently constrained by the measured values and because the interpolation does not necessarily satisfy physical laws.
Note that the temperature estimates were generated following a *nonqualified* process; therefore, the saturation estimates are *nonqualified.* Also, the saturations estimates are considered approximate, as indicated later in this report.

Figures 4.4-4, 4.4-5, and 4.4-6 show the saturation change estimates corresponding to heating days 182, 224, and 258 respectively. The results shown were calculated using Model 2 as described in Ramirez and Daily (1997). Model 1 results are not shown in order to be concise. Note that the Model 2 estimates on Figure 4.4-4 indicate that most of the rock immediately adjacent to the HD and to the wing heaters show saturation ratios below 1.0 These estimates suggest that some drying is occurring close to the HD. A lot more drying is occurring close to the wing heaters. Also note that the drying zone is growing very slowly with time. The tomographs suggest that the drying zone extends farther into the rock above the HD and than below it. The saturation ratio estimates shown in Figure 4.4-6 suggest that the rock showing the maximum amount of drying is located in plane AOD 5, forming a horizontal zone centered on the wing heaters. The tomographs show that this zone has lost about four-fifths of its water (saturation ratio of about 0.20) by mid-August, 1998. When compared to AOD 1, AOD 5 shows a stronger zone of drying that extends beyond the zone where the wing heaters are located.

Saturations ratios greater than 1.0 indicate regions in the rock were water saturation is increasing relative to the pre-heating conditions; we will refer to these zones as wetting zones. Wetting zones are observed in

Figures 4.4-4, 4.4-5, and 4.4-6. Most of these occur below the HD, near the bulkhead as well as in discrete zones closer to the middle of the HD. Another wetting zone appears above and near the edge of the wing heater location, within plane AOD 5.

All of the saturation estimates presented are considered to be approximations. The accuracy of the saturation estimates in may be limited by one or more of the factors listed in Wagner, 1998.

References:

Ramirez, A., and W. Daily (1997). *Electrical Resistivity Monitoring of the Thermomechanical Heater Test in Yucca Mountain.* Milestone report for the CRWMS Management and Operating Contractor, U.S. Department of Energy. (SP9215M4) Livermore, CA: Lawrence Livermore National Laboratory.

Wagner, R., 1998, Drift Scale Test Progress Report No. 1 (BAB000000-01717-5700-00004, Draft A), August 1998, TRW Environmental Safety Systems Inc., Las Vegas Nevada.

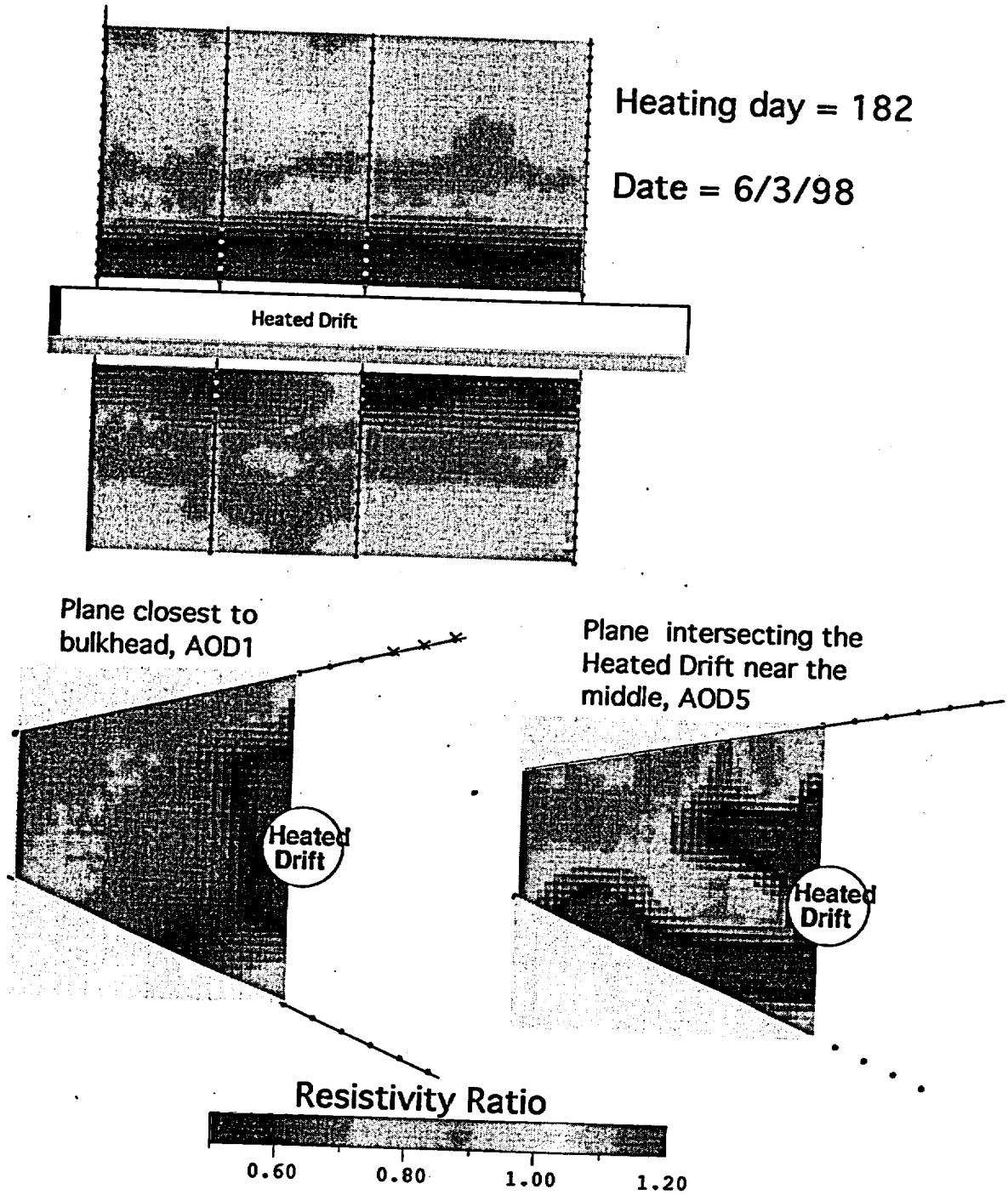

Figure 4.4-1. Tomographs of electrical resistivity ratio for heating day 182. The tomographs show changes relative to the preheating (November 18, 1997) electrical resistivity distribution. A resistivity ratio equal to 1.0 indicates no change; values less than 1.0 indicate that the resistivity is decreasing relative to the baseline.

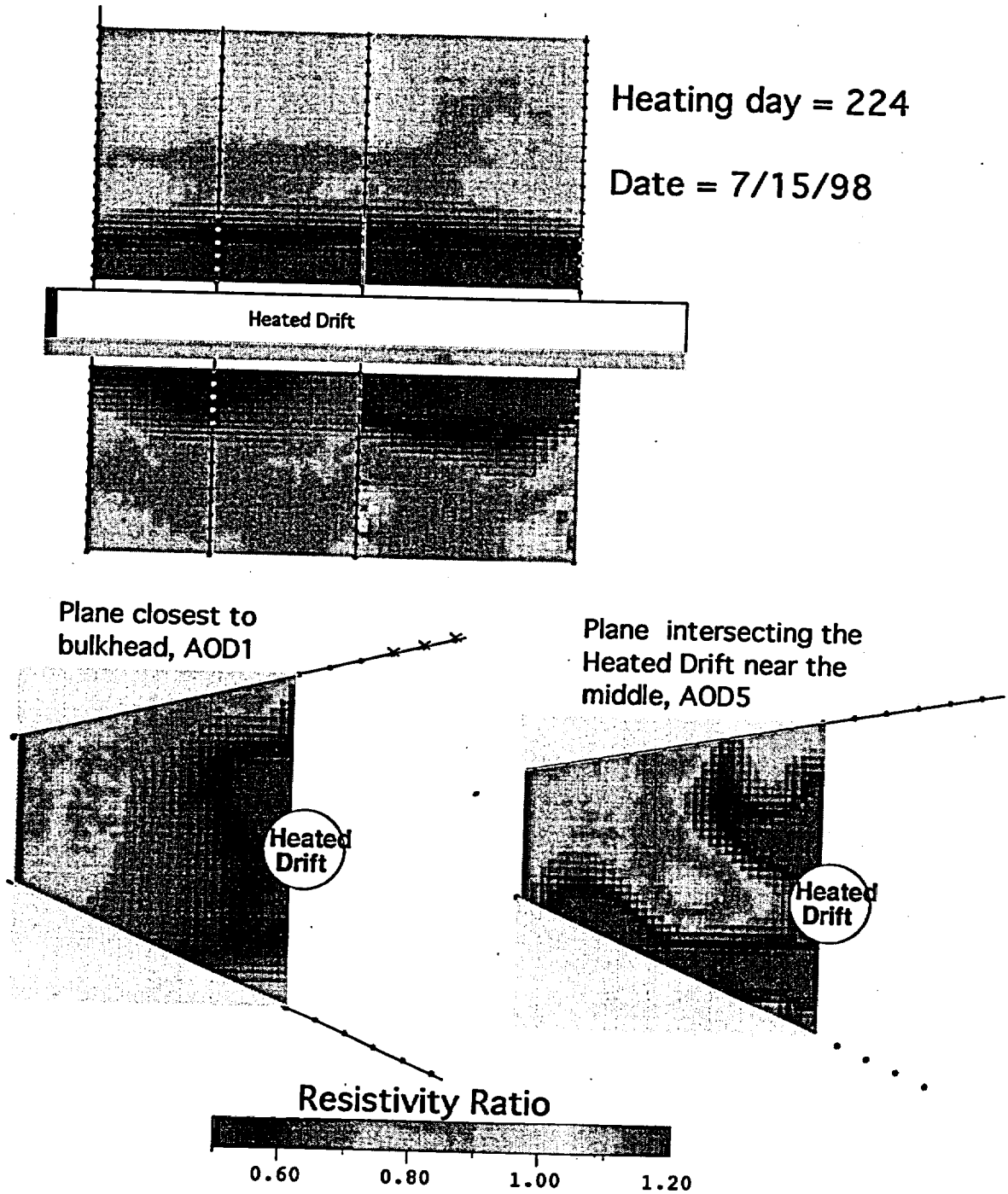

Figure 4.4-2. Tomographs of electrical resistivity ratio for heating day 224. The tomographs show changes relative to the preheating (November 18, 1997) electrical resistivity distribution. A resistivity ratio equal to 1.0 indicates no change; values less than 1.0 indicate that the resistivity is decreasing relative to the baseline.

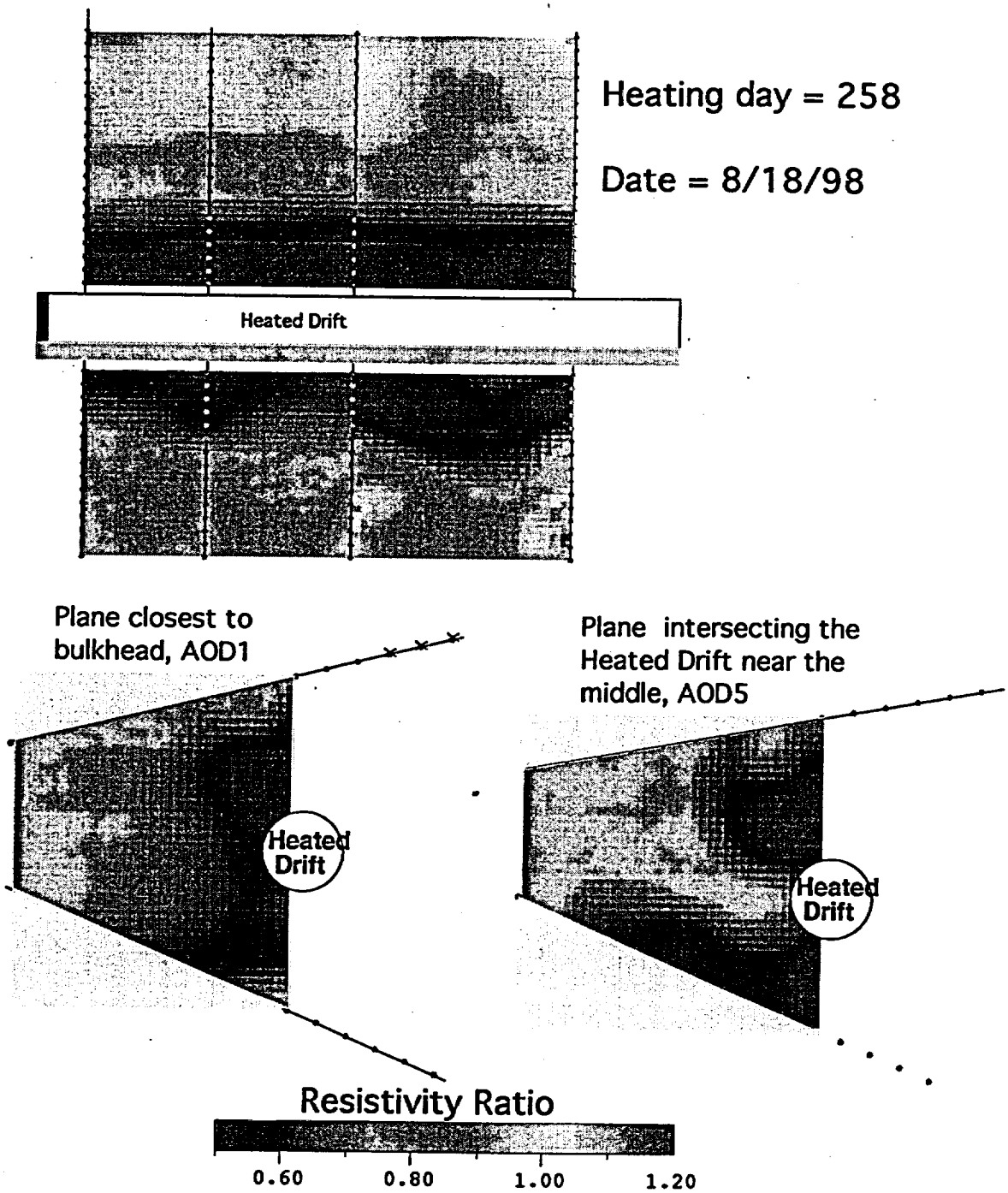

Figure 4.4-3. Tomographs of electrical resistivity ratio for heating day 258. The tomographs show changes relative to the preheating (November 18, 1997) electrical resistivity distribution. A resistivity ratio equal to 1.0 indicates no change; values less than 1.0 indicate that the resistivity is decreasing relative to the baseline.

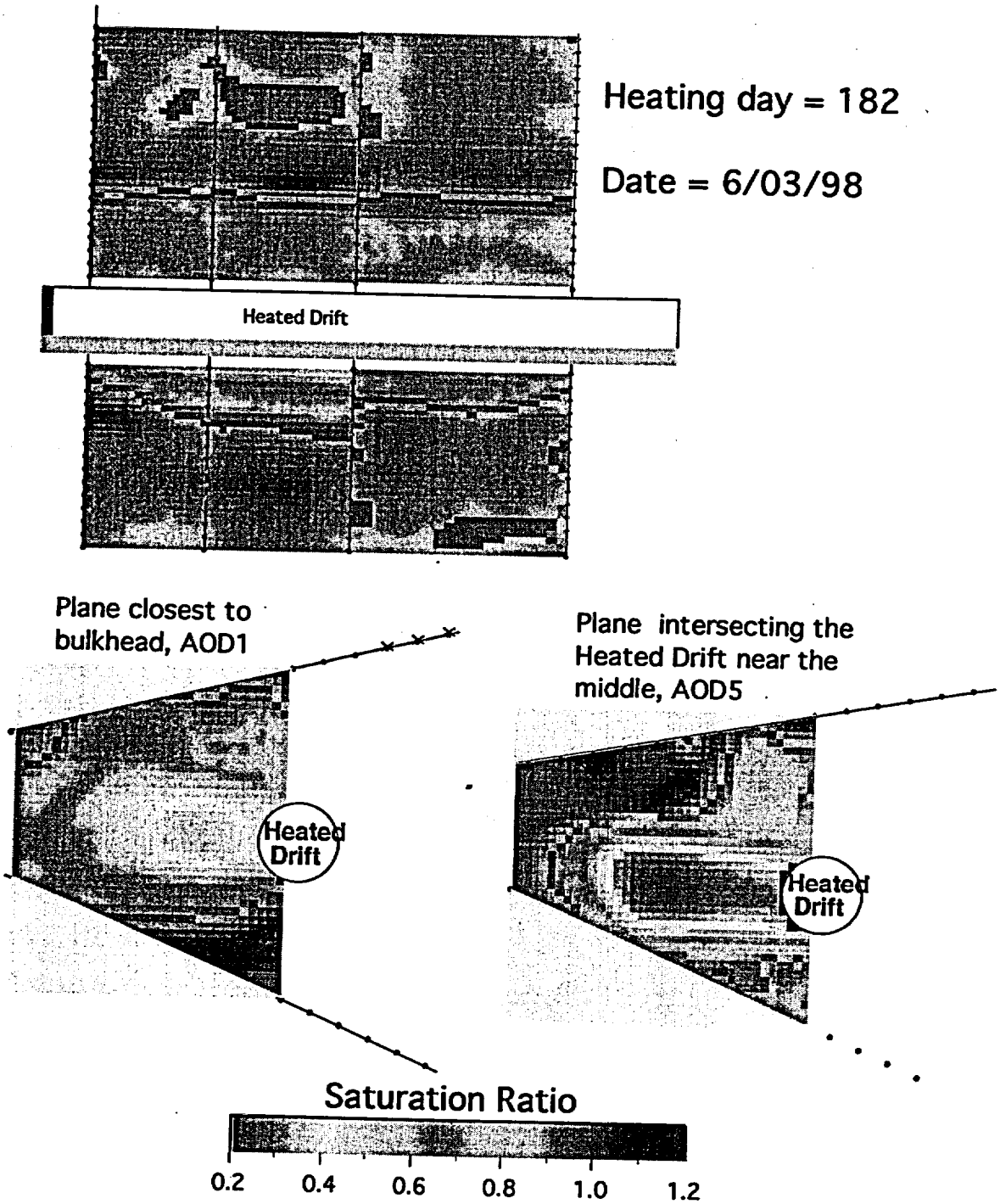

Figure 4.4-4. Tomographs of saturation ratio for heating day 182. The tomographs show changes relative to the preheating (November 18, 1997) saturation distribution. A saturation ratio equal to 1.0 indicates no change; values less than 1.0 indicate that the saturation is decreasing relative to the baseline.

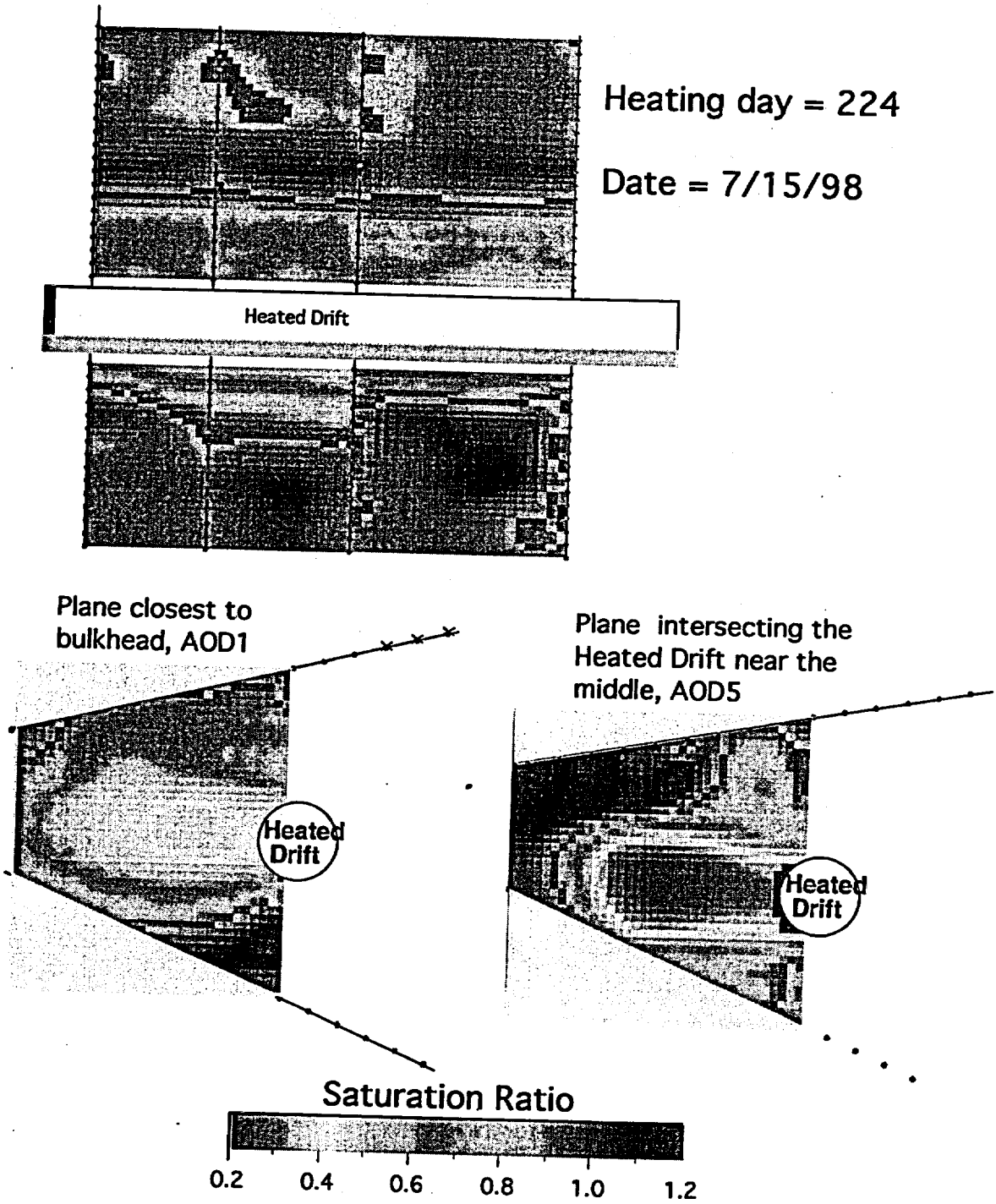

Figure 4.4-5. Tomographs of saturation ratio for heating day 224. The tomographs show changes relative the preheating (November 18, 1997) saturation distribution. A saturation ratio equal to 1.0 indicates no change; values less than 1.0 indicate that the saturation is decreasing relative to the baseline.

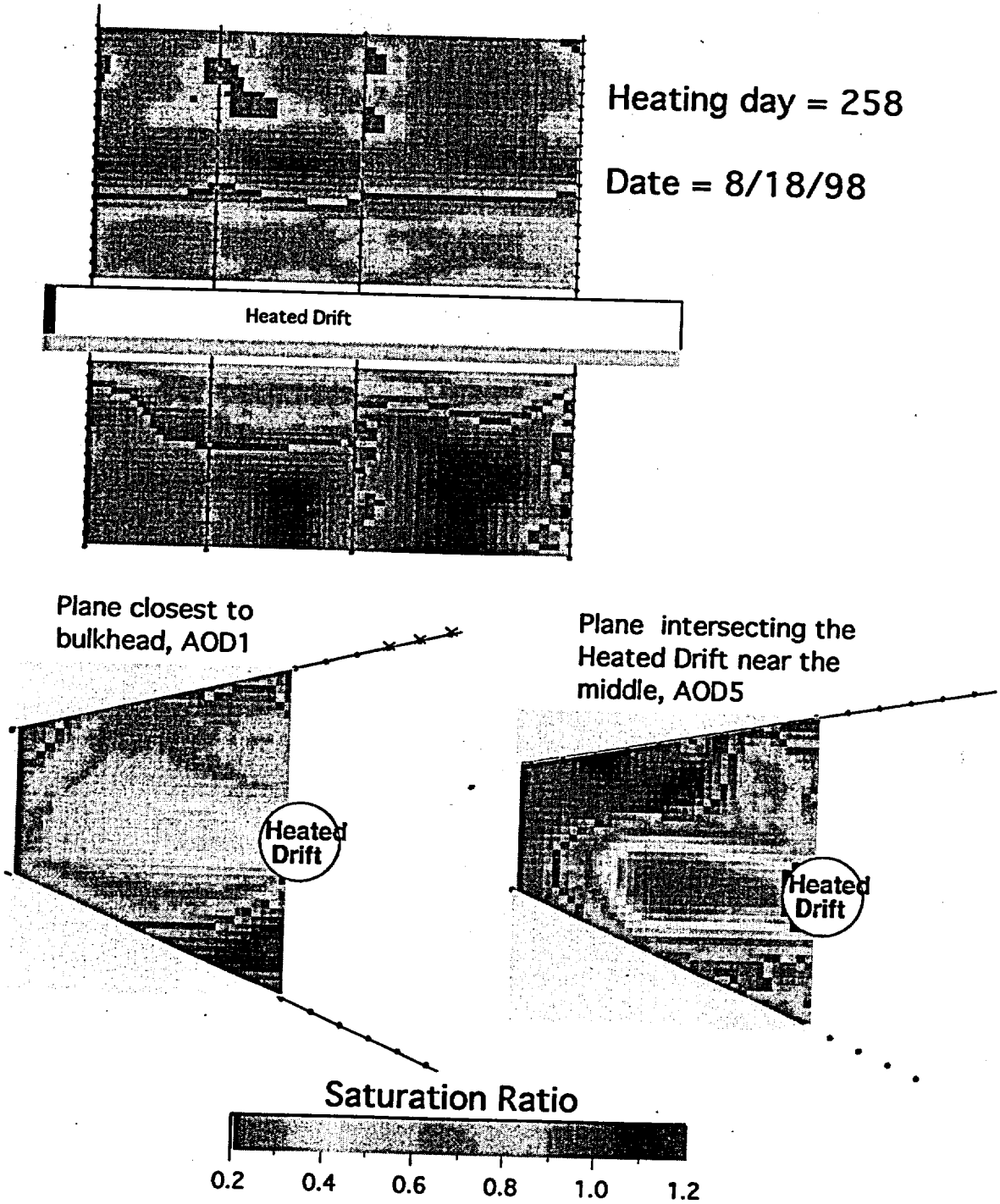

Figure 4.4-6. Tomographs of saturation ratio for heating day 258. The tomographs show changes relative to the preheating (November 18, 1997) saturation distribution. A saturation ratio equal to 1.0 indicates no change; values less than 1.0 indicate that the saturation is decreasing relative to the baseline.

4.5 GROUND PENETRATING RADAR MEASUREMENTS

Over the past several months, a variety of problems have been encountered by the ground penetrating radar(GPR) data acquisition system in support of the Drift Scale Test. The high temperatures present in several of the boreholes have resulted in equipment failures prohibiting successful and timely radar data acquisition. Specifically, it appears that the high temperatures resulting from the close proximity of the boreholes to the wing heaters directly short the radar antennas along weak points and cable connections. Much effort has been expended in determining the exact location of such weak points.

Initially, the focus of our attention was the cable head connection joining the dipole antenna to the coaxial lead-in cable. It was believed that by removing this potential failure point the system would resume normal operation – even at greatly elevated temperatures. A preliminary design was built and tested with no cable head connection. The results were extremely encouraging: the antennas were operated at the highest borehole temperatures with no loss in signal strength or transmitter amplitude over periods of time longer than those expected during normal data acquisition. It should also be noted that although the coaxial cable was not rated for the expected temperature (140ƀC), it performed acceptably and within the standards specified by the manufacturer. Additionally, a small scale GPR survey was undertaken using the prototype system in four of the hottest boreholes (Borehole Numbers 50-51 and 67-68). Because of problems with cable availability, the cables were shorter than the length necessary for a complete survey. As such, the survey was conducted from roughly 23.0 to 18.0 meters down the boreholes. Fortunately, this region is associated with the highest borehole temperatures and the greatest degree of formation drying. Results appear encouraging from a data quality standpoint but final data analysis and interpretation is still underway.

Based on these results, a final design was settled upon and the modified antenna system was fabricated. Unfortunately, cable availability again became a problem and a decision was made to utilize existing coaxial cable for the modified design. The available cable was that coaxial cable previously used at the Drift Scale Test. It was believed that the weak points in this cable were confined to the region nearest the cable head connection. A portion (1-2 meters) of the existing coaxial cable was removed and the dipole antenna directly connected to the shortened cable resulting in a design that would perform similarly to the prototype design and be of a length suitable for the Drift Scale Test survey (35 meters). Subsequent testing proved that our assumptions were partially incorrect. The new antenna design again failed to function properly when subjected to the elevated borehole temperatures. It became clear, however, that temperature was not the only factor in causing antenna failure. Cable stress also appeared to play a role. The first two radar surveys completed at the Drift Scale Test were accomplished by using aluminum push rods to forcibly locate the radar antennas to a desired depth. Especially in the steeply inclined boreholes, the emplacement of the antennas likely caused damage to the coaxial cable at those points where the push rods were strapped to the cable. This location varied depending on the inclination of the borehole and the depth of the survey, and as a result, multiple locations have probably been affected. Thus, when these damaged cable locations were placed under stress and elevated temperatures, electrical shorting and antenna failure was the result (i.e. low or no signal strength).

The failure of the existing cable has forced the procurement and assembly of a new system. The design of the system is to be identical to the one specified above with one notable exception. The new cable will be composed of coaxial cable rated to high-temperature (200+ƀC) covered in a rugged, abrasion-resistant coating also rated for high-temperature (200+ƀC). Additionally, as part of an effort designed to develop a less damaging method for emplacing the radar antennas in the boreholes, a locking pulley system was conceived and built. This device now allows us to lock (and later remove) a pulley at 40 meters depth down a borehole. Using this pulley and an attached high-temperature string, we are able to gently and efficiently pull an antenna to a desired depth. This has proven to be extremely successful and will be very valuable in reducing cable damage in the future. It is now believed that by utilizing the undamaged, high-temperature coaxial cable along with the locking pulley system, the means exists to successfully resume GPR data acquisition in support of the Drift Scale Test.

4.6 Neutron Logging Measurements

There are twelve holes in the Drift Scale Test for measuring the moisture content of the rock by neutron logging.. Ten of these holes in two fans transversely orthogonal to the Heated Drift are from the observation drift. The other two holes are drilled from the connecting drift, parallel to the Heated Drift (HD) at approximately 1m above its crown and approximately 9.5m from the centerline of the HD on either side of it.

A teflon tube is grouted in the neutron holes to facilitate movement of the probe. Since the grout contains moisture, the neutron logging system needs to be calibrated in simulated rock of known moisture content and hole and teflon tube of same diameter and same grout conditions. The neutron count from the logging is processed using the calibration data to yield moisture content of the rock. Although logging in the DST are being performed regularly since before the start of heating, calibration of the tool is not complete. For this reason, true moisture content of the logged intervals in the DST is not yet available. All actual test runs associated with the calibration of the DST neutron tool have been completed and the data is being processed at this time. Data on the true moisture content of the rock will be available in the near future.

Notwithstanding the above, preliminary qualitative conclusions regarding the drying of the rock can be made by analyzing the neutron count obtained by logging. Such analyses indicate that the rock surrounding some sections of neutron holes # 4 , 9 and 12 has been drying. Both neutron holes #4 and 9 are down holes and the drying sections not far from the outer segment of a nearby wing heater. Neutron hole #12 is parallel to the HD and the drying section in this hole is also due to wing heaters below it.

4.7 GAS SAMPLING AND ANALYSIS

Introduction

CO_2 concentrations in the rock around the Heater Drift have increased significantly since the initiation of heating. Numerical models of the system indicate that the source of this CO_2 is exsolution of dissolved inorganic carbon compounds (DIC) such as $CO_3^{=}$, HCO_3^{-} and dissolved CO_2 from the pore waters in the rock during heating. With ~90% of the pore space in the rock filled with water, the capacity of the water to hold carbon in the form of DIC is much greater than the capacity of gas phase to hold CO_2 (on the order of 100 times as much, depending primarily on the pH and temperature). As the temperature rises, the partitioning of inorganic carbon between the gas and liquid phases shifts, with a higher proportion going into the gas phase. When the rock reaches the boiling point of water, the CO_2 concentrations will increase even more quickly until the rock dries out and all the inorganic carbon goes into the gas phase. The changing DIC concentrations in the pore fluids will have a significant impact on the chemistry of the pore fluids (especially on pH), which could strongly affect which mineral phases will be dissolved or precipitated.

The stable carbon isotopic ratios ($\partial^{13}C$ values) of CO_2 from around the heater drift have been measured in order to confirm the source of the increased CO_2 and to constrain parameters such as the changing pH of the pore waters and the nature of gas transport in the heated rock. This is possible because CO_2 and DIC in carbon isotopic equilibrium will have different $\partial^{13}C$ values depending primarily on the temperature and pH of the fluids. As a result, the $\partial^{13}C$ values measured for CO_2 will change as a higher proportion of the DIC in the pore waters is converted to CO_2. The way in which the $\partial^{13}C$ values of the CO_2 vary with time and temperature around the heater drift can then be used to place limits on pH and gas transport in the system.

Data

The $\partial^{13}C$ values of the potential sources of CO_2 in the tunnel were measured. This data is presented in Table 4.7-1. It is significant that the concentrations and $\partial^{13}C$ value CO_2 from the AO Drift and the Heater Drift are similar. This indicates that the Heater Drift is essentially in equilibrium with the air in the tunnel and that the bulkhead separating the Heater Drift from the tunnel is not limiting gas exchange. It should also be noted that the $\partial^{13}C$ value of CO_2 measured for rock air is close to the $\partial^{13}C$ value of CO_2 that would be produced from dissolution of calcite with the $\partial^{13}C$ value measured for the calcite from the AO Drift. This suggests that the $\partial^{13}C$ value of CO_2 in the vicinity of the heater drift may have been fairly constant over time.

The $\partial^{13}C$ values of CO_2 in gas samples collected from the hydrology holes vary depending on both the concentration and temperature of the rock. Figure 4.7-1 is a cross section of the Heater Drift that contains hydrology holes 74-78. The $\partial^{13}C$ values of CO_2 from gas samples collected during August of 1998 are plotted on this figure along with the temperatures and CO_2 concentrations. The $\partial^{13}C$ values are highest in samples from nearest the Heater Drift and drop off significantly in samples from further away. Similar patterns were seen in gas samples from the other intervals that were sampled. The variations in the $\partial^{13}C$ values do not directly correlate with either the temperature measured for the interval sampled or the concentration of CO_2. This is believed to be primarily caused by the large sampling intervals that cross areas with large temperature ranges.

The $\partial^{13}C$ values of the CO_2 also varied with time. Figure 4.7-2 contains data collected from two of the intervals in the hydrology holes that were sampled over the last 8 months. Interval 77-3 is from the hottest part of the system. By February, the temperature was already greater than 80°C. The CO_2 concentrations were also high and increased to greater than 33,000 ppm (3.3%) by August. By October, the temperatures in this interval had increased past the boiling point of water and the CO_2 concentration had dropped down to 2160 ppm, presumably because the pore waters in the area had boiled away (although,

given the large size of this interval, it is unlikely that the whole region had dried out). The carbon isotope data is consistent with this interpretation. In February, the $\partial^{13}C$ value of the CO_2 was already much higher than the background, indicating a significant input of CO_2 from pore water DIC. As the CO_2 concentrations increased, so did the $\partial^{13}C$ values of the CO_2. When the region began to dry out, the $\partial^{13}C$ value of the CO_2 decreased slightly (representing CO_2 coming from cooler areas of the system?).

Conversely, interval 57-3 is from a hole that extends above the Heater Drift at ~10 m from the bulkhead. By early October, when the last sample was taken, the temperature of the interval was only 25.5°C. However, the CO_2 concentrations had increased to approximately twice the initial concentration and the $\partial^{13}C$ values of the CO_2 had dropped down to -16‰. This indicates that CO_2 evolved from pore waters in the hotter areas of the system closer to the Heater Drift is expanding out into the rock, causing CO_2 concentrations in the cooler areas of the system to increase despite no significant increase in temperature. The $\partial^{13}C$ values of the CO_2 in the cooler areas are decreasing because a significant amount of the CO_2 is being absorbed into the pore waters as DIC. The CO_2 dissolving into the pore waters will have higher $\partial^{13}C$ values causing the remaining CO_2 to shift to lower $\partial^{13}C$ values.

Implications

The carbon isotopic data for the CO_2 suggest a couple of initial conclusions. First, the increased concentrations of CO_2 in the rock around the Heater Drift are probably derived from DIC in the pore waters. It is also possible that some of the CO_2 could be from dissolution of calcite in the rock. The second finding is that gas transport around the Heater Drift is relatively fast. In order for the $\partial^{13}C$ values of the CO_2 to increase as much as they have (from -13‰ to greater than -3‰), the system must be open. In a closed system, the $\partial^{13}C$ values of the CO_2 could not increase above the initial $\partial^{13}C$ value of the DIC in the pore waters (approximately -6‰). To rise to greater than -6‰ requires that the initial, lower $\partial^{13}C$ CO_2 that is evolved from pore water DIC be flushed out of the system. Simple calculations suggest that the residence time of CO_2 in the rock is relatively short (complete turn-over every few days). The only reason such high concentrations of CO_2 are maintained in the rock is because of the much higher starting concentration of inorganic carbon in the pore waters.

Reference

Wigley, T.M.L.; Plummer, L.N.; and Pearson, F.J. 1978. "Mass transfer and carbon isotope evolution in natural water systems." *Geochim. et Cosmochim. Acta 42*, 1117-1139.

Table 4.7-1. Average concentrations and $\partial^{13}C$ values of CO_2 from the area of the heater drift.

	# of Measurements	ppm CO_2	$\partial^{13}C_{VPDB}$ (‰)
1. AO Drift Air	4	430	-10
2. Heater Drift Air	2	420	-10
3. Rock Air[1]	1	900	-13
4. Calcite[2]	2		-6

[1] Sample of gas collected from borehole 182 in the

[2] Data for calcite samples taken from fractures in the AO Drift. The $\partial^{13}C$ value given is the measured value for calcite. This is different than the $\partial^{13}C$ value of CO_2 that would be produced from dissolution of the calcite depending on the temperature and the pH of the fluids. At 20°C and a pH of 7, the equilibrium $\partial^{13}C$ value for CO_2 will be approximately -14‰ (Wigley et al., 1978).

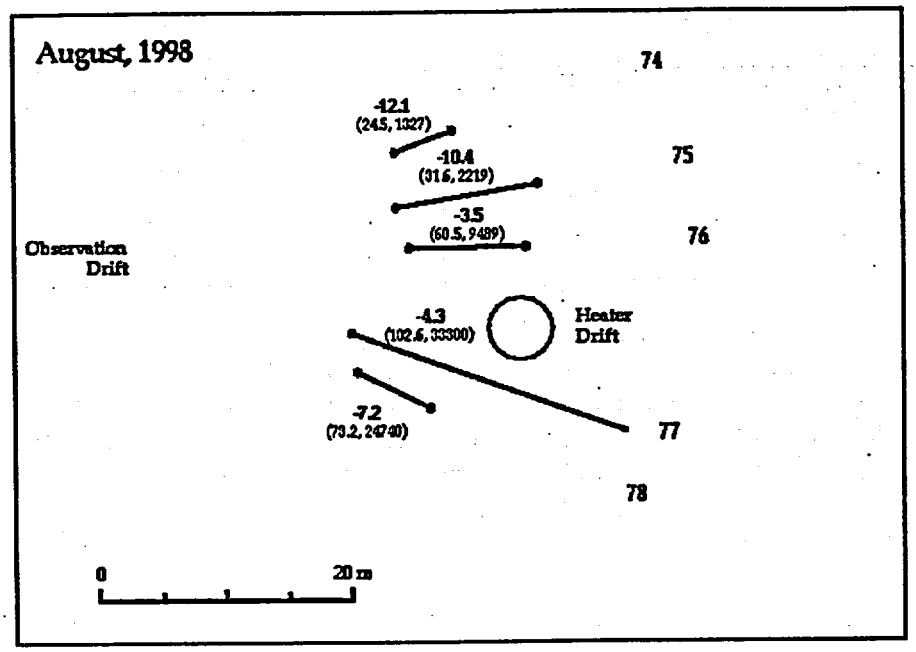

Figure 4.7-1. $\partial^{13}C$ data for CO_2 (in ‰ units relative to VPDB) in gas samples collected during August of 1998 from Hydrology boreholes around the Heater Drift. Also shown are the temperatures (°C) and concentrations of CO_2 (ppmv).

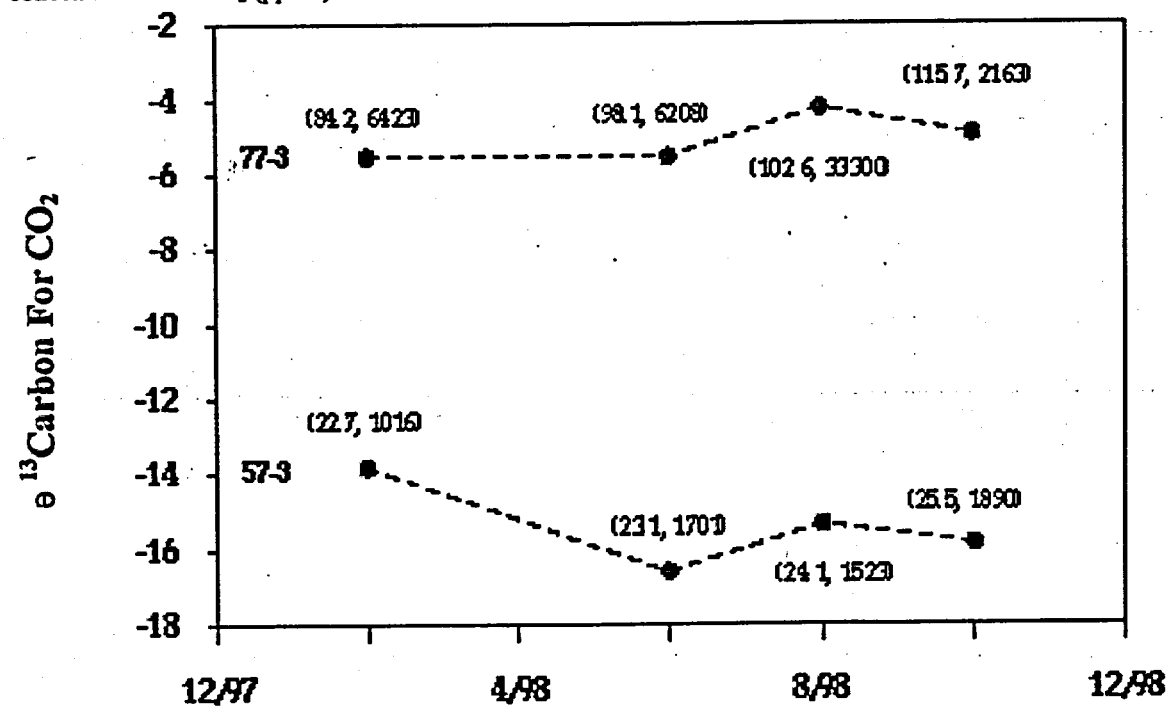

Figure 4.7-2. Plot of $\partial^{13}C$ data for CO_2 (in ‰ units relative to VPDB) in gas samples collected from intervals 77-3 and 57-3 in the LBNL Hydrology boreholes. Also shown are the temperatures (°C) and concentrations of CO_2 (ppmv).

4.8 ANALYSIS OF WATER SAMNPLES

The major cation and anion chemistry of the waters recently sampled from the Drift Scale Test has been analyzed. Several water samples were obtained from the hydrology holes, and pads contacting wet borehole walls were collected from the liners installed in the chemistry boreholes. An aqueous sample was also collected from one of the chemistry boreholes during gas sampling.

The samples were all analyzed with respect to the cations Si, Na, Ca, Mg, Sr, Al, K, Fe, S, B, and Li by the method of Inductively-Coupled Plasma and Atomic Emission Spectrometry (ICP/AES). The anion analyses performed by Ion Chromatography (IC) included F, Cl, Br, NO_2, NO_3, PO_4, and SO_4. A field measurement was also made of pH and temperature in most instances at the time of collection.

Water Samples Collected From The Drift Scale Test

Aqueous samples have been collected from the hydrology boreholes where packed-off intervals separate zones open to the borehole walls. To date, water has been sampled from two of these hydrology boreholes: borehole 60 and borehole 77 occupy corresponding positions in two different borehole arrays. Both boreholes are collared in the observation drift, run normal to the heater drift plane, and angle downward and below the heaters. The first water from the hydrology boreholes was taken 6 months after heater turn-on, in two zones of borehole 60. Samples were collected again from these zones and from borehole 77 about 2 months later.

Water samples taken for chemical analysis from the chemistry boreholes were first collected in April of 1998 (~4 months after the start of heating). At that time the first absorber liner was removed from borehole 55, and the attached absorber pads were collected for analyses. This borehole corresponds in orientation and position within its borehole array to the two hydrology holes from which the previously described water samples were taken. The absorbent pads installed on the liner were positioned every 4m along the length and all appeared to be saturated. One pad, however, located ~18m into the hole was beginning to show signs of drying. Another liner was pulled in June, and again all the pads appeared to be wet. The second liner was pulled from borehole 56, the borehole immediately below 55. In the case of liner 56, the pads visually did not appear to be as wet as for those collected from 55.

Liquid water was also collected on one occasion from the chemistry boreholes. During gas sampling, an in-line water trap collected ~ 30 mls of water as air was pumped from the gas sampling ports to the analysis unit. This water came from borehole 54, within the same array of chemistry holes as 55 and 56, but which is angled upward and immediately above the heaters in the drift. The sampling port which yielded water was located almost at the end of the borehole, at a distance of ~35m in from the collar. This water was collected for sampling and analysis, but it was unexpected, and a formal sampling protocol had not been established.

Sample Handling and Processing

The borehole water samples from the hydrology holes were collected and filtered through a 0.45 Em pore filter. These water samples were stored in polyethylene containers and were either immediately stabilized with HNO_3 for sample splits designated for cations, or the containers simply went into refrigerated storage until they could be sent for analyses. The controlled thermal conditions were unable to be maintained throughout the entire shipping and transfer process, however.

The sample collection of absorber pads included the immediate removal from the retrieved borehole liner and storage in clean, air-tight polyethylene bags. A visual examination showed that the pads suffered from gross contamination of rock and soil particulates that could not easily be excluded during processing in the lab and therefore introduced significant uncertainty into the analytical results. Another potential contaminant was the pervasive presence of mildew on the pads.

Analytical Chemistry Results

The measured cation and anion chemistry of the aqueous samples are reported in Table 4.8-1. Hydrology hole samples are identified by the borehole number and the zone. The chemistry hole sample is identified by the borehole number and the gas sampling port number. In addition to this identification descriptor, all samples have also been given a YMP bar code for sample tracking which is reported as the SMF number. The table includes the sample collection date and field measured values of pH, temperature, and Br concentration if available. All the samples have a Q-pedigree, except for the chemistry borehole water, 54-1. All the analytical data are qualified.

The pad data that have been collected to date are not reported. As previously mentioned, the pads were recognized to be contaminated, and although efforts were made to reduce the contamination from areas analyzed, results are suspect. Additional analyses were also performed to understand the contribution to background levels that the pad generates. These analyses revealed significant heterogeneity of several of the analytes, further complicating the interpretation of potential geochemical changes with respect to depth or distance from heaters. Further examination of the results will determine if some of the data can be utilized.

Discussion

Several liters of water were collected from the hydrology hole #60. The water chemistry in both zones 2 and 3 is inconsistent with a simple condensate which has no history of rock/water interaction. On the other hand, the chemistry of water collected from borehole 77-3 was different; it was dilute by comparison. The temperature readings recorded for 77-3 was 102.8 °C which was generally hotter than the other zones from which water was collected. This borehole yielded only about 200 mls of water, and one possibility is that the sample is simply water vapor stripped from the gas as the hot air is pumped into the cooler atmosphere of the observation drift. At any rate, it is not comparable to the chemistry of the other waters sampled. Finally, borehole 54 port 1 yielded water which also does not appear to be simple condensate. Because its chemistry is suspect, however, since the process of filtration and flushing of the lines were not employed, the results should not be used to make geochemical interpretations. Instead, it may be useful to understand moisture distribution within the test, and to plan for the possibility of future water collections via the same process.

Table 4.8-1. Thermal test water chemistry.

SMF number	Suite 1 SPC00527969	Suite 1 SPC00527977	Suite 2 SPC00527915	Suite 2 SPC00527916	Suite 2 SPC00527917	H2O trap SPC00530268
collection date	06/04/1998	06/04/1998	08/12/1998	08/12/1998	08/12/1998	06/04/1998
temp (C)	36.2	82.1	60.2*	91.6*	102.8*	
field pH	7.5	7.7	6.9	6.8	5.5	7.32
field Br (ppm)*	0.75	0.96	0.385	0.345	0.392	
Na (mg/l)	20.0	24.0	20.4	17	2.4	27.0
Si (mg/l)	56	41	51.8	44	1.48	509
Ca (mg/l)	20	25	19.9	19	2.09	28.8
K (mg/l)	6.0	4.5	5.4	4.5	1.4	n.d. < 0.5
Mg (mg/l)	2.9	5.7	1.21	4.0	0.21	5.79
Al (mg/l)	0.12	n.d.< 0.06	n.d.<0.06	n.d.<0.06	n.d.<0.06	n.d. < 0.06
B (mg/l)	1.2	0.92	1.84	1.1	0.13	1.71
S (mg/l)	5.5	9.2	4.5	5.2	1.4	16.6
Fe (mg/l)	0.04	n.d. < 0.02	0.02	0.12	n.d. < 0.02	n.d. < 0.02
Li (mg/l)	0.07	0.07	0.03	0.04	n.d. < 0.01	0.07
Sr (mg/l)	0.18	0.34	0.11	2.2	0.05	0.4
F (mg/l)	1.00	0.82	0.71	0.43	nd < .007	1.00
Cl (mg/l)	10	16	6.14	5.52	2.15	31.0
Br (mg/l)	0.84	0.73	0.05	0.21	nd < 0.03	n.d. < 0.02
SO4 (mg/l)	17	30	4.88	8.81	1.86	45.0
PO4 (mg/l)	n.d. < 0.07	n.d. < 0.07	0.25	0.16	1.06	n.d. < 0.07
NO2 (mg/l)	n.d. < 0.01	n.d. < 0.01	nd < 0.04	nd < 0.04	nd < 0.04	n.d. < 0.01
NO3 (mg/l)	3.00	3.6	0.46	0.6	0.22	9.00

* These temperatures were downloaded from the data collection system, and are not a measured fluid temperature at the time of collection.

The water sample from borehole 54-1 is not "q" and the analyses likely reflect contaminated sample

4.9 Acoustic Emission / Microseismic

Sixteen accelerometers are installed at various locations in the Drift Scale Test block to monitor micro-seismic or acoustic emissions (AE). Micro-cracking due to heating is thought to be caused by acoustic emissions. Shear movement and rock fracturing are also expected to release micro-seismic emissions. Travel time data to multiple accelerometers can be processed to locate a particular event in space. This information may then be correlated with some of the other measurements such as rock displacement. This information may be useful in understanding the process(es) taking place in the rock.

Three of the sixteen accelerometers are malfunctioning. The remaining thirteen are still adequate for isolating and locating an event. The system is subject to severe interference due to noise from any of the many other electrical systems in the DST.

After the heating started, the AE system in the DST was experiencing both severe noise interference and actual events making it difficult to isolate and locate any event in time and space. One event, considered to have been isolated , took place on January 7, 1998. The processing of the data to locate it is expected to be completed in the near future.

Recent installation of a filter to eliminate high frequency noise and a trigger selection box which will not trigger the system if emmissions reaches multiple accelerometers exactly at the same time is expected to greatly help in isolating events.

4.10 Video Imaging Inside the Heated Drift

The Camera System in the Drift Scale Test is intended to periodically take both video and infrared images inside the Heated Drift. Baseline images were collected before the start of heating in December 1997. The infrared (IR) images after the start of heating did not allow any distinctive features to be identified. This is thought to be due to extremely low temperature gradient on the surfaces being imaged. IR imaging may be useful during the cooling phase to identify any moisture vapor escaping into the Heated Drift from fractures, if there is any such event and the temperature difference between the moisture and rock surfaces in the vicinity is finite and distinguishable by IR imaging.

Video images of the inside of the Heated Drift have been collected in March, July and November of 1998. No changes of any significance has so far been noted.

4.11 Moisture Movement Across the Bulkhead

The Heated Drift is separated from the rest of the thermal testing facility by a bulkhead. The bulkhead is a thermal bulkhead, not a pressure bulkhead. It is made of a steel frame and steel plates and carries the lighting fixtures, viewing windows and the camera door. The bulkhead is insulated on both sides by fiber glass insulation pads.

The ralative humidity (RH) inside the Heated Drift dropped to approximately 15 percent during the first 10 days of heating. Thereafter, the RH inside the HD fluctuated between 10 and 25 percent with a peak to peak interval of approximately 4 days. Measured RH in the HD has been inversely tracking the air pressure in the drift. After some forty days of heating, moisture started to flow out of the Heated Drift as evidenced by condensation on various surfaces near the bulkhead and the formation of a puddle on the floor. Such wet conditions near the bulkhead alternated with dry conditions with the latter coinciding with low RH inside the HD.

The Drift Scale Test System, comprised of the HD and the surrounding heated and unheated rock, is not a closed system. The DST block is exchanging moisture and air with its surroundings through the bulkhead and the fractured rock. Outflows coincide with higher RH in the HD and lower barometric pressure.

As the rock immediately surrounding the drift is heated to above the boiling temperature, the pore water in the rock is mobilized and driven outward creating a dry-out zone around the drift. As the mobilized water in the vapor phase moves outward, it condenses when it reaches cooler regions and vaporizes again, as additional thermal pulse reaches it. A boiling zone is thus formed around the dry-out zone. Phase changes occur continuously in the boiling zone causing pressure to build up. When the barometric pressure and the pressure inside the HD are high, steam and water is confined to the boiling zone. When the barometric pressure and the pressure in the HD drop, steam and water escape from the boiling zone moving into the HD via the fractures and causing the RH in the drift to rise, much like what happens in pressure cooker or geyser.

Ways of measuring the heat loss through the bulkhead, both by conduction and convection, have been investigated. A pair of sensitive heat flux meters has been acquired and will be used to measure the heat loss by conduction in the first part of January 1999.

Measuring the loss by convection is difficult and complicated because flow takes place at numerous locations, at various rates and at different temperatures. A system employing mass flowmeters and mass spectrometers is being investigated.

4.12 THERMAL-HYDROLOGIC ANALYSIS

An interpretive analysis of the thermo-hydrological processes of the Drift Scale Test (DST) at Yucca Mountain was conducted by studying measured temperature data collected in the first 9 months of heating and comparing them with simulated results from the 3-D DST numerical model. In this model, fractures and matrix are each represented as a continuum for flow of liquid, gas and heat. The effective continuum approach (ECM) is applied in three-dimensional simulation runs, while the dual permeability formulation is used for certain two-dimensional runs to study model sensitivity to the fracture-matrix interaction concept. The numerical simulation is exercised for two different infiltration rates—the best estimate of 3.6 mm/yr for the location of the heater, and one-tenth of the expected estimate, 0.36 mm/yr—in order to include a full range of plausible responses. Infiltration is assumed to be constant in time; no episodic events are considered. Model properties are estimated from site-specific measurements whenever possible, otherwise adopted from UZ site-scale model results. Two alternative data sets are used for the DST, one associated with 3.6 mm/yr percolation, the other associated with 0.36 mm/yr percolation. The computational grid designed for the DST honors the designed test conditions as closely as possible, using a total number of 48,249 gridblocks and 157,474 connections between them (Figure 4.12-1).

The model used for the DST simulations is based on the three-dimensional predictive model developed by LBNL in 1997 (Birkholzer and Tsang, 1997). The predictive simulations were carefully reevaluated based on the first 9 months of data, and, as a result, several model refinements have been made. In general, such model refinements can be categorized as follows:

- Modification of test conditions and geometry
- Modification of model conceptualization
- Modification of model rock properties

So far, we have focused on the first two items, i.e., a better representation of the actual test conditions, and a review of the conceptual model. The following model improvements were made:

- Heater power and schedule were adjusted to 77% of maximum power for the canister heaters and 94% of maximum power for the wing heaters, representing the average measured heater power in the DST for the first 4 months of heating
- The concrete invert in the Heated Drift, originally not represented by the model, was added to the computational grid.
- The bulkhead boundary condition was modified to allow for gas transport between the hot and the cold side of the heated drift.
- The initial temperature and moisture conditions close to the Heated Drift were adjusted to account for the impact of elevated drift temperature and drift ventilation prior to heating.

Our observation so far is that the simulation results for the first 9 months of heating compare favorably with temperature data as well as with results from active hydrological testing. The model refinements all contribute to a better match between simulation results and field data, in particular the introduction of the gas-permeable bulkhead boundary condition. Our results also indicate that thermal radiation is quite effective within the Heated Drift, and can be approximated in the model by assuming totally effective black body heat radiation. Simulation runs performed for a heating period of several years show that the current heater power can probably be maintained for about 24 months of heating before the wall temperature in the Heated Drift reaches 200°C (Figure 4.12-2).

So far, no model calibration has been performed. Sensitivity studies, however, indicate that the temperature match between measured and simulated results may be further improved by using adjusted rock property sets. Hence in future modeling efforts, the model properties for the DST will have to be carefully evaluated. Sensitivity studies have also been conducted to study the impact of model conceptualization, i.e., the validity of ECM or DKM approaches, respectively. The simulated temperatures are almost identical for the two model concepts; however, obvious differences between ECM and DKM are obtained for saturation results, as the DKM method promotes gravity-driven liquid flux in the fractures (Figure 4.12-3). We may conclude from this analysis that temperature data will probably not diagnostically discriminate the ECM and DKM concepts in the DST. However, we believe that a thorough analysis of the air-permeability tests

performed in different borehole intervals at different heating phases could provide such information, since the ECM and the DKM modeling concept clearly results in different fracture saturation fields. Further analysis of the different modeling concepts will be performed in future studies.

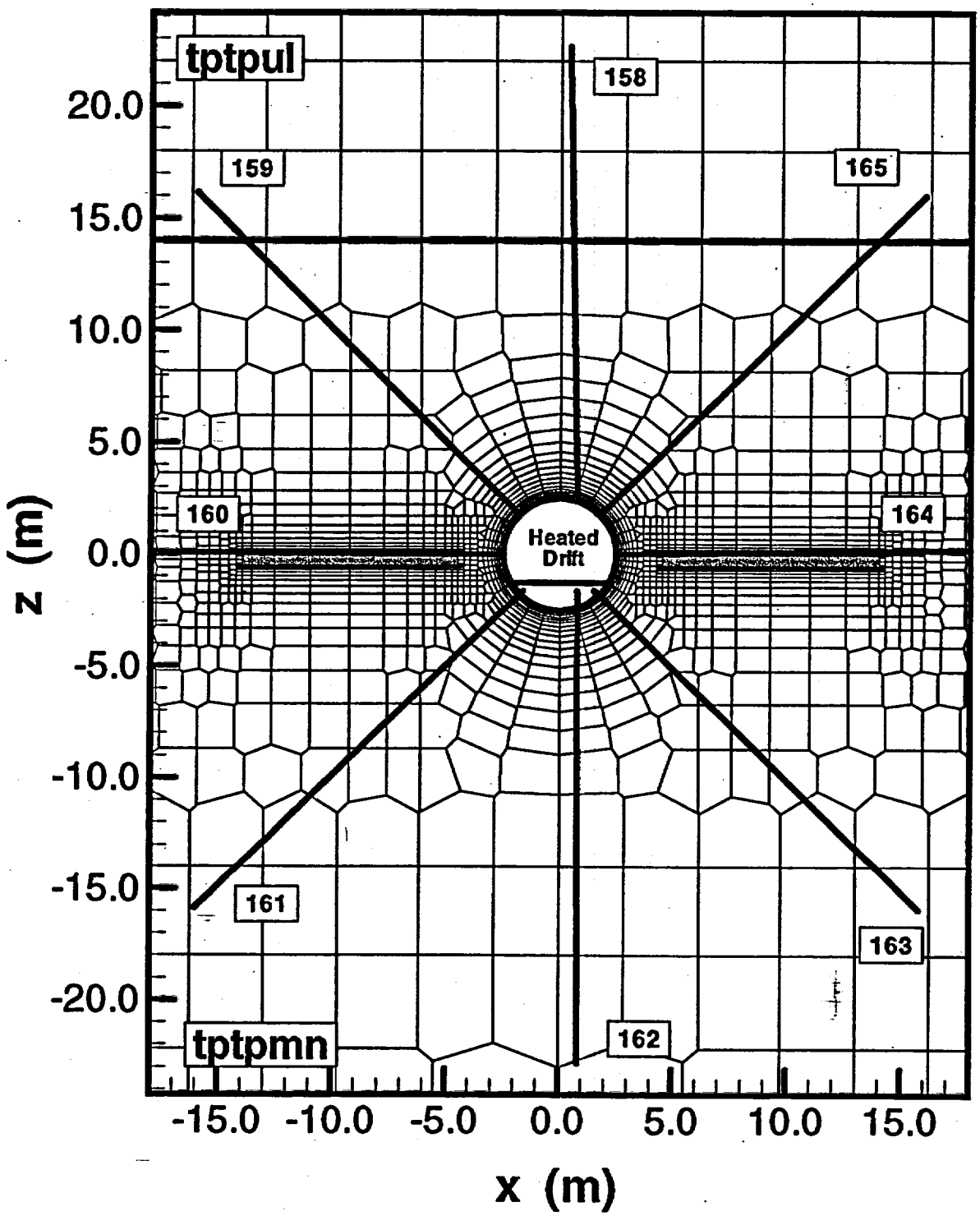

Figure 4.12-1. Close-up view of model grid in a vertical cross section at y = 23 m from the bulkhead with RTD borehole 158 through 164. The blue area indicates location of wing heaters.

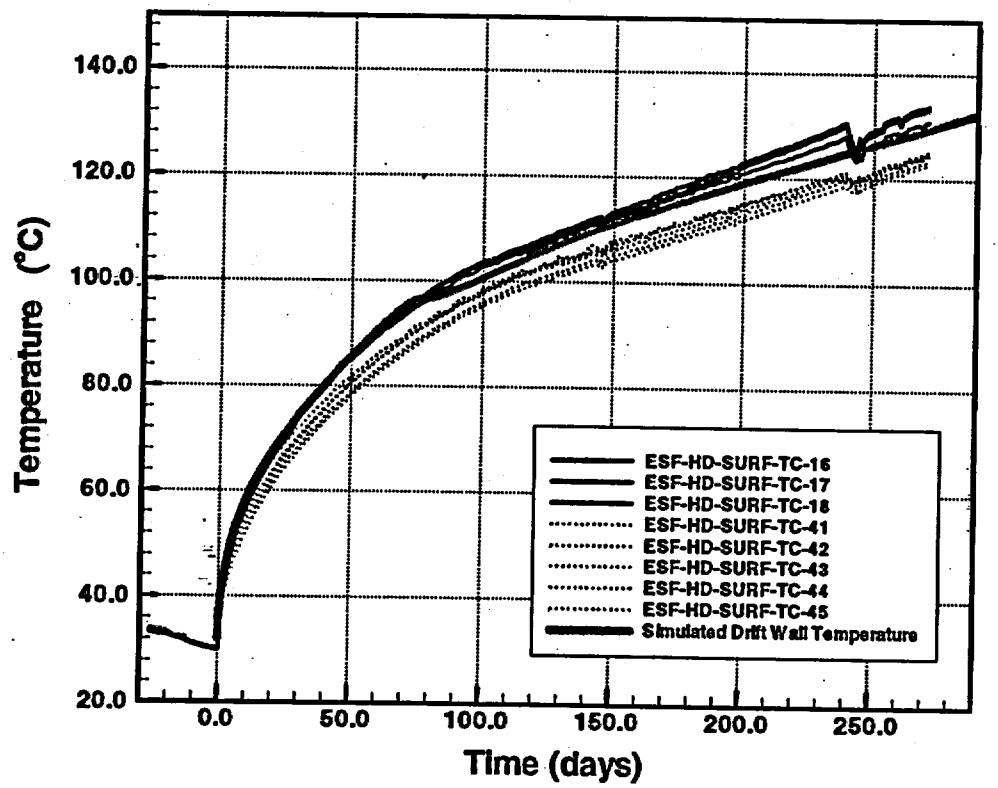

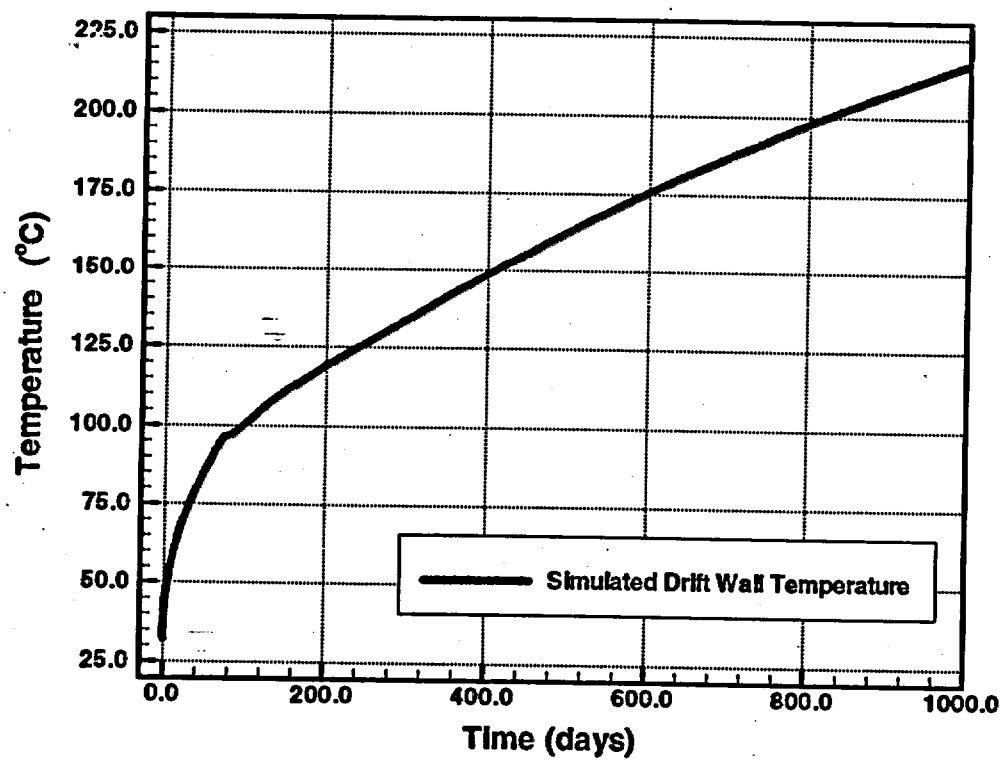

Figure 4.12-2. Measured and simulated temperature evolution at the Heated Drift wall. Measured temperature is shown at two different cross sections along the Heated Drift.

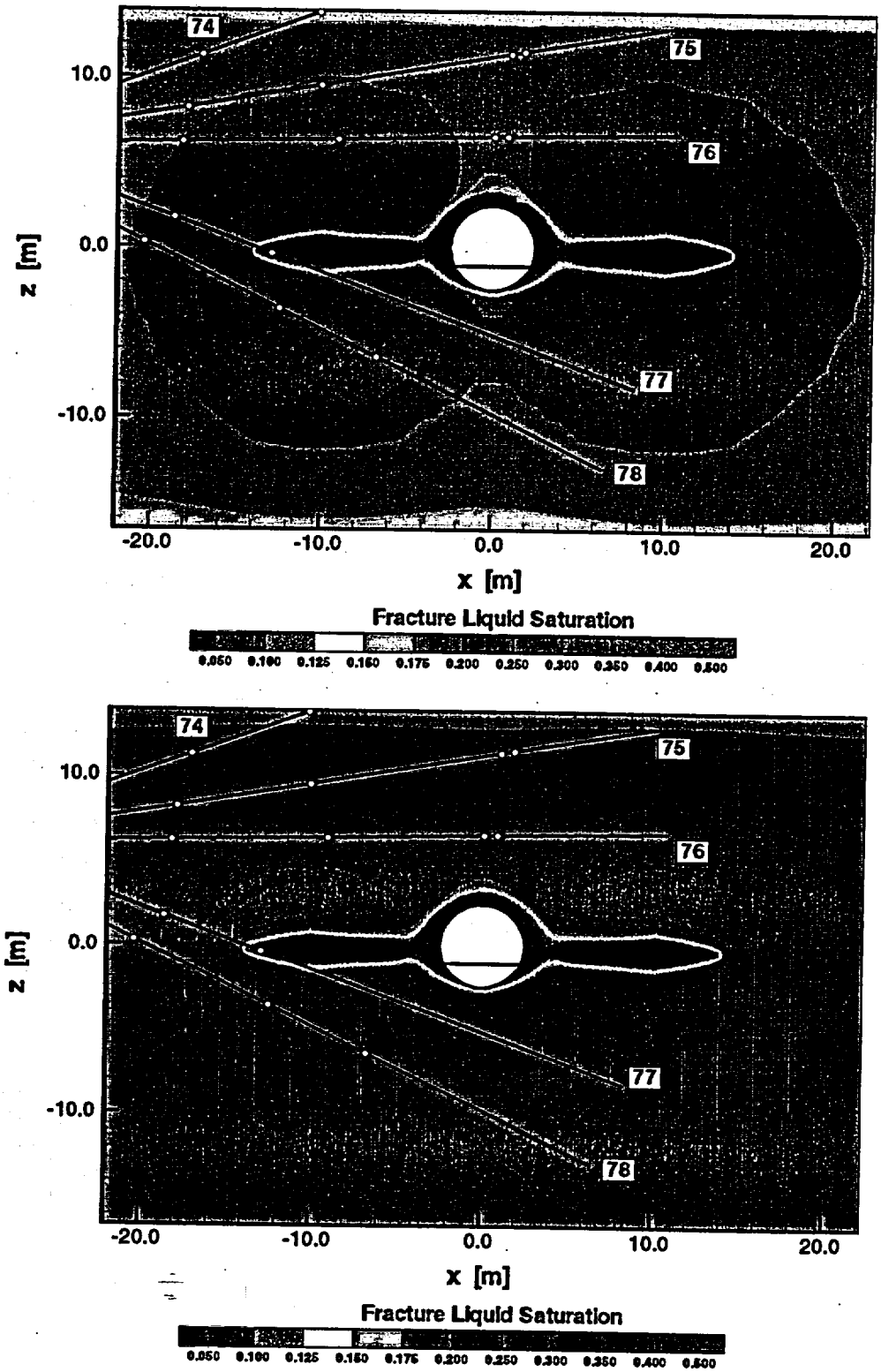

Figure 4.12-3. Fracture liquid saturation at 3 months of heating, using an ECM representation (top) and a DKM representation (bottom). Saturation contours are presented in a vertical cross section with hydrology boreholes 74 through 78,

4.13 THERMAL-CHEMICAL ANALYSIS

The modeling of THC processes for the DST included updates to the chemical model and sensitivity studies on the effects of increased fracture porosity. New gas measurements allowed for some qualitative comparisons to the model results. Refinements of the model included the consideration of CO_2 degassing and transport for full heating and cooling phases of the DST.

Model results show a large region of increased partial pressure of CO_2 (PCO2) beyond the heat pipe zone into areas of near-ambient temperatures. Because of the dissolution of the CO_2 into the aqueous phase the pH of fracture waters in these areas has declined from 8.2 to a minimum of about 6.9. Except for one anomalous water sample, having a pH of 5.5, this agrees favorably with the waters that have been collected from boreholes. The increased PCO2 also agrees qualitatively with measurements from gas samples taken from the hydrology holes. Direct comparisons between model results and measured data is limited by the large packer intervals from which the gas samples are taken, where large spatial gradients in chemistry and temperature are predicted.

The model results indicate that dissolution of cristobalite on fracture walls occurs predominant in the high temperature region of the condensate zone (approximately 90 to 95 degrees C). Most amorphous silica precipitation takes place in an even narrower region at the boiling front and closer to the heater than the center of the cristobalite dissolution region. Calcite dissolution in fractures takes place over a wider area as it is related to the decreased pH due to increased PCO2, and the drainage of lower pH waters into cooler fractures below the heated area. Calcite precipitation is dominant near the drift wall and along the wing heaters owing to its reverse solubility with increasing temperature. The drainage of more dilute condensate waters below the drift is also shown clearly by the chloride concentrations in fracture waters below the drift

Modifications of the "base case" fracture porosity by factors of 5 and 10 were done to evaluate the uncertainty in the THC calculations due to the possibly higher fracture porosities indicated by in-situ tracer testing. While not changing the overall behavior of the system, an increased fracture porosity leads to lower liquid saturations in fractures below the drift and modified water chemistry in the high temperature condensate region. In the most dilute region, chloride concentrations are a little higher for the larger fracture porosity case whereas silica concentrations are significantly higher.

4-14 Heating Plan

The heating phase of the DST was initiated in December 1997 with the wing heaters at 100% of full capacity i.e a total of approximately 143 kW and the canister heaters at 80% of design capacity i.e 6 kW per canister for a total of 54 kW. There were three principal objectives behind the heating plan. These were : a) drift wall temperature not to exceed 200°C; b) a volume of over 10,000 cubic meters of rock to be heated above 100°C; and c) a boiling zone at approximately 95°C will be maintained for approximately 3 years.

Modeling analysis before the start of heating had indicated that with the above power outputs from the heaters, drift wall temperature will reach 200°C in approximately 12 to 14 months. Actual heater power during the first year of heating has averaged approximately 188 kW and some heat loss has been taking place through the bulkhead. The rate of rise of the drift wall temperature has slowed down in recent months with the drift wall temperature at the end of November 1998 at approximately 154°C. The models have been refined based on measured temperatures. Recent modeling indicates that it will take some 20 to 22 months of heating at the current heater power setting for the drift wall temperatures to reach 200°C.

The idea that the heater outputs may be adjusted so that the temperature goals are met sooner, was thoroughly discussed in the October 1998 workshop in Livermore. The consensus was that no adjustment to the heater outputs will be made even though 200°C drift wall temperature may not be attained for another year or so. It was decided that the matter will be reconsidered in 10 to 12 months and adjustments to heater powers will be made if deemed necessary at that time.

The goal of 200°C drift wall temperature was adopted before the start of the heating phase with the expectation that increase in the coefficient of thermal expansion due to phase changes of silica polymorphs may manifest and be observed. However, it is now known that phase changes from cristobalite and trydamite do not occur below 230°C. Thus, the goal of 200°C drift wall temperature was considered unnecessary. Consultation with the repository designers on the other hand indicated that they would like to maintain the goal of 200°C drift wall temperature to observe the stability and integrity of the drift at these elevated temperatures. Maximum drift wall temperature of 200°C, therefore, remains a goal of the DST.

4.15 UPDATING THERMAL TEST STRATEGY

This presentation dealt with the issue of revisiting and ultimately updating the strategy for the DST. Basically, the presentation was divided into three categories: background discussion, the need for a strategy update, and a proposed framework. Background discussion related to the current thermal test strategy as delineated in the report entitled "Updated In Situ Thermal Testing Program Strategy" released in April, 1997. Much of the strategy in that document related to evaluation of specific thermal tests ranging from laboratory testing to a large-scale, long-duration thermal test. Specific details and methodologies such as those corresponding to the 8-year duration of the DST were beyond the scope of this report. Experiences gained from the near completion of the SHT and LBT were also part of the background discussion.

The need for an update to the DST strategy was the second category in this discussion. Factors cited included pre-occupation with the planning, implementation, and early stages of the DST, the comparatively long duration of the test, shortcomings of adhering to the strategy applied to the SHT and LBT, merit of developing a consensus among the TTT, the possibility of the DST becoming a major component of DECOVALEX III, and the benefit of producing a written document with details of the process and its linkage to key program milestones.

The last category dealt with a proposed framework from which to develop an updated strategy to the DST. Components presented included the consideration of various levels of couplings (e.g. one-way, two-way, and full), a process that integrates TTT resources, the interaction with the group responsible for development of near-field process models, and the notion that updating the DST strategy will be an iterative process. Discussion concluded with an agreement to schedule a full-day meeting with PIs, POCs, and technical leads to begin the process of producing a more comprehensive strategy for the DST.

4.16 DRIFT SCALE TEST and DECOVALEX

DECOVALEX is an international consortium of governmental agencies associated with the management/disposal of high level nuclear waste and spent nuclear fuel in Canada, Japan, Finland, France, Spain, Sweden, and the United Kingdom. DECOVALEX stands for **DE**velopment of **CO**upled models and their **VA**lidation against **EX**periments, signifying the overall objective of the consortium. The United States Nuclear Regulatory Commission participated in the first DECOVALEX project, DECOVALEX I, which was from 1992 to 1995. DECOVALEX II, underway since then, is scheduled to be completed in March 1999. Meanwhile, DECOVALEX III is being organized at this time and last summer the Department of Energy applied to join the consortium with the proposal that the Drift Scale Test be a test case for DECOVALEX III.

In November 1998, the consortium invited DOE to join DECOVALEX. The DOE has since decided to participate in DECOVALEX III. The consortium is planning to perform four tasks in DECOVALEX III. These are:

Task 1. Numerical simulation of the FEBEX in-situ THM experiment in Switzerland, proposed by ENRESA, Spain.

Task 2. Numerical simulation of the Drift Scale Test, proposed by the Yucca Mountain Site Characterization Office, DOE, USA.

Task 3. Treatment of coupled THM processes in performance assessment (PA) of Repositories, based on a number of suggestions from DECOVALEX II participants.

Task 4. A forum for outside PA experts to be invited to interact with DECOVALEX III participants to discuss application of THM process models in the performance assessment in other projects.

Organizational meetings for DECOVALEX III are scheduled in January and March, 1999. Actual work is not expected to start until the second half of FY 1999.

11/30/98

ieer

INSTITUTE FOR ENERGY AND ENVIRONMENTAL RESEARCH

Washington, D.C. office:
6935 Laurel Avenue
Takoma Park, MD 20912
Phone: (301) 270-5500
FAX: (301) 270-3029
e-mail: ieer@ieer.org
http://www.ieer.org

30 November 1998

Dr. Lake Barrett,
Acting Director,
Office of Civilian Radioactive Waste Management
US Department of Energy
1000 Independence Avenue, SW
Washington, D.C. 20585

Dear Lake,

Please find enclosed Dr. Yuri Dublyansky's final report prepared for IEER on his examination of fluid inclusions. Copies of five reviews of the draft have been included as appendices to the final report, including the review that you arranged by Joe Whelan, James Paces, Brian Marshall, Zell Peterman, John Stuckless, Leonid Neymark (all of the USGS) and Edwin Roedder (Harvard University). The final report also contains a detailed reply by Dr. Dublyansky to the Whelan et al. review. The final report also contains the detailed exchanges between Dr. Dublyansky and Dr. Diamond. IEER believes that these exchanges exemplify the kind of scientific discourse that is essential to sound research and healthy scientific discourse on what is, admittedly, an exceedingly complex subject.

We were dismayed by the personal remarks, derogatory tone, and factual inaccuracies and misrepresentations in the Whelan et al. review. Furthermore, we found many of the charges made in the review to be illogical and unfounded. If Dr. Dublyansky's motive had been to mislead the public by making "shrewd and nonscientific arguments that seem to be crafted for readers unfamiliar with the specific Yucca Mountain geologic relations," as alleged (see the cover memorandum), why would he have allowed IEER to send you his *draft* report for review? If he were not in fact interested in careful examination of the issues (as is implied in the memorandum) why would he have sent some his samples to an independent researcher (Dr. Larryn Diamond) for examination? Why would he have gone the laboratory of Dr. Robert Bodnar, who is an expert consultant on fluid inclusions to the Congressionally-mandated Nuclear Waste Technical Review Board, for further study and documentation of his samples?

We found other serious problems with the Whelan et al. review related to the data as well. It contains a gross misrepresentation of some of the reviewers' own work that is relevant to the one calculation regarding dating of a calcite sample presented in Dr. Dublyansky's draft report. The review also derides other people's work and implicitly misrepresents both Dr. Dublyansky's draft report and the paper by Grow et al.

Printed on recycled paper.

Since you arranged for the review, I am requesting you to ask the reviewers to issue a public correction of some of their comments on the draft report and to issue a retraction of their personal remarks on the following specific points:

1. The reviewers misrepresented their own data on the concentration of uranium in calcite (please see page 12 of Dr. Dublyansky's reply). Whether done deliberately or in haste, the effect was to falsely undercut the indicative evidence of relatively young calcite deposits discussed in Dr. Dublyansky's report. The reviewers should correct the public record about the range of values in calcite deposits shown by their own research. They should also note that the one value cited in Dr. Dublyansky's report from his samples is within that range.
2. Whelan et al. state that "the coarse crystal forms of calcite found in the Yucca Mountain unsaturated zone do not occur along steep flowpaths that would be analogous to water films producing flowstones" (point number 14, page 7). This is incorrect. Figure 1 of Dr. Dublyansky's report clearly shows evidence of flow along steep flowpaths. I am enclosing additional photographs showing the same thing for your information. The reviewers' comment is particularly puzzling because, as you can see from the photographs, two of the locations examined by Dr. Dublyansky were marked by Dr. Zell Peterman, one of the reviewers.
3. The reviewers derided an article by Mattson et al. cited by Dr. Dublyansky as "an unknown reference" (point number 19, p. 8). In fact, *Geotimes*, the magazine cited, is published by the American Geological Institute, a non-profit organization that represents scientific societies of geoscientists. Further, the authors of the specific article on Yucca Mountain in question were from Science Applications International Corporation (SAIC), the DOE, and the US Geological Survey. If the authors or the magazine were unknown to the reviewers that was their problem -- and one that could have easily been corrected -- and not a defect in Dr. Dublyansky's work.
4. The reviewers state that, instead of using Mattson et al., Dr. Dublyansky should have referred to Grow et al. on the potential of the Yucca Mountain site for oil and gas deposits (page 8, paragraph 9). Dr. Dublyansky has looked at the Grow et al. paper. The paper presents evidence of hydrocarbon deposits in the general area, though these are not thought to be *commercially* viable. The presence of oil and gas even in small amounts is compatible with Dr. Dublyansky's finding of minor amounts of hydrocarbons in some of the calcite samples. A figure from the Grow et al. paper is included in Dr. Dublyansky's reply to the review. Even if there was a misunderstanding of the draft report as referring to commercial deposits, this is very clearly not the main point of the report or the data. Dr. Dublyansky has clarified the matter in his final report. The reviewers comments imply that the Grow et al. paper contradicts Dr. Dublyansky's data about hydrocarbons, which is clearly incorrect.
5. The reviewers should retract the following personal remarks and innuendoes:
    - The allegations about Dr. Dublyansky's intentions made in the cover memorandum, which are discussed above.
    - The allegation that Dr. Dublyansky was "trying to misrepresent geologic information to those unfamiliar with the Yucca Mountain area" by citing the Paintbrush fault when he possibly intended to invoke the Bow Ridge Fault

(point 10, page 4 of the review). Dr. Dublyansky re-asserts that he did intend to refer to the Paintbrush fault. The reviewers and Dr. Dublyansky may disagree on his interpretation, but the allegation of attempted misrepresentation was an incorrect speculation by the reviewers.

- In view of the discussion above of the Mattson et al. and the Grow et al. papers, the reviewers should withdraw the comment that "Dr. Dublyansky seems to know little about this [hydrocarbons in relation to the study of Yucca Mountain] subject." In addition, their comment that his failure to review the Grow et al. paper before "may represent another example of the selective use of information" (point 19, p. 8) is inappropriate. It is quite normal for reviewers to refer researchers to additional papers or contrary evidence. It is not at all normal for them to speculate on the motives of the researchers. This remark is especially unwarranted inasmuch as the reviewers themselves were unaware of an article in a readily-available magazine that contains the work of researchers from institutions centrally involved in investigating Yucca Mountain, including the USGS, where all but one of the reviewers currently work.

If the reviewers other than Dr. Whelan are not responsible for the comments in the cover memorandum, then they should publicly disassociate themselves from them.

I know that the subject of fluid inclusions is one on which are widely differing views that are strongly held. Indeed, that is one of the main reasons that I sent the draft report to you for review. Scientific disagreements are common and, in an area as complex as the geology of Yucca Mountain, they are to be expected. But these disagreements can and should be addressed through respectful discussion of the issues. For instance, despite our different points of view, you and I have had a fruitful exchange of views. I really appreciate the openness with which you have approached our discussions and the scientific integrity that has led you to propose joint sampling and study of fluid inclusions in which Dr. Dublyansky would be among the principal researchers.

We owe electricity ratepayers, taxpayers, and future generations the benefit of honest, open, and respectful scientific discourse. The review by Whelan et al., because of its *ad hominem* remarks, seems aimed at stifling debate. This is a disservice to the public. I sent you the report for review, trusting that we would get a response that would do justice to the gravity of the task at hand. In that spirit, I look forward to hearing from you and from the reviewers.

Yours sincerely

Arjun Makhijani, Ph.D.
President